Generation of transgenic mice with regulated expression of manganese superoxide dismutase (MnSOD)

Doctoral Thesis

submitted to

Mathematisch-Naturwissenschaftlich-Technische Fakultät

Martin-Luther-Universität Halle-Wittenberg

by

Tomasz Loch

born 22.11.1971 in Siemianowice Śląskie, Poland

Reviewers:

1. **Prof. Thomas Braun**
2. **Prof. Thomas Noll**

Datum der Verteidigung: 15.09.2006, Halle (Saale)

urn:nbn:de:gbv:3-000010674
[http://nbn-resolving.de/urn/resolver.pl?urn=nbn%3Ade%3Agbv%3A3-000010674]

Contents

1 INTRODUCTION

1.1 Free radicals, oxidative stress and antioxidant enzymes

1.1.1 Free radicals

Free radicals are highly reactive atoms or molecules that have unpaired electron in their outer orbital. The term 'reactive oxygen species' (ROS) is often used instead but the latter may also include nonradical compounds having high oxidative properties such as hydrogen peroxide (H_2O_2). ROS can be generated by a variety of processes in biological systems. A range of external stimuli contribute to the formation of oxidants. The most important include UV light, ionizing radiation, environmental toxins, inflammatory response, hyperthermia and chemotherapeutic drugs. In addition, ROS are generated in many physiological processes in the course of aerobic metabolism. The main source of endogenous ROS are mitochondria which were originally believed to convert 1-2% of consumed oxygen into superoxide anion ($O_2^{\bullet-}$) (Boveris and Chance, 1973). More recently this rate of conversion was re-estimated at 0.1% which still is a very significant amount (Fridovich, 2004). Superoxide production in mitochondria is a side-effect of aerobic metabolism and occurs as a consequence of electron leakage in the electron transport chain. The main sites of $O_2^{\bullet-}$ formation are complex I (NADH dehydrogenase) and III (ubiquinone-cytochrome c reductase) of the respiratory chain (Turrens, 1997).

Free radicals are produced in various cellular compartments and have divergent properties. Most important ROS include:

- superoxide ($O_2^{\bullet-}$) – present in cells at an approximate concentration of 1.0×10^{-11} M (Skulachev, 1997). It is produced mainly in mitochondria but also in microsomes and nuclei (Aust et al, 1972; Patton et al., 1980); in addition, superoxide is produced during autooxidation of many biological compounds and by NADPH oxidase at the plasma membrane of inflammatory cells (Misra and Fridovich, 1972; Jackson et al., 2004); $O_2^{\bullet-}$ is less reactive than hydroxyl radical, its transformation in the presence of water (Haber-Weiss reaction) generates hydroxyl radical
- hydroxyl radical ($OH^{\bullet}$) – is extremely reactive and the least stable ROS, its half-life is 10^{-9} seconds (Pryor, 1986). It is produced in the cytoplasm and mitochondria as a result of Haber-Weiss and Fenton reaction (from H_2O_2 in the presence of transition metals)

- hydrogen peroxide (H_2O_2) – estimated concentration in cells about 1.0×10^{-8} M (Shackelford et al., 2000) is generated mainly in the process of superoxide dismutation by class of enzymes called dismutases. Sites of production include mitochondria, peroxisomes, endoplasmic reticulum and cytoplasm. In the presence of transition metals it can be converted to $OH^{\bullet}$ (Fenton reaction)
- nitric oxide ($NO^{\bullet}$) – is produced from L-arginine by a class of enzymes called nitric oxide synthases. $NO^{\bullet}$ is highly diffusible and hydrophobic, its half-life ranges from 2×10^{-3} to 2 seconds and it is produced in mitochondria, caveoli and cytosol. Its production depends on cellular environment since it can be converted to nitrosonium cation (NO^{+}), nitroxyl anion (NO^{-}) or peroxynitrite ($ONOO^{-}$). The latter has a reactivity comparable with $OH^{\bullet}$ (Stamler et al., 1992; Thomas et al., 2001; Dröge, 2002; Brookes et al., 2002)

1.1.2 Free radicals in physiology

Free radicals have dual function in cellular physiology. They participate in physiological processes and inflict widespread damage to macromolecules. Nitric oxide regulates smooth muscle tone and inhibits platelet aggregation (Radomski et al., 1987). ROS are produced in high amounts by activated macrophages during "oxidative burst" which eliminates environmental pathogens. In the course of this response hydrogen peroxide may reach concentration of 10-100 μM (Dröge, 2002). $O_2^{\bullet-}$, $OH^{\bullet}$, H_2O_2 and $NO^{\bullet}$ stimulate formation of a common second messenger – cGMP (Mittal and Murad, 1977; Arnold et al., 1977; White et al., 1976). Free radicals interfere also with Ca^{2+} signalling pathways through increasing Ca^{2+} influx from extracellular and intracellular stores (Dröge, 2002). They may induce a number of signalling pathways through activation of extracellular signal-regulated kinase (ERK), c-Jun amino-terminal kinase (JNK), p38 mitogen-activated protein kinase (MAPK) and phosphoinositide 3-kinase (PI(3)K)/Akt pathway. Besides ROS act on transcription factors increasing AP-1 level, inducing NF-κB translocation to the nucleus, and activating p53. Free radicals themselves can act as second messengers downstream of receptors for TGF-β1, PDGF, FGF-2, TNF-α, IFN-γ, angiotensin II, endothelin and more. Taken together, physiological effects of free radical action range from stimulation or arrest of growth to induction of apoptosis (Finkel and Holbrook, 2000; Yoon et al., 2002; Giordano, 2005; Thannickal and Fanburg, 2000).

1.1.3 Oxidative stress

Damaging effects of free radical species affect such molecules as DNA, RNA, proteins, lipids and carbohydrates. DNA oxidation leads to single or double-strand breaks, cross-links, telomere shortening and mutations and has far reaching consequences. The best studied marker of oxidative damage to DNA is the formation of the 8-oxo-2-deoxyguanosine (oxo8dG) adduct. Oxidants affect both nuclear and mitochondrial DNA, however, only the former can be fixed by the base excision repair pathway. Accumulation of damage in mitochondrial DNA contributes to age-associated decline in mitochondria function (Hudson et al., 1998; Hamilton et al., 2001; Evans and Cooke, 2004). RNA modifications seem to have less severe consequences. Much fewer studies deal with RNA oxidation although 8-hydroxyguanosine (8OHG) is the most frequently used marker of oxidatively damaged RNA. Although RNA is not heritable, abundant in many copies, and renewable, its damage appears to play a role in the development of Alzheimer disease (Nunomura et al., 2004; Honda et al., 2005). Proteins are the major component of organisms. Proteins' modifications resulting from oxidative stress include fragmentation, cross-linking, unfolding and conformational changes. Oxidation of side chains or backbones may lead to the generation of other reactive species. A typical marker of protein oxidation is the formation of carbonyl compounds. Most protein damages are not repaired but damaged molecules are removed by proteases (Davies, 2005). Lipids, the common building blocks of membranes, are frequent targets of oxidation. They are damaged as a consequence of a self-propagating chain reaction of peroxidation. Hence, the initial oxidation of few molecules can result in a significant damage. The most often studied products of lipid oxidation are aldehydes (malondialdehyde, MDA, being the most popular), which have oxidative capacity and can react with thiol and amino groups of proteins, with lipids and with DNA (Mylonas and Kouretas, 1999; Meagher and FitzGerald, 2000).

1.1.4 Antioxidant enzymes (AOEs)

Cells defend themselves by various means against oxygen toxicity. Among these are enzymes that have evolved to detoxify reactive oxygen species. The major AOEs are superoxide dismutases (three isozymes, Table 1), catalase and glutathione peroxidases. Each of these enzymes is capable of neutralizing or transforming particular ROS species and altogether they create a powerful detoxification system.

superoxide dismutase (SOD)	MW (kDa)	number of subunits	metal in active site	cellular localization
CuZnSOD (SOD1)	32	2	2 atoms Cu^{2+} 2 atoms Zn^{2+}	cytoplasm, nucleus, lysosomes, peroxisomes, mitochondrial intermembrane space
MnSOD (SOD2)	88	4	4 atoms Mn^{2+}	mitochondrial matrix
ECSOD (SOD3)	135	4	4 atoms Cu^{2+} 4 atoms Zn^{2+}	extracellular space, plasma membrane (outer surface)

Table 1. Comparison of eucaryotic superoxide dismutases.

1.1.4.1 Copper zinc superoxide dismutase (CuZnSOD)

Copper zinc superoxide dismutase, also known as SOD1 or cytosolic SOD, dismutates superoxide radicals to hydrogen peroxide and oxygen:

$$2\ O_2^{\bullet -} + 2H^+ \rightarrow H_2O_2 + O_2$$

The SOD1 gene contains five exons and is located on chromosome 21q22.1 (Tan et al., 1973; Huret et al., 1987; Orrell et al., 1997). CuZnSOD is formed by two identical subunits joint by at least one disulfide bond. The homodimer has a molecular weight of 32,500 Da and contains two atoms of copper and two atoms of zinc at its active site. Copper is essential for enzymatic activity while zinc provides stability to the protein (Keele et al., 1971; Fridovich and Freeman, 1986). CuZnSOD is localized primarily in the cytosol but a fraction was also detected in peroxisomes, lysosomes, nucleus and intermembrane space of mitochondria (Chang et al., 1988; Keller et al., 1991; Geller and Winge, 1982; Sturtz et al., 2001; Okado-Matsumoto and Fridovich, 2001). This enzyme is present in all mammalian tissues with the highest abundance in the liver, erythrocytes, brain and neurons. CuZnSOD is not required for normal development and survival in mice, since CuZnSOD gene knock-out mice develop normally to adulthood and show no apparent evidence of oxidative damage (Tsan, 2001). Only later in life these mice show reduced life-span and significantly increased incidence of hepatomas (Elchuri et al., 2005). Overexpression of this enzyme protects brain and heart from ischemia/reperfusion induced injury (Kinouchi et al., 1991; Chen et al., 2000) and extends life-span in *Drosophila* (Parkes et al., 1998). On the other hand CuZnSOD overexpression contributes to the premature senescence in individuals with Down syndrome (de Haan et al., 1996).

1.1.4.2 Extracellular superoxide dismutase (ECSOD)

Extracellular superoxide dismutase, known as SOD3, also dismutates superoxide radicals to hydrogen peroxide and oxygen. Human and rat ECSOD show a high similarity at DNA and amino acid level to CuZnSOD but ECSOD is coded by a distinct gene located on human chromosome 4 (Hjalmarsson et al., 1987; Folz and Crapo, 1994; Hendrickson et al., 1990). It consists of four subunits and has a molecular weight of 135 kDa (Marklund 1984). It also contains Cu and Zn in its active site. Expression of SOD3 can be induced by IFN-γ and LPS and repressed by TNF-α, TGF-β and IL-1α (Marklund, 1992; Loenders et al., 1998). ECSOD is the predominant extracellular antioxidant enzyme and possesses affinity for heparan sulfate proteoglycans (Sandstrom et al., 1992). This dismutase has been found in the uterus, umbilical cord, placenta, arteries, serum as well as cerebrospinal, ascitic and synovial fluids (Marklund et al., 1982; Oury et al., 1996a). The highest ECSOD expression can be found in the lung tissue where it plays an important role in protection against oxygen toxicity (Folz et al., 1997). Additionally a function in the regulation of nitric oxide availability was proposed for ECSOD (Oury et al., 1996a, 1996b). ECSOD knock-out mice are normal but appear more susceptible to induced lung injury (Carlsson et al., 1995). Overexpression of this enzyme protects mice from effects of hyperoxia (Folz et al., 1999).

1.1.4.3 Manganese superoxide dismutase (MnSOD)

Manganese superoxide dismutase, MnSOD or SOD2, is considered to be one of the most important intracellular antioxidant enzymes. It provides the first line of defense against ROS by dismutation of superoxide at the site of its synthesis. It is encoded by a nuclear gene while the protein is localized in the mitochondrial matrix. SOD2 is a homotetrameric enzyme with manganese ions in its active site and a molecular weight of 88 kDa. MnSOD is synthesized as a 26 kDa precursor protein containing a 24 amino acids-long mitochondria targeting sequence at the N-terminus. After transport to mitochondria the precursor protein is cleaved to a mature 24 kDa monomer, which is then assembled into a homotetrameric enzyme. MnSOD constitutes approximately 10-15% of the total SOD activity in most tissues and has been shown to be essential for the survival of animals (Tsan 2001; Borgstahl et al., 1992; Fridovich, 1975; Weisiger and Fridovich, 1973; Wispe et al., 1989). It is broadly discussed in chapter 1.2.

1.1.4.4 Catalase (CAT)

Catalase is a tetrameric hemoprotein which degrades hydrogen peroxide to water by two mechanisms:

catalatic: $2H_2O_2 \rightarrow 2H_2O + O_2$

peroxidatic: $H_2O_2 + AH_2 \rightarrow 2H_2O + A$

Decomposition of H_2O_2 by the catalatic activity of catalase is a first-order reaction with the rate dependent on substrate concentration (Ho et al., 2004). The gene coding for human CAT has been mapped to chromosome 11 band p13 and found to consist of 13 exons (Quan et al., 1986). This homotetrameric enzyme has molecular weight of 240 kDa and contains Fe^{3+} ions in its active site. It is most abundant in erythrocytes, hepatocytes, kidney and highly oxidative muscles (Powers et al., 1994; Forsberg et al., 2001). Subcellular localization of CAT include cytoplasm, peroxisomes and, to lesser extent, mitochondria (Powers et al., 1999; Radi et al., 1991). Hyperoxia, oxidants and cytokines increase expression of catalase (White et al., 1989; Shull et al., 1991; Tsan et al., 1990). Mice lacking CAT develop normally and show no phenotypical changes. Only mitochondria of the brain of these mice are susceptible to hyperoxia induced injury (Ho et al., 2004). Transgenic models with heart-specific catalase overexpression are protected against doxorubicin generated cardiac injury while no protection was found in strains with a ubiquitously overexpressed CAT (Kang et al., 1996).

1.1.4.5 Glutathione peroxidase (GPx)

Detoxification of hydrogen peroxide by glutathione peroxidase is considered more important than the corresponding action of catalase. Enzymes of GPx pathway are widely distributed in the cytoplasm. K_m value for GPx is lower than for CAT and this pathway is also capable of neutralizing hydroperoxides other than H_2O_2 (Kinnula et al., 1995). In these detoxification reactions GPx uses reduced glutathione (GSH) as an electron donor and GSH is oxidized to glutathione disulfide (GSSG). Regeneration of GSH is accomplished by glutathione reductase (GR) which requires NADPH for this reaction (Dringen et al., 2005):

$$2GSH + H_2O_2 \xrightarrow{Gpx} GSSG + 2H_2O$$

$$GSSG \xrightarrow[GR + NADPH]{} 2GSH$$

There are four distinct glutathione peroxidases that contain selenocystein at their active sites. The best studied cytosolic or classical (cGPx or GPx1) peroxidase is 85 kDa homotetrameric protein that consists of four 22-23 kDa subunits, each having one selenocysteine compound (Nakagawa, 2004). The prevalent GPx enzyme is present ubiquitously in cytoplasm and in mitochondria (Esworthy et al., 1997). GPx1 is induced by hyperoxia and TNF-α (Jornot and Junod, 1995; Tsan et al., 1990). A knock-out of the Gpx1 gene leaves very weak peroxidase activity in main organs. This remnant activity can be attributed to other GPx isoforms. $Gpx1^{-/-}$ mice are normal and no pathological changes were observed. Analysis of oxidatively damaged proteins and lipids revealed that under normal conditions these mutant mice do not differ from their wild type mates. Only paraquat and ischemia/reperfusion susceptibility is increased in these animals (Ho et al., 1998; Crack et al., 2001). Overexpression of GPx1 provides increased resistance to hyperoxia, paraquat toxicity and ischemia/reperfusion injury (Ho et al., 1998). In addition to the cytosolic GPx, three other peroxidases were described:

- gastrointestinal GPx (GPx-GI, GPx4) is a tetrameric enzyme present in the cytosol in the gastrointestinal tract (Chu et al., 1993)
- phospholipid hydroperoxide GPx (PH-GPx, PL-GPx, GPx2) is a monomeric protein of 20-22 kDa with affinity to biomembranes; it can reduce phospholipid and cholesterylester hydroperoxide; it has been detected in cytosol, mitochondria and nucleus; it shares 30-40% homology with GPx1; GPx4 is ubiquitously expressed with the highest expression in testis (Nakagawa, 2004)
- extracellular GPx (eGPx, GPx3), also known as plasma GPx (pGPx, GPx3), is a homotetrameric protein found in plasma, milk and proximal tubules of kidney; it is also secreted by some cell lines; subunit of this protein has 23 kDa (Avissar et al., 1994; Whitin et al., 2002)

1.1.4.6 Other antioxidants

In addition to the main antioxidant enzymes mentioned above, there are many low and high molecular weight substances with antioxidant properties. This group comprises both enzymes and organic compounds. In particular heme oxygenases (HO) and thioredoxins (Trx) have to be mentioned. There are 3 isoforms of the former: HO-1, HO-2 and HO-3. Only HO-1 is inducible, while the other two are constitutively expressed. Heme oxygenases catalyze degradation of heme to biliverdin and carbon monoxide. Both biliverdin and bilirubin are potent antioxidants and HO-1 is considered an antioxidant enzyme (Vile et al., 1994; Lim et

al., 2000; Foresti et al., 2004). Thioredoxins are small proteins (about 12 kDa) that have two neighbouring thiol groups which form disulfide bond during reduction of oxidized cysteine groups on proteins. Oxidized Trx undergoes a NADPH-dependent reduction by thioredoxin reductase. Major thioredoxins are: Trx-1 of cytoplasm and nucleus and Trx-2 found in mitochondria (Powis and Montfort, 2001). Known is also a group of enzymes called peroxiredoxins (Prx) which, among other functions in cell physiology, utilize thioredoxin as the electron donor for conversion of hydrogen peroxide to water (Butterfield et al., 1999). It seems that several proteins that are present in living organisms at high concentrations may act as ROS scavengers. Certainly, the most abundant protein of the plasma, albumin has antioxidative properties and protects other less abundant proteins by absorbing the impact of oxidants (Bourdon et al., 2005). Another group of small cysteine-rich proteins are metallothioneins (MT) which participate in homeostasis and detoxification of heavy metals as well as scavenging of free radicals (Miles et al., 2000). Additional low molecular weight antioxidants include vitamines A, C, E, flavonoids, anthocyanins, cysteine, uric acid and melatonins (Reiter, 1995; Rice-Evans, 2001; Tsuda et al., 2000; Atmaca, 2004; Becker, 1993; Reiter et al., 1999).

1.2 Manganese superoxide dismutase (MnSOD)

1.2.1 Gene structure and regulation of transcription

Mitochondrial superoxide dismutases are highly homologous between species. At the protein level mouse MnSOD shows 94% and 88.5% identity with rat and human proteins, respectively (Jones et al., 1995). Nucleotide sequence of cDNAs of human, bovine and murine MnSOD share more than 90% homology, although they differ in their promoter sequences (Meyrick and Magnuson, 1994). MnSOD is a nuclear DNA encoded single-copy gene localized on chromosome 6q25 in humans and 17 in mouse (Wan et al., 1994; Matsuda et al., 1990). The structure of the genes is essentially conserved among species. It consists of 5 exons interrupted by 4 introns. It has been shown that the promoter of MnSOD gene contains no TATA or CAAT box but includes GC-rich region, containing multiple specificity protein 1 (Sp1)-binding sites. Such TATA-less promoters with GC-rich region are frequently found in housekeeping genes. Sp1 sites are essential for basal transcription of MnSOD gene. Upstream Sp1 sites activating protein 1 (AP-1) consensus sequence can also be found. Ap-1 transcription factor is activated by MAPK pathways and has been shown to be stimulated by

different oxidative stress-inducing stimuli. The MnSOD promoter contains also consensus sites for the AP-2 complex, which negatively regulates transcription and which cooperates with Sp1 in regulation of transcription. An additional regulatory element in the MnSOD promoter is the antioxidant response element (ARE) which, possibly, upon ROS-induced Nrf2 factor translocation to the nucleus and ARE binding confers responsiveness to oxidative stress. Moreover, the promoter contains two NF-κB-binding sites that contribute redox-sensitive regulation of transcription. In the far 5' upstream region of human MnSOD promoter sequences corresponding to consensus p53 binding element were found. Indeed, p53-dependent upregulation of MnSOD transcription was observed in some cell lines, although this regulation appears to be cell type and species variable (Hussain et al., 2004). Other *cis*-acting elements in MnSOD promoter include interleukin 6 response element (IL6RE), simian virus 40 enhancer core sequence and CCAAT/enhancer binding protein (C/EBP) site (Jones et al., 1995; Xu et al., 2002; Lee and Johnson, 2004).

MnSOD transcription can be activated by a number of stimuli. It is induced by tumor necrosis factor α (TNFα) and interleukin-1β (IL-1β). Both factors act via binding to sequences in the second intron. It was also shown that TNF-α induces generation of ROS and activates NF-κB transcription factor (Jones et al., 1997). Additional inflammatory mediators that also induce MnSOD expression are interleukin-6 (IL-6) and lipopolysaccharide (LPS) (Dougall and Nick, 1991; Visner et al., 1991). Another cytokine, interferon-γ (IFN- γ), was also shown to activate MnSOD expression (Raineri et al., 1996). A number of physical stimuli have influence on MnSOD gene activity. Both hyperoxia and peroxynitrite are potent inducers of MnSOD transcription (Ho et al., 1996; Jackson et al., 1998). It must be mentioned that $ONOO^-$ by nitration of tyrosine residues might inactivate MnSOD protein. Thus reactive oxygen species and stimuli (like irradiation) which lead to their production, influence the rate of mitochondrial dismutase gene expression (Akashi et al., 1995).

1.2.2 Post-transcriptional regulation of MnSOD activity

Transcription of the murine MnSOD produces two mRNA species which differ in their 3'UTR: the major, inducible – 960 bp and the less stable – 4 kb. The first corresponds to previously reported cDNA and the latter arises due to the usage of alternate polyadenylation site. Multiple mRNA species are also characteristic of human and rat MnSOD gene (Jones et al., 1995). Though MnSOD mRNA concentration and stability increase in rats exposed to hyperoxia, the regulation of MnSOD occurs also at the translational level. A region involved

in translational control was mapped approximately 100 nucleotides downstream of the stop codon and was found present in all mRNA species. Moreover, it was very similar in mouse, rat and human 3' UTRs. This 41 base long *cis*-element acts as translational enhancer. Sensitive to tyrosine residue phosphorylation MnSOD RNA-binding protein (MnSOD-BP) binds this *cis*-element when it is in the hypophosphorylated state activating translation of the message. Experiments that eliminated MnSOD-BP binding showed 60% decrease in translation efficiency. Thus, it appears that a yet unknown kinase/phosphatase pathway controls MnSOD activity through binding of MnSOD-BP to the mRNA molecule (Clerch, 2000; Knirsch and Clerch, 2001). Regulation of MnSOD activity occurs also at post-translational level. It seems that inducible nitric oxide synthase (iNOS) induction leads to transcription-independent inactivation of MnSOD for which peroxynitrite formation is probably responsible (Nilakantan et al., 2005).

1.2.3 Effects of MnSOD deficiency

Two groups have independently generated MnSOD knock-out mice. In both cases inactivation of the gene led to early-onset mortality of the animals. The first group produced $MnSOD^{-/-}$ mice on a CD1 genetic background by deleting exon 3 of the gene (Li et al., 1995). Homozygous animals showed no gross phenotypical changes at birth and no deaths were observed before delivery. The animals were found to have lower body temperature and pale appearance. Few days after birth growth retardation and worsened physical fitness became apparent. Blood analysis revealed metabolic acidosis. Almost all animals died by day P10. Post-mortem examination discovered dilated cardiomyopathy with enlarged left ventricle and thinning of the chamber wall. Microscopic observations revealed myocardial hypertrophy and endocardial fibrosis. Besides, lipid deposits were found in the liver and skeletal muscle. The intestine showed signs of calcification. Surprisingly, no changes were observed in the brain. No increase in lipid peroxidation and morphological changes in mitochondria were detected. Cardiac arrythmia was the postulated cause of death of these mice.

The other group produced MnSOD knock-out mice on a mixed C57BL/6J and 129/Sv background by deleting exons 1 and 2 together with a part of the gene promoter (Lebovitz et al., 1996). Similarly to the first strain, no embryonic lethality or any gross abnormalities after birth was discovered. Differences between $MnSOD^{-/-}$ and wild type mice became visible few days after birth. Mutants were paler and smaller than control animals while their adipose tissue and skeletal muscle mass were significantly reduced. In addition, MnSOD knock-outs

exhibited motor disturbances manifested by rapid onset of fatigue and circling behaviour. Histological examinations revealed reduction in all hematopoietic cells in bone marrow which led to marked anemia at the time of their death. Animals survived up to 18 days. This group discovered lesions in neurons of the brainstem and basal ganglia. This injury was manifested by extensive mitochondrial damage and some abnormalities of the rough and smooth endoplasmic reticulum and nuclear membrane. Only 10% of mutants suffered from dilated cardiomyopathy with marked aberrations in mitochondria structure and morphology. The activity of CuZnSOD was increased by 25% in these mice, probably as a compensatory mechanism. This slight induction of cytosolic dismutase may have a somewhat protective effect on mitochondria as CuZnSOD was found in their intermembrane space. It seems likely that the induction of CuZnSOD is partially responsible for the extension of life-span of $MnSOD^{-/-}$ mice. Certainly, the other factor that has an influence on the survival of MnSOD deficient mice and development of cardiomyopathy is the genetic background. Genetic modifiers certainly influence the severity of symptoms that $MnSOD^{-/-}$ mice encounter though, all mutant mice die eventually of heart or central nervous system failure, or due to metabolic acidosis (Huang et al., 2001). Attempts to compensate MnSOD deficiency in $MnSOD^{-/-}$ mice by overexpressing CuZnSOD do not prevent perinatal lethality. This finding underlines the central role of MnSOD and its compartmentalization in cellular physiology (Copin et al., 2000).

Interesting data were obtained during analysis of $MnSOD^{+/-}$ mice. Such animals are viable and do not show any gross abnormalities. Tissues from heterozygous MnSOD knock-out mice show 30-80% reduction in MnSOD activity and lack of any compensatory up-regulation of other antioxidant enzymes. In particular a 80% reduction in the MnSOD activity was observed in brains and a 50% reduction in hearts and livers. The ratio of reduced to oxidized glutathione was decreased in these animals, indicating augmented oxidative stress (Van Remmen et al., 1999). Implications of the latter include: 1) increased levels of 8-hydroxydeoxyguanosine in mitochondrial DNA; 2) increased carbonylation of proteins; 3) decreased activities of iron-sulfur cluster-containing enzymes i.e. mitochondrial complexes I and II, aconitase; 4) increased proton leak and inhibition of respiration in mitochondria. Interestingly, the level of oxidative damage in nuclear DNA is also higher in aged $MnSOD^{+/-}$ mice than age-matched controls (Melov et al., 1999; Kokoszka et al., 2001; Van Remmen et al., 2003). In the experimental model of focal cerebral ischemia, the release of cytochrome c to the cytosol and nuclear DNA laddering were more prominent in $MnSOD^{+/-}$ mice as compared to wild types (Fujimura et al., 1999). Reduction of MnSOD expression also leads to

an increase of the level of oxidized form of LDL (oxLDL) and vascular cells from MnSOD$^{+/-}$ mice are more sensitive to oxLDL-induced cell death (Guo et al., 2001). In the DMBA/TPA-induced multistage skin carcinogenesis model histological examinations revealed higher mitotic and apoptotic indices in tissues from MnSOD$^{+/-}$ mice (Zhao et al., 2002). Cardiomyocytes isolated from newborn MnSOD$^{-/-}$ and MnSOD$^{+/-}$ mice appeared to be more susceptible to apoptosis induction. All these data implicate the pivotal function of MnSOD in the regulation of the mitochondrial pathway of apoptosis (Van Remmen et al., 2001). On the other hand, heterozygous mice were equally resistant to hyperoxia and there were no differences in the oxidative stress markers in lungs of wild type and MnSOD$^{+/-}$ mice. Probably, 50% decrease in MnSOD activity is not critical for some tissues and organs. At least in the case of the lung ECSOD seems to play a more important role in the antioxidant defense (Tsan et al., 1998; Jackson et al., 1999).

1.2.4 Effects of MnSOD overexpression

Similarly to MnSOD$^{-/-}$ mice, transgenic mouse strains with an engineered MnSOD overexpression show a high degree of phenotypic variability dependent on the genetic background. Raineri et al. (2001) showed that the same transgene maintained in two different mice strains produced different levels of the active enzyme. On a C57BL/6J (B6) background mice displayed up to 10-fold increase of MnSOD activity, which was associated with decreased body size, male infertility and attenuated female fertility. On a DBA/2J background only a 2-fold higher MnSOD activity was achieved and no linked phenotypical changes were observed in these animals. Indeed, high level of MnSOD was shown to inhibit growth of cells in culture (Li et al., 1998). Electron microscopy revealed abnormal mitochondrial cristae structure in testicular Leydig cells of MnSOD overexpressing B6 mice. Mitochondrial pathology might involve either defects in their development and segregation or alterations in their physiological functions (Harris et al. noticed impaired mitochondria segregation in yeast overexpressing MnSOD). Leydig cells are essential for synthesis of testosterone, which is necessary for sperm development. Arrested sperm production in MnSOD overexpressing B6 mice results in male infertility. Since it has been shown that high CuZnSOD level inhibit ovulation in rabbits, MnSOD overexpression may also reduce the number of released ova (Raineri et al., 2001; Harris et al., 2003).

Many experiments showed beneficiary effects of MnSOD overexpression. Low, mild and high level overexpression protected heart mitochondria from doxorubicin induced injury (Yen

et al., 1996). Three-fold higher MnSOD activity significantly attenuated myocardial necrosis following induced ischemia/reperfusion. Transgenic mice subjected to this procedure showed no alterations in cardiac output or fraction shortening while their littermates did (Jones et al., 2003). Also in the DMBA/TPA-induced multistage skin carcinogenesis model MnSOD overexpression inhibited tumor promotion by delaying and reducing AP-1 activation. It was shown that MnSOD attenuated TPA-induced PKCε activation which is responsible for activation of JNK and AP-1 (Zhao et al., 2001). Experiments attempting to estimate protective effect of MnSOD overexpression in lungs of mice challenged with hyperoxia produced inconsistent results. An increase in MnSOD activity by 160% prevented acute pulmonary pathology after exposure to 95% oxygen (Wispe et al., 1992). Conversely, other group produced mice exhibiting similar MnSOD overexpression but no protection was observed after hyperoxia (Ho, 2002).

A large amount of data comes from studies on different cell lines engineered to overexpress MnSOD. As it was previously mentioned, MnSOD overexpression inhibits growth of cells in culture (Li et al., 1998). Rodriguez et al. (2000) showed that this effect was caused by increased H_2O_2 level in these cells. In addition, higher MnSOD activity led to decrease in the ATP content. Coexpression of catalase in MnSOD overexpressing cells reversed both effects pointing to the influence of H_2O_2 on activation of p21 and inactivation of mitochondrial enzymes including ATP synthase. Overwhelming evidence proves a protective effect of MnSOD on receptor- and mitochondria-mediated pathways of programmed cell death. However, there are some reports that contradict its generally accepted anti-apoptotic properties (reviewed in Kahl et al., 2004). Furthermore, MnSOD appears to participate in the process of differentiation. Induced MnSOD overexpression in mouse fibroblast treated with 5-azacytidine significantly enhanced differentiation of these cells into myoblasts. This effect seemed to be mediated by up-regulation of Raf1, ERK and NF-κB (Zhao et al., 2001). Since MnSOD overexpression-induced H_2O_2 increase leads to the activation of ERK1/2 and AP-1, many genes and cellular processes are affected. Activation of matrix metalloproteinases (namely MMP -1, -2, -3, -7, -9, -10 and -11) is one example of such an effect, leading to the elevation of metastatic potential of MnSOD overexpressing fibrosarcoma cells. An association of high MnSOD activity with poor prognosis in certain cancers has been made (Wenk et al., 1999; Ranganathan et al., 2001; Nelson et al., 2003). The role of MnSOD in cancer progression, metastasis and treatment will be discussed in the following chapter.

1.2.5 MnSOD in cancer

Though the term 'tumor suppressor gene' is more and more frequently used for MnSOD, the literature is full of conflicting reports on an involvement of MnSOD in cancer. Repression of mitochondrial dismutase was observed in liver, breast, pancreas and prostate cancer (Galeotti et al., 1989; Li et al., 1998; Cullen et al., 2003; Baker et al., 1997). High MnSOD activity was reported in brain, thyroid, colon, gastric and esophageal cancer (Cobbs et al., 1996; Nishida et al., 1993; Janssen et al., 1999; Janssen et al., 2000). Experimental data show that MnSOD activity is in inverse correlation with p53 status. p53 mutation or inactivation leads to high MnSOD activity while low activity is found in tumors with high amount of functional p53. This findings are in line with the observation that MnSOD overexpression prevents apoptosis induced by several agents (e.g. LPS, TNF-α, pro-oxidants, chemotherapeutics, irradiation) that activate p53. Moreover loss of p53 function is often associated with therapy resistance and poor prognosis (Pani et al., 2000). In contrast to these reports it was shown that MnSOD and Gpx1 are up-regulated by p53 in human lymphoblastoid cell line. Other studies showed an inhibition of apoptosis in cells with a down-regulated MnSOD gene or stimulation of cell death following MnSOD induction (Hussain et al., 2004; Kinscherf et al., 1997, 1998). Nevertheless, most data indicate beneficiary effect of MnSOD overexpression in suppressing tumorigenicity of mammalian tumor cell lines. Increased MnSOD activity has been shown to repress human melanoma, glioma, oral carcinoma, prostate and breast cancer and mouse fibrosarcoma. It can also reverse promotion sensitive phenotype of murine JB6 epithelial cells (Church et al., 1993; Zhong et al., 1997; Liu et al., 1997; Li et al., 1998; Li et al., 1995; Zhao et al., 2001; Amstad et al., 1997). Postulated mechanisms of the tumor suppressive action of MnSOD include a delay of G0/G1 in the cell cycle, a reduction of the ratio of GSH/GSSG thereby increasing oxidative stress, activation of p53, phosphorylation of MAP kinase, induction of senescence or activation of the maspin tumor suppressor gene in breast and prostate cancer cells (Li et al., 1998; Zhong and Oberley, 2001; Plymate et al., 2003; Duan et al., 2003). It was also shown that MnSOD overexpression can sensitize tumor cell lines to anticancer drug BCNU thereby decreasing tumor volume in mice (Darby Weydert et al., 2003).

Many efforts were made to associate polymorphism in mitochondria targeting sequence (MTS) of MnSOD and risk of developing a cancer. The polymorphism pertains to a genetic dimorphism that encodes either alanine (Ala) or valine (Val) in the codon 16 of human precursor MnSOD protein. Sutton et al. (2005) showed that the Ala variant produced more

enzymatically active MnSOD protein probably due to impaired import to mitochondria of the Val variant and attenuated stability of its transcript. Thus, according to observations of MnSOD overexpression in certain tumors, the allele coding for the Ala variant of the protein should be associated with an increased incidence of tumors. Indeed, an increase in the risk of developing prostate and breast cancer has been observed in men and women homozygous for Ala allele, respectively (Woodson et al., 2003; Ambrosone et al., 1999; Mitrunen et al., 2001; Cai et al., 2004). Taking into account the low level of MnSOD in both tumors and the fact that introduction of MnSOD cDNA inhibits tumor growth, these population-based data seem confusing. It seems possible that other exogenous and endogenous antioxidants override the prognostic value of MTS polymorphism as suggested by recent epidemiological study in prostate patients (Li et al., 2005). However a number of reports indicate the lack of a correlation between MTS and carcinogenesis or even show that Val variant predisposes to breast cancer (Tamimi et al., 2004; Millikan et al., 2004; Bergman et al., 2005).

The role of MnSOD in cancer is still controversial. Anti-apoptotic effect of MnSOD overexpression suggests that induction of mitochondrial dismutase should offer a survival advantage to tumor cells and lead to treatment resistance. In agreement with this is the poor prognosis in some cancers with high MnSOD activity (Nakano et al., 1996; Janssen et al., 1998). Probably other internal and external factors control the clinical outcome of MnSOD deficiency or up-regulation. In this context, the role of MnSOD in carcinogenesis and tumor therapy needs further research.

1.2.6 Aims of the project

The general purpose of the work was to investigate the effects of MnSOD deficiency and overexpression on cellular functions and the physiology of living organisms i.e. the mouse. In particular, I intended to improve understanding of the role of MnSOD in heart physiology at the molecular level. My primary aim was to unveil - both in cell culture and in transgenic mice - the effects of an increase and decrease of MnSOD activity on other antioxidant enzymes, apoptosis, cellular senescence and oxidative stress. Several experimental model systems were established to achieve these objectives.

The creation of the following model systems were part of the project:

- generation of a transgenic mouse strain that allows a regulated expression of MnSOD by the administration of tetracycline
- generation of a stable fibroblast cell line with tetracycline-dependent overexpression of MnSOD
- establishment of MnSOD deficient primary fibroblast cell line

2 MATERIAL AND METHODS

2.1 Material

3MM paper	(Whatman)
BioTrace®NT Membrane	(Pall)
Biodyne® Nylon Membrane	(Pall)
Cell culture plasticware	(Nunc, Greiner)
Glass slides, coverslips	(Menzel-Gläser)
NAP-5™ Column	(Amersham)
Sterile filters 0.2 and 0.45µm	(Sartorius)
Plasticware	(Nunc, Greiner)
X-ray film	(Kodak)
X-ray developer	(Kodak)
Cloning cylinders, glass	(Sigma)

2.1.1 Reagents

All basic reagents, unless otherwise stated, were of analytical or molecular biology grade and were purchased from the following companies: Roth, Invitrogen, Merck, Sigma, Promega, Molecular Probes, Roche, New England Biolabs, Fermentas, Stratagene, Fluka, Serva.

2.1.2 Specific reagents

[α-^{32}P] dCTP	(Amersham Biosciences)
Carboxy-H_2DCFDA	(Molecular Probes)
Cytochrome c, partially acetylated	(Sigma)
DAB (3,3'- Diaminobenzidine)	(Sigma)
DNA Polymerase I Large Klenow	(Promega)
Doxorubicin	(Sigma)
Doxycycline	(Clontech, Sigma)
Dulbecco's Modified Eagle Medium (D-MEM) 1,000 mg/L D-	

glucose, L-glutamine and sodium pyruvate	(Invitrogen)
Dulbecco's Modified Eagle Medium (D-MEM) 4,500 mg/L D-glucose, 25 mM HEPES without sodium pyruvate	(Invitrogen)
FBS, Tet System Approved	(Clontech)
FCS	(PAA)
Geneticin G-418	(Gibco BRL)
Hygromicin B	(Invitrogen)
In Situ Cell Death Detection Kit, TMR red	(Roche)
IPTG (Isopropyl-β-D-thiogalactopyranoside)	(Roth)
MEM Non-Essential Amino Acids Solution (100×) 10mM	(Invitrogen)
Mitomycin C	(Sigma)
NBT (4-Nitro-blue-tetrazolium-chloride)	(Roth)
Oligo $(dT)_{12-18}$	(Promega)
Opti-MEM® with GlutaMAX™-I	(Invitrogen)
Penicillin-Streptamycin-Glutamine (100×)	(Invitrogen)
RNasin® Ribonuclease Inhibitor	(Promega)
SuperScript™ II Reverse Transcriptase	(Invitrogen)
Taq DNA Polymerase	(Eppendorf)
TRIzol	(Gibco BRL)
Trypsin 2.5% (10×)	(Invitrogen)
Trypsin-EDTA (0.5% Trypsin with EDTA 4Na) 10×	(Invitrogen)
Vectabond™	(Vector Laboratories)
X-Gal (5-bromo-4-chloro-3-indolyl β-D-galactopyranoside)	(Roth)
Polyfreeze™ Tissue freezing medium™	(Polysciences)
Prestained Protein Ladder, ~10-180 kDa	(Fermentas)
Protein Assay ESL	(Roche)
RQ1 RNase-Free DNase	(Promega)
Superoxide Dismutase #S2515	(Sigma)
Vectastain ABC Kit (mouse IgG or rabbit IgG)	(Vector Laboratories)
Xanthine	(Sigma)
Xanthine oxidase	(Calbiochem)

2.1.3 Kits

EndoFree Plasmid Mega Kit	(Qiagen)
In Situ Cell Death Detection Kit, TMR red	(Roche)
QIAEX II Gel Extraction Kit	(Qiagen)
Vectastain® *Elite*® ABC Kit	(Vector Laboratories)

2.1.4 Oligonucleotides

For most applications primers were designed with the help of 'Primer Select' software (DNA-Star, Lasergene 99).

name	**sequence** (5' to 3')	**product**	**application**
3forSOD	TGAGGAGAGCAGCGGTCGTGT	343 bp	library screening
3revSOD	TCGGTGGCGTTGAGGTTGTTC		
5'endSOD/ BamHI	GCGGATCCCGCCACCACACCAC CATAGCATTTTG	950 bp	probe for mapping of 5' UTR of MnSOD gene
5'endSOD/ HindIII	GCAAGCTTCGCTTCCCTGGGGCC TAACCTGACAT		
3'endSOD/ BamHI	GCGGATCCCGTTCTTCCAAAATA AAAACT	491 bp	probe for mapping of 3' UTR of MnSOD gene
3'endSOD/ HindIII	GCAAGCTTCGTCAAGGCTCTAA CGAAAAT		
totSOD/ BamHI	GCGGATCCCGACGGCCGTGTTCT GAGGAG	735 bp	cloning of MnSOD cDNA
totSOD/ HindIII	GCAAGCTTCGCAATGTGGCCGT GAGTGAGG		
INTRN/C1	GCATCGATGCCTGTAGGAAAAA GAAGAAGGCATGAAC	573 bp	cloning of rabbit β-globin intron
INTRN/Pv2	GCCAGCTGGCGTGAGTTTGGGG ACCCTTGATT		

fIRES2/PstI	GCCTGCAGCGGGTTTCCACAACT GATAAAACTCGTG	1306 bp	cloning of IRES-EGFP cassette
rEGFP/SpeI	GCACTAGTGCTCAGTTATCTACT TGTACAGCTCGTCCATGCCGA		
SODorf/E1	GCGAATTCGATGTTGTGTCGGGC GGCG	700 bp	cloning of MnSOD cDNA open reading frame; PCR genotyping of ES clones and transgenic mice; MnSOD expression
SODorf/P1	CGCTGCAGCGCAATGTGGCCGT GAGTGAGG		cloning of MnSOD cDNA open reading frame
EGFPseq.	ACACGATGATAATATGGCC		sequencing of EGFP cassette
TL-GFP	CTTTACATGTGTTTAGTCGAGG		
M13 reverse	GGAAACAGCTATGACCATG		sequencing from pKS polylinker
T3 primer	AATTAACCCTCACTAAAGGG		
T7 primer	GTAATACGACTCACTATAGGGC		
pTRE2/5seq	CGCCTGGAGACGCCATC		sequencing from pTRE2 polylinker
pTRE2/3seq	CCATTCTAAACAACACCCTG		
5'HPRT	GCTGGTGAAAAGGACCTCT	249 bp	HPRT expression
3'HPRT	CACAGGACTAGAACACCTGC		
EGFP-SE	AAGTTCATCTGCACCACCG	450 bp	EGFP expression
EGFP-ASE	TGCTCAGGTAGTGGTTGTCG		
for-RE-oligo	GATCGTTTAAACGATATCGC		introduction of additional restriction sites into pKS polylinker
rev-RE-oligo	GGCCGCGATATCGTTTAAAC		
3'probe I-for	CGCGAATTCACTGATCCAGGTTA TTCTGGTAAGAATGC	290 bp	probe for genotyping ES clones and transgenic mice
3'probe I-rev	CGCAAGCTTTCAATACTCTGCCA GGTGTGGATTAC		
ex2-for	CGCGAATTCCACGGGCAGGAGG CTGGGCC	200 bp	probe for genotyping ES clones and transgenic mice

ex2-rev	CGCAAGCTTCCTTGGCCAGAGC CTCGTGGTACTTC		probe for genotyping ES clones and transgenic mice; PCR genotyping of ES clones and transgenic mice; MnSOD expression
pTG-seq	TTCTGACCAGCAGCAGAGCC		sequencing from 5' homologous arm
pTG-seq2	GATAGGAAAGGACGTTTATGCG		sequencing from intron 2 of MnSOD gene
Neo-seq	CTGTGGTTTCCAAATGTGTCAG		sequencing from Neo cassette
5'gt-for1	CACCTTTAATCCCAGGAGACAG GC	2682 bp	PCR genotyping of ES clones and transgenic mice
5'gt-Neo	CTACCGGTGGATGTGGAATGTG		
ROSA 1	TTCCCTCGTGATCTGCAACTCC	522 bp and/or 873 bp	PCR genotyping of ROSA t1d mice
ROSA 2	GAGAGCAAGGCACATCTGAAGC		
ROSA 7	GAGTCATCAGACTTCTAAGATC AGG		
tTA 2-for	TACACGGCCTACAGAAAAACAG T	370 bp	PCR genotyping of αMHC-tTA mice; tTA expression
tTA 2-rev	AGCAGGCCCTCGATGGTAGA		

2.1.5 Antibodies

Anti-myc monoclonal antibody 9e10	made on site
Rabbit Anti-Manganese Superoxide Dismutase Polyclonal Antibody #SOD-110	(Stressgen)

2.1.6 Bacterial strains

JM110 E. coli	(Stratagene)	*rps*, (Str^r), *thr, leu, thi-1, lacY, galK, galT, ara, tonA, tsx, dam, dcm, supE44, D (lac-proAB),* [F'*tra*D36, *pro*AB, *lac*I^qZD M15]

Stbl2 E. coli	(Invitrogen)	F⁻ *mcr*A Δ(*mrr-hsd*RMS-*mcr*BC) *rec*A1 *end*A1 *lon* *gyr*A96 *thi*-1 *sup*E44 *rel*A1 λ⁻ Δ(*lac-pro*AB)
SURE® E. coli	(Stratagene)	*e14⁻(mcrA⁻)*, D (*mcrCB-hsdSMR-mrr)171, endA1, supE44, thi-1, gyrA96, relA1, lac, recB, recJ, sbcC, umuC*::Tn5(Kan^r), *uvrC*, [F' *proAB, lacI^q*D*M15*, Tn10(Tet^r)]
XL1-Blue E. coli	(Stratagene)	*recA1, endA1, gyrA96, thi-1, hsdR17(rK-,mK+), supE44, relA1, l-, lac-, [F' proAB, lacIqZD M15, Tn10(Tetr)]*

2.1.7 Plasmids and vectors

pBluescript II KS(+)	(Stratagene)	Standard cloning vector
pCRE-ERT2		Plasmid containing rabbit β-globin intron
pCS2+MT	Turner, D.L., and Weintraub, H. (1994)	Contains 6 copies of the myc epitope recognized by the 9e10 monoclonal antibody; constructed for production of epitope-tagged fusion proteins; backbone is from pBluescript II KS+
pIRES2-EGFP	(Clontech)	Plasmid containing multiple cloning site followed by IRES site and EGFP
pK-11	Meyers, E.N., Lewandoski, M., Martin, G.R. (1998)	Plasmid containing neomycin (Neo) resistance cassette flanked by frt sites; neomycin resistance gene expression is driven by phosphoglycerol kinase promoter (PGK); backbone is from pBluescript II SK
pTet-On/Off	(Clontech)	Expression plasmid coding for tetracycline receptor; pTet-On coded receptor binds TRE in the presence of tetracycline, pTet-Off coded receptor binds TRE in the absence of the drug
pTRE2hyg	(Clontech)	Tetracycline receptor regulated expression plasmid with tetracycline responsive element (TRE) followed by CMV minimal promoter; multiple cloning site lies downstream of CMV_{min} and is followed by β-globin

		poly A signal
pUC19	(Invitrogen)	Standard cloning vector

2.1.8 Cell lines

C3H/10T1/2	murine fibroblasts; ATCC No. CCL-226
Hybridoma cell line	murine hybridoma cell line for anti-myc 9e10 monoclonal antibody IgG1 isotype synthesis; ATCC No. CRL-1729
Mouse Embryonic Fibroblasts (MEF)	acquired from mice that have been engineered to be resistant to neomycin
Mouse Embryonic Stem cells v6.5	hybrid ES cell line: C57BL/6 × 129/Sv
Phoenix	human embryonic kidney cell line transformed with adenovirus E1a

2.1.9 Mice strains

αMHC-tTA	Transgenic mouse strain designed to express tTA tetracycline receptor exclusively in the heart; expression is driven by αMHC promoter. Generous gift from Prof. T. Braun
C57BL/6	Black coat inbred strain commonly used in the production of transgenic mice; used for blastocyst preparation, transfer of injected embryo to foster mother and for backcrossing chimeric mice to obtain congenic strains; used also for preparation of primary fibroblast culture
FLP-deleter	Mouse strain engineered to express constitutively Flp recombinase; used to excise frt flanked genes. Generous gift from Prof. T. Braun
ROSA t1d	Mouse strain designed to express ubiquitously rtTA tetracycline receptor from ROSA26 locus. Generous gift from Prof. T. Braun

2.2 Methods

Unless otherwise stated, all molecular biology techniques were performed in accordance with standard protocols described in "Molecular Cloning" (Sambrook et al., 1989) or "Current Protocols in Molecular Biology" (Ausubel et al., 1992). All cloning steps as well as PCR and RT-PCR products were confirmed by restriction digestions and DNA sequencing. All solutions were made in double-distilled water or demineralized MilliQ water. Solutions were either autoclaved or filter-sterilized.

2.2.1 Generation of cell culture and targeting constructs

2.2.1.1 Genomic library screening

Mouse strain 129 genomic library was provided in pools by RZPD Deutsches Ressourcenzentrum für Genomforschung GmbH. Pools were screened for MnSOD locus by PCR reaction with 3forSOD (exon 1) and 3revSOD (exon 2) primers. Positive pools that produced 343 bp product in PCR reaction were used to order genomic clones which were provided in Lawrist 7 cosmids. Primers 3'endSOD/BamHI with 3'endSOD/HindIII and 5'endSOD/BamHI with 5'endSOD/HindIII were used in further PCR reactions to prove the presence of 3' and 5' part of MnSOD gene as well as to generate probes for mapping of the locus. Primers produced 491 bp and 950 bp products, respectively.

2.2.1.2 Mapping of the MnSOD locus

The partial sequence of MnSOD locus was published by Jones et al. in 1995 and is available under the following GenBank accession numbers: L35525, L35526, L35527 and L35528. Standard molecular biology techniques were used to map unknown restriction sites and identify desired fragments which after cloning into pKS vector served either as probes or homologous arms for construction of the targeting vector. Further mapping was greatly facilitated by nucleotide sequence retrieved from mouse genome database available at www.ensembl.org

2.2.1.3 Generation of cell culture construct pTRE2hyg/SOD2ex

TRIzol extracted wild type liver RNA was reverse transcribed according to general protocol – see 2.2.5.1. cDNA for MnSOD was amplified with totSOD/HindIII and totSOD/BamHI primers. 735 bp fragment was digested with HindIII and BamHI restriction enzymes and cloned to pKS vector (pKS/totSOD). Cloned fragment was sequenced and compared to known cDNA sequence. Then SODorf/E1 and SODorf/P1 primers were used to amplify 691 bp fragment containing MnSOD ORF and introduce EcoRI site in front of start codon.

Myc epitope sequence (260 bp) was cut out from pCS2+ MT plasmid with ClaI and EcoRI enzymes and cloned to pKS (pKS/tag). Next, PCR amplified 691 bp MnSOD coding region was cut with EcoRI and PstI and introduced into relevant sites in pKS/tag (pKS/tagSOD). Obtained fusion of myc epitope and MnSOD was sequenced with particular attention paid to the fusion site.

Then fIRES2/PstI and rEGFP/SpeI primers were used to amplify IRES-EGFP cassette (1306 bp) from pIRES2-EGFP vector. This fragment was cloned to PstI-SpeI sites in pKS/tagSOD and obtained pKS/tagSOD IRES-EGFP plasmid was verified by sequencing.

Rabbit β-globin intron was PCR amplified from pCRE-ERT2 plasmid with INTRN/C1 and INTRN/Pv2 primers (573 bp) cut with ClaI and PvuII restriction enzymes and cloned to pTRE2 vector (pTRE2/INTRN).

Subsequently whole tagSOD IRES-EGFP expression cassette was cut out from pKS/tagSOD IRES-EGFP plasmid with ClaI and XbaI enzymes and cloned to respective sites in pTRE2/INTRN plasmid (pTRE2/SOD2ex). Finally, hygromycin resistance cassette was cut out from pTRE2hyg vector with XhoI enzyme and cloned into XhoI site in pTRE2/SOD2ex. Obtained pTRE2hyg/SOD2ex cell culture construct was used in further work.

Partial digestions of pTRE2hyg/SOD2ex plasmid with XhoI enzyme were done to inactivate one of the two XhoI sites (at position 2). The obtained pZK/SOD construct was linearized with XhoI and used exclusively in stable cell line generation. This modification had no influence on functionality of the construct.

2.2.1.4 Generation of targeting construct pTG/TRE

Homologous arms were cloned as follows. Lawrist 7 cosmid with MnSOD gene was digested with HindIII restriction enzyme and 2445 bp HindIII fragment (5’ arm) was

identified by means of Southern blot hybridization. Primers 5'endSOD/BamHI and 5'endSOD/HindIII were used to synthesize probe. This HindIII fragment was cloned to pKS vector (pKS/5').

For 3' arm cloning BamHI digestions of MnSOD cosmid were done and 8.75 kb BamHI fragment (3' arm) was identified with a probe prepared with 3'endSOD/BamHI and 3'endSOD/HindIII primers. BamHI fragment was cloned to pKS vector (pKS/3').

Then 3' arm fragment was cut out from pKS/3' with XmaI and SacII restriction enzymes and ligated to respective sites in pKS/5' (pKS/5'-3').

Neomycin resistance cassette flanked by frt sites (1.96 kb) was cut out from pK-11 with SacI and KpnI enzymes and subcloned to pUC18 vector (pUC/Neo). Subsequently it was cut out with XmaI together with EcoRI and ligated to relevant sites in pKS/5'-3' (pKS/5'-Neo-3'). Correct ligation was verified by sequencing of junction points with pTG-seq and Neo-seq primers.

MnSOD expression cassette together with CMV_{min} promoter, TRE and β-globin poly A was cut out from pTRE2hyg/SODex construct with XhoI and BsrBI enzymes. This 4.7 kb fragment was blunt-ended and ligated to SmaI site in modified pKS vector (PmeI and EcoRV sites introduced between BamHI and NotI). Then whole expression cassette was cut out with EcoRV enzyme and blunt end ligated to SmaI site in pKS/5'-Neo-3'. Desired orientation of the expression cassette was identified and pTG/TRE targeting construct was completed. NotI restriction site located downstream of the 3' arm was used to linearize the construct before transfecting into ES cells.

2.2.1.5 Generation of targeting construct pTG/TRE tetR

Tetracycline receptor (Tet-Off) coding sequence together with CMV promoter and SV40 poly A was cut out from pTet-Off plasmid with XhoI and PvuII enzymes, blunted and ligated to SmaI site in modified pKS vector. The whole tetracycline receptor cassette was cut out with EcoRV and modified with AscI linkers. The PmeI site in pTG/TRE construct was also changed with AscI linkers. Finally, the AscI linkered tetracycline receptor cassette was cloned into the AscI site in pTG/TRE to complete the pTG/TRE tetR targeting construct. Two orientations of tetR were obtained. After functional test of both orientations (transient transfections and GFP spectrophotometric measurement) the plasmid with the reverse orientation of tetR was used for further work. Similarly NotI restriction site was used to linearize this construct.

2.2.1.6 Principles of Tetracycline-regulated expression system

Tetracycline (Tet) regulated expression system is based on two separate vectors. The response vector (pTRE2 or pTRE2hyg) contains tetracycline responsive element (TRE) upstream of the inherently inactive minimal CMV promoter (CMV_{min}) and multiple cloning site (MCS). Binding of tetracycline receptor to TRE element activates the promoter and leads to transcription of the gene cloned in the MCS.

Regulation of the system is achieved through vectors coding for different types of tetracycline receptors: pTet-On – codes for a receptor which binds to TRE element and activates transcription in the response vector only in the presence of doxycycline; pTet-Off – codes for a tetracycline receptor which binds TRE element in the absence of tetracycline, so administration of the antibiotic stops transcription.

Originally, tetracycline was used to control this system. However the Tet-Off system is equally inducible with doxycycline (Dox), while the mutated version of Tet-Off is responsive only to doxycycline. Moreover there are some other more important reasons to use Dox: it has longer half-life and much lower concentrations of Dox are required to operate the system. Therefore, doxycycline was used in all experiments as well as, when required, during animals' maintenance. Principles of Tet-regulated expression system are shown on Fig. 1.

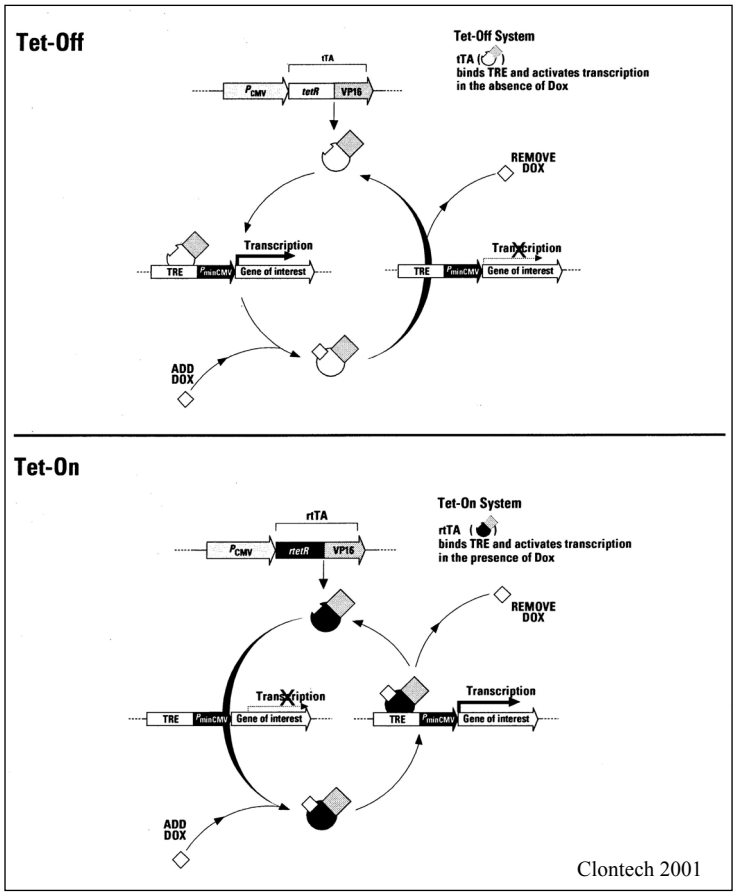

Fig. 1. Schematic representation of tetracycline regulated gene expression system. Doxycycline is used instead of tetracycline. Abbreviations: P_{CMV} – CMV promoter, tTA – tetracycline controlled transactivator, rtTA – reverse tTA, rtetR – Tet repressor protein, VP16 – Herpes simplex virus VP16 activation domain, TRE - tetracycline responsive element, P_{minCMV} – minimal CMV promoter, Dox – doxycycline

2.2.2 Cell culture methods

2.2.2.1 Basic maintenance

C3H/10T1/2 and Phoenix cell lines were grown in D-MEM (1,000 mg/ml glucose) medium containing 10% FCS, 100 U/ml of penicillin, 100 μg/ml of streptomycin and 0,292 mg/ml L-glutamine.

Cells transiently transfected with pTet-On/Off and pTRE2hyg/SODex plasmids as well as cell lines stably transfected with pTet-Off and double-stable pTet-OFF/ pTRE2hyg/SODex were cultivated in identical medium except that instead of FCS Tet System Approved FBS was used.

Cells were grown for 2-3 days to 80-90% confluence in humidified atmosphere containing 10% CO_2 at 37° C. Cells were detached from dishes with trypsin solution (0.05% trypsin, 0.02% EDTA in 1×PBS) and split 1 to 6.
Frozen stocks were made in freezing medium: 20% FCS and 10% DMSO in D-MEM.

2.2.2.2 Primary fibroblast culture

Nineteen 14 days old embryos were isolated from two $SOD^{+/-}$ pregnant females crossed with $SOD^{+/-}$ male. Heads of the embryos were cut off and saved for DNA extraction. Organs were dissected and the carcasses transferred to separate, fresh 6-cm plates filled with 0.25% trypsin in HEPES/EDTA buffer. Each embryo was chopped to tiny pieces with a sterile scalpel and then incubated for 40 minutes in the cell culture incubator. Next, tissues were disaggregated by vigorous pipetting and returned to the incubator for 10 minutes. Then the volume was made to 20 ml with Mouse Embryonic Fibroblast (MEF) medium i.e. D-MEM (4,500 mg/ml glucose) medium containing 15% FCS, 100 U/ml of penicillin, 100 μg/ml of streptomycin and 0,292 mg/ml L-glutamine. Each pool of cells was transferred to separate 15-cm plate. After overnight incubation fibroblasts attached to the cell culture plate and debris was removed by aspirating the medium. Fresh medium was added and the cells were grown to 90% confluency. In the meantime MnSOD locus genotype of each embryo was determined according to the procedure described under 2.2.6.2. Primary cell lines of interest were expanded and frozen stocks were made at passage 2.
For further work cells were cultured in D-MEM (1,000 mg/ml glucose) medium containing 10% FCS, 100 U/ml of penicillin, 100 μg/ml of streptomycin and 0,292 mg/ml L-glutamine. Cells were grown for 2-3 days to 90% confluence in humidified atmosphere containing 3% oxygen and 10% CO_2 at 37° C. Cells were detached from dishes with trypsin solution (0.25% trypsin in HEPES/EDTA buffer) and split 1 to 3.

2.2.2.3 Transient transfections

2.2.2.3.1 Calcium phosphate

On the day before transfection cells were trypsinized and plated at 10 000 – 15 000 cells per cm^2 (C3H/10T1/2) or 30 000 cells per cm^2 (Phoenix). Typically 6-well plates were used. Next day cells should reach 60-70% confluence. 3 hours before transfection medium was

aspirated and changed to fresh growth medium. 30 minutes before transfection the following coctail was prepared: 5 μg plasmid DNA and 750 μl HBS (100 mM NaCl, 6.5 mM KCl, 0.8 M $Na_2HPO_4 \cdot 2H_2O$, 210 mM HEPES) pH 7.05. To this mixture 48 μl of 2 M $CaCl_2$ was added dropwise and shaked after each drop. Transfection coctail was incubated for 30 minutes at room temperature. After incubation, coctail was transferred to a single well of a 6-well plate in dropwise fashion. After 12-16 hours medium was changed. Cells were photographed or collected by trypsinization after 24-72 hours.

2.2.2.3.2 Electroporation

On the day of electroporation cells were 70-80% confluent. Cells were detached with trypsin, centrifuged and 2 mln cells were suspended in 400 μl of electroporation buffer: Opti-MEM and cytosalts (1 M KCl, 10 mM $CaCl_2$, 0.5 M K_2HPO_4 pH 7.6, 100 mM $MgCl_2$) in 25 to 75 ratio. Up to 60 μg of plasmid DNA was added to this electroporation coctail and the whole volume was transferred to 4 mm gap electroporation cuvettes. Electroporation was performed in BTX ECM 600 electroporator with the following settings:

Low Voltage Mode
Voltage: 475 V
Pulse Length: 1 millisecond
Number of Pulses: 4

Cells were plated in 10-cm plates 5-10 min. after pulsing. After 12-16 hours medium was changed. Cells were photographed or collected by trypsinization after 24-72 hours.

2.2.2.4 Double-stable cell line generation

C3H/10T1/2 cells were transfected with 1 μg of pTet-Off by means of standard electroporation protocol except that cells were plated in 3 separate 10-cm plates at concentrations: 50, 100 and 200 thousand per plate. The following day medium was replaced with selection medium i.e. standard growth medium supplemented with G418 at 1 mg/ml concentration. Medium was replenished every second day. Cells were cultivated for 10-14 days until considerable number of large colonies was obtained. Single colonies were isolated by trypsinization in cloning cylinders. Each trypsinized colony was transferred to single well of a 96-well plate and expanded in standard growth medium containing 0.5 mg/ml G418.

29 stable clones were isolated and screened for the presence of integrated plasmid by Southern blot hybrydization with a probe specific for neomycin resistance gene.
9 stable clones were subjected to functional screening to test inducibility of the Tet-Off system: cells were transiently transfected with pTRE2hyg/SODex plasmid by the standard electroporation protocol. Following electroporation cells were split to two 6-cm dishes and allowed to grow in the presence or absence of doxycycline at 1 μg/ml. Cells were collected by trypsinization when they reached confluence and proteins were extracted according to the described procedure (see 2.2.4.1). Then intensity of fluorescence of EGFP reporter molecule was determined in protein extracts in Hitachi F-2000 fluorescence spectrophotometer set at: excitation – 488 nm, emission – 509 nm. EGFP Relative Fluorescence Units (RFU) were normalized to the protein concentration. Normalized values for cells grown without doxycycline (induced state) were related to cells grown in the presence of the drug (repressed state). These ratios were compared between all analyzed clones. The clone with the highest induction of expression and the lowest background (clone OFF2) was selected for the next transfection.
OFF2 cell line was stably transfected with 1 μg of XhoI linearized pZK/SOD plasmid. All procedures were carried out as mentioned above except that selection medium contained 0.5 mg/ml G418 and 800 μg/ml Hygromicin B. Following selection and thereafter double-stable clones were grown in selection medium containing 0.5 mg/ml G418 and 200 μg/ml Hygromicin B. Clones were subjected to functional screening procedure as described above. Four double-transfected clones with the highest expression induction and the lowest background were selected and grown for few weeks. During this period EGFP fluorescence was monitored under the fluorescence microscope and the clone showing the most stable and consistent expression of the transgene was chosen for further experiments.

2.2.2.5 Mouse embryonic stem cells culture

2.2.2.5.1 Preparation of mitomycin C treated MEFs

Mouse embryonic fibroblasts (MEFs) were isolated as described in 2.2.2.2 from a neomycin resistant mouse strain. One frozen stock was thawed in a 10-cm plate. After the cells reached 90% confluence they were detached with 0.25% trypsin in HEPES/EDTA buffer and plated on 15-cm plate which after reaching 90% confluence was split to three 15-cm plates. Subsequently cells from three 15-cm plates were collected and plated on ten 15-cm

dishes. Day after the cells reached 90% confluence MEF medium was replaced with 5% FCS MEF medium supplemented with Mitomycin C at 10 μg/ml and incubated for 2-4 hours in cell culture incubator. Then cells were washed two times with HEPES buffer and collected by trypsinization. 3 frozen stocks of ready to use feeder cells were made from each 15-cm plate. Typically 1-2 frozen stocks were plated on one 10-cm plate, 6-well plate, 24-well plate or 96-well plate.

2.2.2.5.2 Basic maintenance

Tissue culture plates used in embryonic stem (ES) cells culture were routinely covered with 0.2% gelatine in water. Then this solution was aspirated and feeder cells (protocol 2.2.2.5.1) were plated a day before planned ES cells plating. Throughout the work with ES cells ES-medium was used. Cells were grown for 3-4 days in humidified atmosphere containing 10% CO_2 at 37° C. Medium was changed every day. Before trypsinization cells were washed with HEPES buffer and detached with 0.25% trypsin in HEPES/EDTA buffer. ES cells were split 1:6.

2.2.2.5.3 Electroporation of ES cells

For electroporation ES cells were split 1:4 and grown for 2 days. Two hours before electroporation cells were fed with fresh medium. Then cells were detached and counted in hemacytometer. 13-16 mln cells were suspended in 600 μl of Opti-MEM medium and transferred to 4 mm gap electroporation cuvette. 25 μg of linearized pTG/TRE or pTG/TRE tetR plasmid in 100 μl of Opti-MEM was added to cells and mixed. Electroporation was performed under the following conditions:

Low Voltage Mode
Voltage: 250 V
Pulse Length: 1 millisecond
Number of Pulses: 1

Cells were resuspended in ES-medium 10 min. after pulsing. Then cells were plated in 10-cm dishes as follows: 3 plates with 4 mln cells each and 2 plates with 0.7 mln cells each. 24 hours after transfection medium was changed to selection medium: ES-medium supplemented with G418 at 400 μg/ml. Henceforth medium was changed daily and growth of ES colonies was monitored for 10-14 days.

2.2.2.5.4 Isolation of recombinant ES cell clones

Once colonies reached appropriate size they were picked with tips mounted on 50 µl automatic pipette. Only colonies with irregular shape and sharp boundaries were picked. Those, showing signs of differentiation (dark center surrounded with light ring and growing upwards) were not collected. Shortly before picking of clones medium was aspirated and replaced with HEPES/EDTA buffer. Open dishes were placed under inverted microscope and clones were picked with the help of the microscope and transferred to V-bottomed 96-well plate filled with 0.25% trypsin in HEPES/EDTA buffer. After picking of 16 colonies the 96-well plate was incubated for 10 min. in cell culture incubator. Then colonies were dissociated by vigorous pipetting and transferred to previously prepared flat bottom 96-well plate with feeder cells. Thereafter ES-medium without G418 was used. All the operations were done under tissue culture hood.

After 3-4 days of growth ES clones were split. Trypsinized cells were divided 1:4 i.e. one part was trasferred to previously prepared 24-well plate with feeder cells and four parts left in 96-well plate were mixed with freezing medium, covered with mineral oil and frozen at -80° C. From these frozen stocks only selected clones with successfully targeted locus were expanded and used in balstocyst injections. ES clones in 24-well plates were grown for 7-10 days until they reached confluence. As these cells were used only for DNA isolation medium was not changed during their growth.

2.2.2.5.5 DNA extraction from ES cells

24-well plates with confluent ES cells were washed with 1×PBS and covered with 500 µl of ES-lysis buffer. Cells were incubated in cell culture incubator for 24-72 hours. Then plates were shaked for 1 hour at room temperature. After that 500 µl of isopropanol was added and plates were shaked for next 1 hour. Finally, white DNA precipitate was lifted with a needle bent at the end and transferred to 1.5 ml tubes with 100 µl TE buffer. DNA was dissolved overnight at 55° C with shaking. ES clones were screened for desired recombination by PCR and Southern blot hybridization (see 2.2.6).

2.2.3 ROS measurement by Fluorescence Activated Cell Sorting (FACS)

Cells were cultured in triplicates on 6-cm plates. For FACS analysis they were detached with trypsin and washed with PBS two times. Then cells were resuspended in 0.5-1 ml of prewarmed HBS medium with carboxy-H_2DCFDA at 5 μM and incubated for 30 minutes at 37° C. Then cells were transferred to ice and 2 μl of propidium iodide (PI) at 100 μg/ml was added immediately before analysis. Cells were sorted in FACSFlow cytometer (Becton Dickinson) and data were analyzed in CellQuest™ software. Instrument calibrations were performed on unstained and stained with single dye cells. FACS settings were as follows:

Detector	Voltage	AmpGain	Mode
FSC	E-1	6.55	log
SSC	272	1.00	log
FL-1	420	1.00	log
FL-2	430	1.00	log

Thershold:	Compensation:
Parameter: FSC	FL-1 – 1.0% FL-2
Value: 52	FL-2 – 21.0% FL-1

Fluorescence was analyzed in the continuous presence of both dyes. Carboxy-H_2DCFDA was analyzed in FL-1 channel, PI in the FL-2 channel. PI was used to exclude non-viable cells from analysis.

2.2.4 AOE's activity methods

2.2.4.1 Protein extraction

Cells from confluent 15-cm plate were resuspended in 100-150 μl cell homogenization buffer pH 7.2 and homogenized with a handheld teflon homogenizer. Then the homogenate was subjected to two cycles of freezing and thawing followed by 10 minutes centrifugation at 600×g at 4° C. Supernatant was transferred to new tubes, aliquoted and stored at -80° C.

Tissues were weighted and appropriate volume of tissue homogenization buffer pH 7.2 was added to make a 4-5% (w/v) solution. Ultra Turrax (IKA Works) homogenizer was used for disintegration of heart tissue and teflon homogenizer for brain and liver. All steps were performed on wet ice. Then extracts were centrifuged at 600×g at 4° C. Supernatants were saved, aliquoted and frozen at -80° C.

Protein concentration in extracts was determined according to the procedure provided with Protein Assay ESL kit (Roche).

2.2.4.2 Superoxide Dismutase (SOD)

2.2.4.2.1 SOD activity gel

In gel SOD activity assay was done as described by Beauchamp and Fridovich (1971). Native polyacrylamide gel was made of separating gel – 12% and stacking gel – 6%. Non-denaturing loading buffer was mixed with 80-120 μg protein and loaded to a single well. The gel was run for 2-3 hours at 15-20 mA. Following electrophoresis the gel was soaked in 2.45 mM NBT for 20 min. with gentle rocking. Then NBT was replaced with the solution: TEMED 28 mM, riboflavin 0.028 mM, K-phosphate buffer pH 7.8 36 mM. If MnSOD was visualized only KCN was added to this solution to final concentration 8 mM. Gel was incubated in this solution for 15 min. with gentle rocking. Finally, the gel was briefly washed with water and illuminated on light box for 15-30 min. until blue colour developed.

2.2.4.2.2 Cytochrome C method

In order to determine precisely SOD activities the method of inhibition of cytochrome c reduction was used (McCord and Fridovich, 1969). Cytochrome c buffer was prepared as follows: 50 mM potassium phosphate buffer pH 7.8, 50 μM xanthine and 0.248 mg/ml cytochrome c. The optimal concentration of xanthine oxidase (XO) in the assay was established by adding 12-20 μl of XO (0.8 U/ml) to 960 μl of cytochrome c buffer. Changes of cytochrome c absorbance measured against cytochrome c buffer without XO were followed during 3 min. incubation at 550 nm. Changes of absorbance in time (ΔA_{550nm}/min) from 60^{th} to 120^{th} second were recorded every 10 seconds and the average value from 6 measurements was calculated. ΔA_{550nm}/min in the range of 0.023-0.025 was considered optimal for SOD activity assay. Once the volume of XO giving this ΔA_{550nm}/min range was established, it was used throughout whole experiment.

For determination of total SOD activity in tissues 960 μl of cytochrome c buffer was mixed with 12-20 μl of xanthine oxidase and 10-40 μl of tissue protein extract (to obtain ΔA_{550nm}/min in the range 0.010-0.020). To differentiate between MnSOD and CuZnSOD KCN was used to inhibit specifically cytosolic SOD. Inhibition was achieved by incubation of the protein extract with 10 μl of 0.2 M KCN for 2 minutes.

Commercially available SOD of known activity was also measured and used to establish a standard curve from which activities of unknown samples were read. CuZnSOD activity was calculated by substracting MnSOD activity from total SOD. Hitachi U-2000 thermostatted spectrophotometer was set at kinetic mode. Assay was done at 30° C, each sample was measured at least 3 times. Activities were normalized to protein concentration and expressed in U/min/mg protein.

2.2.4.3 Catalase (CAT)

Catalase activity buffer was prepared as follows: 50 mM potassium phosphate buffer at pH 7.2-7.4, 1 mM EDTA and 0.05% Triton X-100. Hydrogen peroxide was added to 990 µl of catalase buffer to 10 mM final concentration and absorbance was read in a quartz cuvette at 260 nm. Absorbance in the range 0.4-0.45 was regarded as optimal for catalase activity measurements. For determination of CAT activity in tissues 980 µl of buffer with hydrogen peroxide was mixed with 20 µl of extracts. After 15 seconds incubation absorbance change in time (ΔA_{260nm}/min) was measured against catalase buffer with the same amount of tissue extract but without hydrogen peroxide. Reaction was followed for 2 minutes and average read-outs were recorded. Obtained ΔA_{260nm}/min values were in the range of 0.02-0.05. To calculate units of CAT activity, it was assumed that decomposition of 1 µM of H_2O_2 gives ΔA_{260nm}/min = 0.0394. Assay was done at room temperature, each sample was measured at least 3 times on a Hitachi U-2000 spectrophotometer. Activities were normalized to protein concentration and expressed in µmole/min/mg protein.

2.2.4.4 Glutathione Peroxidase (GPX)

Reaction buffer was prepared as follows:

48 ml of 75mM sodium phosphate buffer pH 7.0

1 ml of 60 mM reduced glutathione

2 ml of glutathione reductase (30 U/ml)

1 ml of 120 mM sodium azide

2 ml of 15 mM EDTA

2 ml of 3 mM NADPH

pH of this reaction buffer was adjusted to 7.0. All components of this mix as well as 1 mM DTT solution were prepared in 75 mM sodium phosphate buffer pH 7.0. 933 µl of reaction buffer was mixed either with 30 µl tissue extract or the same volume of 1 mM DTT (to substract non-enzymatic glutathione oxidation) which served as reference cuvette. Reaction was started with addition of 33 µl 7.5 mM H_2O_2. Decrease in absorbance at 340 nm was followed for 5 minutes in Hitachi U-2000 spectrophotometer. ΔA_{340nm}/min values in the range of 0.02-0.05 were considered optimal for the reaction. GPX activity was calculated assuming that millimolar extinction coefficient of NADPH is 6.22. Assay was done at room temperature, each sample was measured at least 3 times. Activities were normalized to protein concentration and expressed in nmole/min/mg protein.

2.2.5 General PCR and RT-PCR methods

2.2.5.1 Reverse transcription (RT)

Total RNA was extracted with TRIzol reagent according to manufacturer's protocol. Concentration of RNA was determined with Eppendorf BioPhotometer by measuring absorbance at 260 nm and assuming that 1 unit of absorbance corresponds to 40 µg of RNA. In the first step, RNA extract was purified from DNA contamination:

3 µg	total RNA
1 µl	RQ1 RNase-Free DNase 10×buffer
1 µl	RQ1 RNase-Free DNase [1 U/µl]
to 10 µl	water

Incubation at 37° C for 30 minutes followed by addition of 1 µl of Stop Reaction buffer and incubation at 65° C for 10 minutes.

Then 1 µg of DNase-treated RNA (3.5 µl from above reaction) was reverse transcribed:

3.5 µl	DNase-treated RNA
1 µl	oligo $d(T)_{12-18}$ [500 µg/ml]
5 µl	dNTP's [2 mM]
3 µl	water
12.5 µl	total

This coctail was incubated at 65° C for 10 minutes and then immediately placed on ice. Following reagents were added to the above mix:

4 µl	RT SSII buffer [5× conc.]
2 µl	DTT [0.1 M]
0.5 µl	RNasin [40 U/µl]
	Super Script II Reverse
1 µl	Transcriptase [200 U/µl]
20 µl	total

RNA was reverse transcribed for 1 hour at 42° C followed by incubation at 70° C for 15 minutes. Obtained cDNA was used immediately in PCR reaction or frozen at -20° C.

2.2.5.2 Polymerase chain reaction (PCR)

Typical PCR reaction was done as follows:

1.5 µl	Taq buffer [10×, with 15 mM $MgCl_2$]
1.5 µl	dNTP's [2 mM]
3 µl	TaqMaster PCR Enhancer [5×]
0.15-0.3 µl	forward primer [10 µm]
0.15-0.3 µl	reverse primer [10 µm]
1-3 µl	DNA
0.15 µl	Taq DNA Polymerase [5 U/µl]
to 15 µl	water

All PCR conditions were optimized experimentally for each primer pair. When necessary $MgCl_2$ was added to final concentration of 2-5 mM. Thermal cycling conditions were also optimized empirically.

2.2.5.3 Reverse transcription - Polymerase chain reaction (RT-PCR)

Reactions were performed as in 2.2.5.2 except that typically 3 µl of cDNA from 2.2.5.1 was used as template.

2.2.6 Genotyping of recombinant ES cells and transgenic mice

2.2.6.1 Tail DNA isolation

Approximately 5 mm tip of a tail was immersed in 0.5 ml tail lysis buffer and incubated overnight at 56° C with shaking. Next day samples were centrifuged for 10 min. at 13 000 rpm. DNA was precipitated from supernatant with 0.5 ml isopropanol, centrifuged at 13 000 rpm for 15 min. and pellet was washed with 70% ethanol, dried and dissolved in 100 µl TE.

2.2.6.2 PCR

SOD locus

Two primer pairs were employed. External primers allowed the detection of successful targeting of the MnSOD locus with targeting construct. The forward primer was designed to bind sequence upstream of the modified region. This pair of primers was used to screen neomycin resistant ES cell clones in search for desired recombination events. Occasionally they were also used in verification of homozygosity in transgenic mice. PCR amplification with external primers produced a specific 2.7 kb band.

Internal primers are complementary to sequences in two neighbouring exons to allow discrimination between cDNA in targeting construct and DNA of native MnSOD locus. These primers produced 226 bp and 340 bp bands, respectively. They were mainly used to assess genotype of transgenic mice.

Prior PCR reactions tail or ES cell DNA was diluted in water 1:10.

external primers

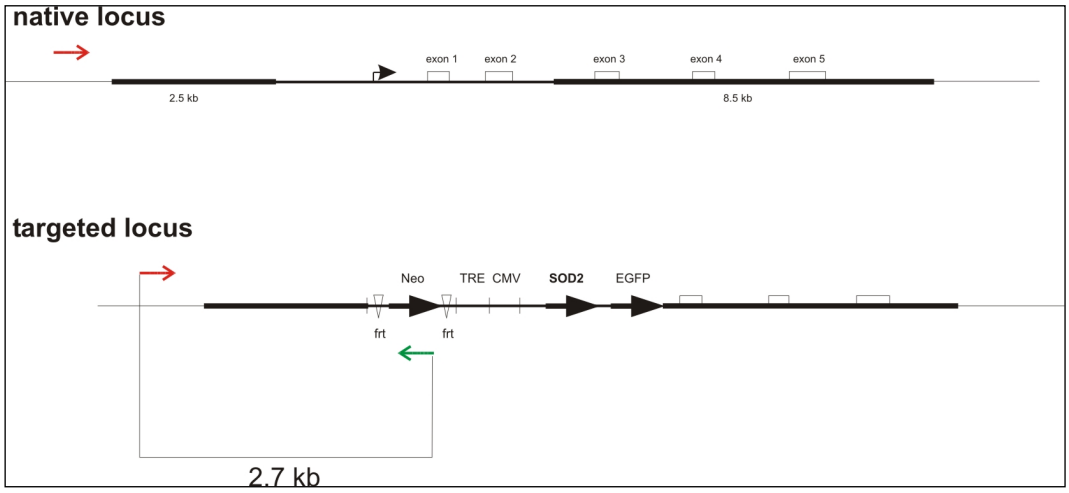

PCR:

10x Taq buffer	1.5 µl
2mM dNTP's	1.5 µl
5x enhancer	3 µl
10µM 5'gt-for2	0.3 µl
10µM 5'gt-Neo	0.3 µl
DNA [1:10]	1 µl
Taq Pol [5U/µl]	0.15 µl
water	7.25 µl
total	15 µl

Profile: "touch-down"

95º C – 7 min.

95º C – 1 min.
65º, 63º, 61º, 59º, 57º, 55º C – 45 sec.
72º C – 3 min. 10 sec.
| 2 cycles each

95º C – 1 min.
53º C – 45 sec.
72º C – 5 min.
| 23 cycles

72º C – 10 min.

internal primers

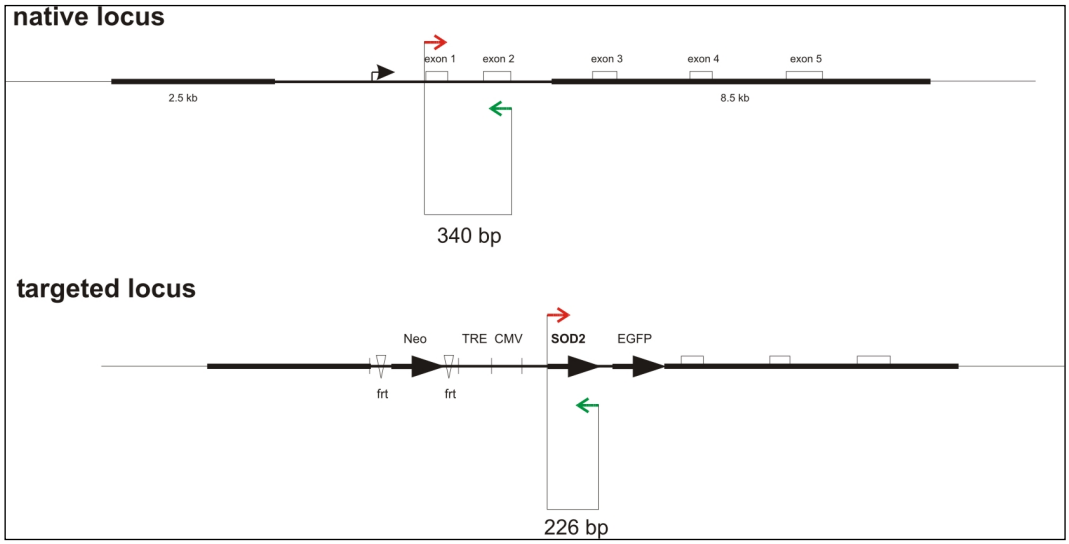

PCR

10x Taq buffer	1.5 µl
2mM dNTP's	1.5 µl
25mM $MgCl_2$	1.5 µl
5x enhancer	3 µl
10µM SOD orf E1	0.15 µl
10µM ex2-rev	0.15 µl
DNA [1:10]	1 µl
Taq Pol [5U/µl]	0.15 µl
water	6.05 µl
total	15 µl

Profile:

95º C – 7 min.

95º C – 45 sec.
65º C – 20 sec.
72º C – 30 sec.
| 40 cycles

72º C – 10 min.

αMHC-tTA locus

Primers detect tetracycline receptor sequence and do not discriminate between homozygous and heterozygous mice (370 bp product).

PCR

10x Taq buffer	1.5 µl
2mM dNTP's	1.5 µl
25mM $MgCl_2$	1.5 µl
5x enhancer	3 µl
10µM tTA2-for	0.15 µl
10µM tTA2-rev	0.15 µl
DNA [1:10]	1 µl
Taq Pol [5U/µl]	0.15 µl
water	6.05 µl
total	15 µl

Profile:

95º C – 7 min.

95º C – 40 sec.
55º C – 30 sec.
72º C – 40 sec.
} 40 cycles

72º C – 10 min.

ROSA-rtTA locus

Combination of three primers allows to discriminate between wild type (522 bp), heterozygous and homozygous (873 bp) animals.

PCR

10x Taq buffer	1.5 µl
2mM dNTP's	1.5 µl
5x enhancer	3 µl
10µM ROSA1	0.3 µl
10µM ROSA2	0.3 µl
10µM ROSA7	0.3 µl
DNA [1:10]	1 µl
Taq Pol [5U/µl]	0.15 µl
water	6.95 µl
total	15 µl

Profile:

95º C – 7 min.

95º C – 45sec.
55º C – 30 sec.
72º C – 40 sec.
} 40 cycles

72º C – 10 min.

2.2.6.3 Southern blot hybridization

An external probe, which hybridized to sequences localized outside targeted area (in 3' region), was used in Southern blot hybridization to screen for ES clones with correctly targeted locus. This probe was also used to corroborate the genotype of homozygous mice. The template for probe synthesis was produced in PCR reaction with MnSOD cosmid DNA as a template:

PCR

10x Taq buffer	1.5 µl
2mM dNTP's	1.5 µl
5x enhancer	3 µl
10µM 3'probeI-for	0.15 µl
10µM 3'probeI-rev	0.15 µl
DNA [1 ng/µl]	1 µl
Taq Pol [5U/µl]	0.15 µl
water	7.55 µl
total	15 µl

Profile:

95º C – 5 min.

95º C – 30sec.
50º C – 20 sec.
72º C – 30 sec.
} 40 cycles

72º C – 10 min.

Product of this reaction (290 bp) was gel purified and used as a template for probe synthesis by primer extension.

Genomic DNA was digested with EcoRI restriction enzyme and separated on 0.7% agarose gel. Southern blot hybridization was performed according to standard protocol (Sambrook et al., 1989). Signals from two bands were expected : 24 kb – for wild type, 12 kb – for targeted MnSOD locus.

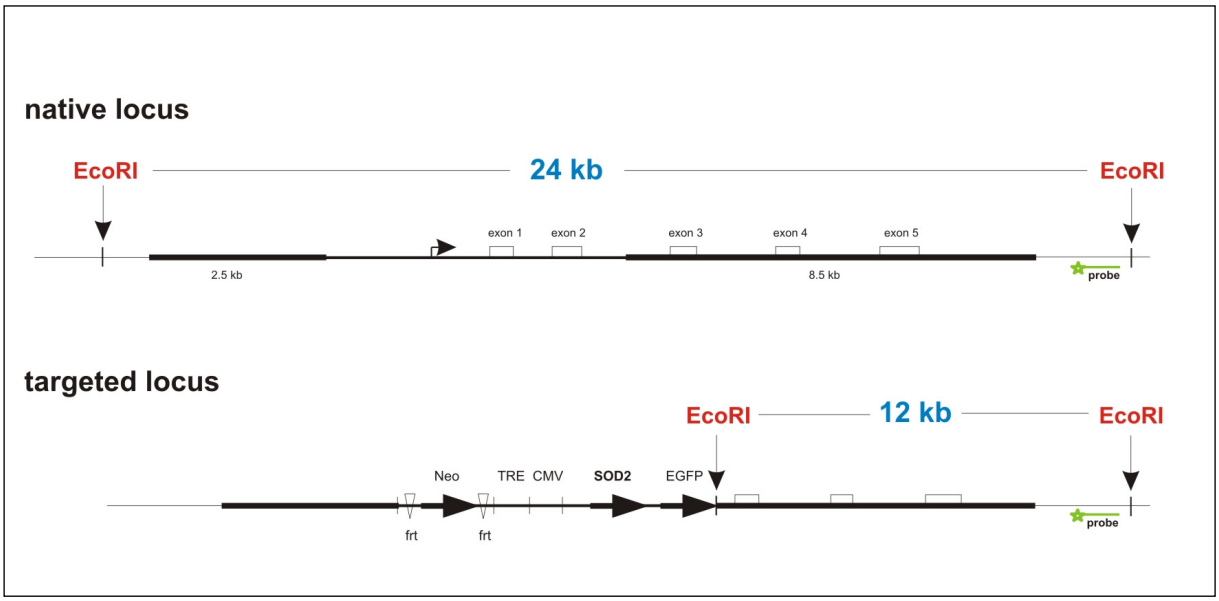

2.2.7 Tissue sections

2.2.7.1 Paraffin embedding and sectioning

After excision organs were thoroughly washed in ice-cold PBS and fixed in 4% PFA in PBS overnight. Then dehydration was performed as follows: 1 hour in 25% EtOH, 1 hour in 50% EtOH, 1 hour in 75% EtOH, 1 hour in 96% EtOH, then 100% EtOH two times 10 minutes followed by overnight incubation in 100% EtOH at -20° C. On the next day organs were soaked in EtOH/xylol (1:1) for 1 hour, followed by two 1 hour washes in xylol, 2 hour wash in xylol/paraffin (1:1) at 60° C and overnight incubation in xylol/paraffin (1:1) at room temperature. The following day tissues were incubated in xylol/paraffin (1:1) at 60° C for 1 hour and then washed two times (1 hour incubations) with paraffin at 60° C. Finally, tissues were embedded in paraffin. Tissue sections (7-15 μm thick) were cut from paraffin-embedded blocks on Leica microtome and mounted from warm water (40°C) onto adhesive microscope slides (prepared with Vectabond). Sections were allowed to dry on heating block (40° C) for 1-4 hours and then stored at room temperature.

2.2.7.2 Cryosectioning

Immediately after excision and washing in ice-cold PBS organs were embedded in Polyfreeze™ Tissue freezing medium™. Sections (8-40 μm thick) were cut with Leica cryotome and immediately mounted on adhesive microscope slides. Then sections were briefly fixed (15 minutes) in 4% PFA in PBS, washed in PBS and subjected to SA-β-Gal staining.

2.2.8 In situ hybridization

2.2.8.1 Probe synthesis

Riboprobe was synthesized in the following reaction mix:

1 μg	linearised plasmid
4 μl	5× transcription buffer
2 μl	DTT [0.1 M]
2 μl	Dig-Mix
1 μl	RNA polymerase (T3,T7 or Sp6)
1 μl	RNasin [40 U/μl]
to 20 μl	water

Reaction was incubated at 37º C for 2 hours. Next DNA template was digested with DNase I for 30 min. at 37º C and inactivated at 65º C for 15 min. The probe was ethanol precipitated and redissolved in water supplemented with RNasin. Quality of cRNA was checked on 1% agarose gel.

2.2.8.2 In situ hybridization

The procedure involved preparation of slides for hybridization, hybrydization, posthybridization wash and staining. Preparation of slides for hybridization consisted of the following steps performed at room temperature:

99.8% Ethanol	2 min.
99.8% Ethanol	2 min.
96% Ethanol	1 min.
70% Ethanol	1 min.
50% Ethanol	1 min.
30% Ethanol	1 min.
PBS	5 min.
4% PFA	15 min.
PBS	5 min.
Proteinase K (10µg/ml)	5 min.
Glycine (2mg/ml)	10 min.
PBS	5 min.
4% PFA	15 min.
Acetic Anhydrate/0.25% TEA/H_2O	10 min.
2x PBS	5 min.
Hybridization Buffer	15 min. at 65º C
Hybridization	overnight at 65º C

Hybridization was performed overnight at 65º C in hybridization buffer containing 1-5 µl of synthesized riboprobe per 1 ml. Then slides were washed 3 times in solution I at 65º C for 15 min. each, 3 times in solution III at 65º C for 15 min. each, 3 times in TBST at room temperature for 10 min. each and once in blocking solution at room temperature for 30 min. Then slides were incubated with anti-digoxygenin antibody (1:2000) in TBST at 4º C overnight. Next day antibody was washed away by washing 3 times in TBST 15 min. each and 3 times NTMT 10 min. each. Staining solution contained NBT/BCIP (4.5 µl and 3.5 µl respectively) in NTMT. Staining was performed in darkness until desired intensity was achieved.

2.2.9 Senescence Associated β-Galactosidase staining (SA-β-Gal)

Accelerated senescence in cells was achieved as follows. Cells were plated at density of 100 000 per well of a 6-well plate. Next day doxorubicin was added to medium to final concentration 200 – 800 nM. After two days incubation medium was replaced with fresh medium containing doxorubicin. On the third day cells were given fresh medium without doxorubicin and allowed to recover for the following 4 days with medium changes every second day.

SA-β-Gal staining was essentially performed as described in Dimri et al. (1995). Cells were washed 2 times with PBS and fixed in 5% formalin in PBS for 5 minutes. After fixation cells were washed with PBS 2 times. Then SA-β-Gal staining solution was applied: 40 mM sodium phosphate pH 6.0, 5 mM potassium ferrocyanide, 5 mM K-ferricyanide, 150 mM NaCl, 1 – 4 mg/ml X-gal. Cells were stained for 48 – 96 hours. The reaction was stopped with PBS.

2.2.10 Immunoprecipitation

Protein A sepharose was equilibrated by washing three times in washing buffer: 250 mM NaCl, 0.25% NP-40, 10 mM Tris·HCl pH 7.5, 5 mM EDTA. 25 μl of typical protein extract from cells was incubated with 10 μl of purified anti-myc 9e10 monoclonal antibody at room temperature for 20 minutes. Then 100 μl of washing buffer and 40 μl of equilibrated Protein A sepharose were added and immunoprecipitation was carried out at 4° C with rotation overnight. Next day sepharose beads were washed 4 times with 500 μl of washing buffer. Finally beads were mixed with 25 μl of SDS-loading buffer, denatured at 95° C for 5 minutes and loaded on SDS-gel.

2.2.11 In-situ anti-myc staining

Cells remaining on plates were washed 2 times with PBS and then fixed with 70% methanol/30% aceton mixture for 5 minutes at room temperature. Then cells were washed 3 times with PBS/ 0.1% Triton X-100. Next cells were incubated overnight at 4° C with 2 ml of anti-myc 9e10 monoclonal antibody diluted in 1 ml PBS/ 1% horse serum. After that cells were washed 4 times (5 minutes each) with PBS containing 0.1% Triton X-100 and 1% BSA. Then incubation with biotinylated secondary antibody (1:600 in PBS with 1% horse serum) was performed at room temperature for 60 minutes. Cells were washed 2 times (5 minutes

each) in PBS with 0.1% Triton X-100 and 1% BSA. Then again washed 2 times in PBS/0.1% Triton X-100 and two times in PBS. After washings cells were incubated with ABC solution (2 drops of 'label A' and 2 drops of 'label B' in 5 ml PBS prepared 30 minutes in advance, Vector Laboratories) for 30 minutes. Specimens were washed with PBS 4 times (5 minutes each) and incubated with staining solution: 2.5 mg/ml DAB in 10 ml 0.1 M Tris·HCl pH 7.2 with 5 µl 30% H_2O_2. Staining was stopped by replacing DAB solution with PBS.

2.2.12 Western blotting

Proteins were separated on standard denaturing SDS-PAGE gels. Stacking gel was 6%, separating gel – 12%. 15-50 µg of crude protein extract was loaded per well. Upon completion of electrophoresis proteins were transferred onto nitrocellulose membrane by semi-dry electroblotting (Fastblot B 43, Biometra). 4 pieces of Whatman 3MM paper and 1 piece of BioTrace® Nitrocellulose Membrane were cut to the size of the gel and together with the gel they were soaked for few minutes in electroblotting buffer. Two layers of 3MM paper were placed on the anode. On top of the pile a nylon membrane was placed. Gel was laid on the membrane and covered with 2 layers of 3MM paper. The whole stack was covered with the cathode and pressed. Electroblotting was run at a current of 5 mA per cm^2 of the blot for 45 minutes. The membrane was blocked in 1% non-fat dry milk in TBST solution for 1-2 hours at room temperature. Next the membrane was incubated at 4° C overnight with anti-MnSOD rabbit polyclonal antibody diluted (1:10 000) in blocking buffer. Three 5 minutes' washings in TBST preceded 1 hour incubation (room temperature) with biotinylated secondary antibody (anti-rabbit IgG) diluted 1:600 in TBST with 1% horse serum. After 3 washings (5 minutes each) in TBST, the membrane was incubated with ABC solution (2 drops of 'label A' and 2 drops of 'label B' in 5 ml TBST prepared 30 minutes in advance, Vector Laboratories) for 30 minutes. After that, the membrane was washed three times with TBS buffer. Bound antibodies were detected with DAB (2.5 mg/ml) in 10 ml of 0.1 M Tris·HCl pH 7.2 with 5 µl 30% H_2O_2. Staining was stopped by thorough rinsing of the membrane in water.

2.2.13 Northern blotting

Procedure was performed essentially as described in Sambrook et al. (1989). 20 or 50 μg RNA was denatured in glyoxal mixture at 65° C for 10 minutes, chilled on ice, mixed with RNA gel loading buffer and separated in 1.2% agarose gel in 1× BPTE. Electrophoresis was run at 5V/cm of the gel. Then RNA was transferred onto a Biodyne® Nylon Membrane. The hybridization probe (approximately 700 bp) for detection of MnSOD mRNA was synthesized using the complete MnSOD cDNA as a template. cDNA was produced in standard PCR reaction with primers: SODorf/E1 and SODorf/P1. The probe was synthesized by a primer extension reaction. Signals from two bands were expected: 1 kb from native MnSOD mRNA and 3.45 kb from targeting construct mRNA.

Blot was stripped and reprobed with GAPDH probe to provide a control for even loading and integrity of RNA. Template for probe synthesis (primer extension) was made by standard PCR with primers: 5'GAPDH and 3'GAPDH. Signal from 1.25 kb band was expected.

2.2.14 Echocardiography

Blinded studies were done in mice, which were anesthetized with 1.5% isoflurane. Examination was performed with a 10MHz Toshiba PSK-70LT ultrasound probe during 10-20 min. sessions. During that time, both 2-D and M-mode echocardiography were repeated 3 times for each mouse at midpapillary level.

In the 2-D echocardiography endocardial borders were traced at the end of diastole and systole and thereby endsystolic area (ESA) and end-diastolic area (EDA) were determined. 2-D image acquisition was performed at 168 frames per second. Heart rate (HR) during each scanning was calculated as the mean value from three RR-distances during M-mode measurements. Left ventricle internal diameter in systole and diastole (LVIDS and LVIDD) was obtained from M-mode images. Left ventricle fractional area change (FAC) and fraction shortening (FS) were calculated according to the following formulas:

$$FAC\ [\%] = [(EDA - ESA)/EDA] \times 100$$

$$FS\ [\%] = [(LVIDD - LVIDS)/LVIDD] \times 100$$

Ejection fraction (EF) was calculated according to Teichholz equation:

$$LVEDV = [7.0/(2.4 + LVIDD)] \times LVIDD^3$$
$$LVESV = [7.0/(2.4 + LVIDS)] \times LVIDS^3$$

$$EF\ [\%] = [(LVEDV - LVESV)/LVEDV] \times 100$$

2.2.15 Statistics

Unless otherwise stated all data are means ± SD. Statistical analysis was performed using Statistica software (StatSoft). Student's t tests were used. Data were considered significant when $p<0.05$.

3 RESULTS

3.1 Generation of the expression construct pTRE2hyg/SOD2ex

Cloning of MnSOD cDNA, modifications of the coding sequence and functional analysis of the cloned gene were prerequisites for further work. Based on the pTRE2hyg vector the following expression construct was generated:

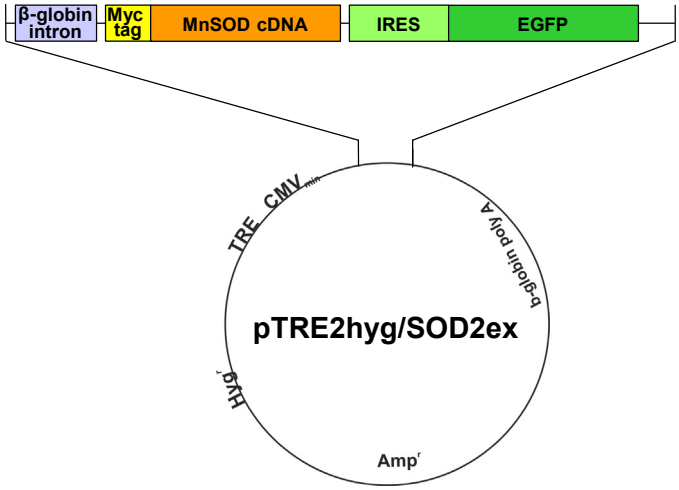

Fig. 2. Schematic representation of pTRE2hyg/SOD2ex expression construct. Abbreviations: CMV_{min} – minimal CMV promoter, TRE - tetracycline responsive element, Myc tag – myc protein epitope, IRES – internal ribosome entry site, EGFP – enhanced green fluorescence protein, Hyg^r – hygromycin resistance gene, Amp^r – ampicillin resistance gene.

The construct included a rabbit β-globin intron for better transcription of the cloned gene. MnSOD coding sequence was fused to myc epitope sequence to facilitate detection of the protein in *in situ* stainings and on Western blots. The internal ribosome entry site allows the translation machinery to synthesize both MnSOD and EGFP reporter molecule from a single bicistronic mRNA molecule. EGFP greatly facilitates the work with cells expressing this construct since the functional assay for MnSOD activity is laborious and time-consuming.

The construction of pTRE2hyg/SOD2ex expression plasmid allowed the following experimental approaches:

- to test the performance of tetracycline regulatory system in a cell culture model
- to study the effects of MnSOD overexpression in a cell culture environment
- was a source of proved and adjusted MnSOD expression cassette for further generation of targeting construct used in the generation of transgenic mice

The next chapters describe the experiments that were used to verify that all the elements of the prepared expression construct are fully functional.

3.1.1 The pTRE2hyg/SOD2ex construct can be regulated at the transcriptional level

C3H/10T1/2 mouse fibroblasts were transiently transfected with the pTRE2hyg/SOD2ex expression construct and either pTet-On or pTet-Off regulatory vector. After electroporation, cells were cultivated in the presence or absence of doxycycline to compare the induction level and background activity of the expression construct under the regulation mediated by pTet-On or pTet-Off.

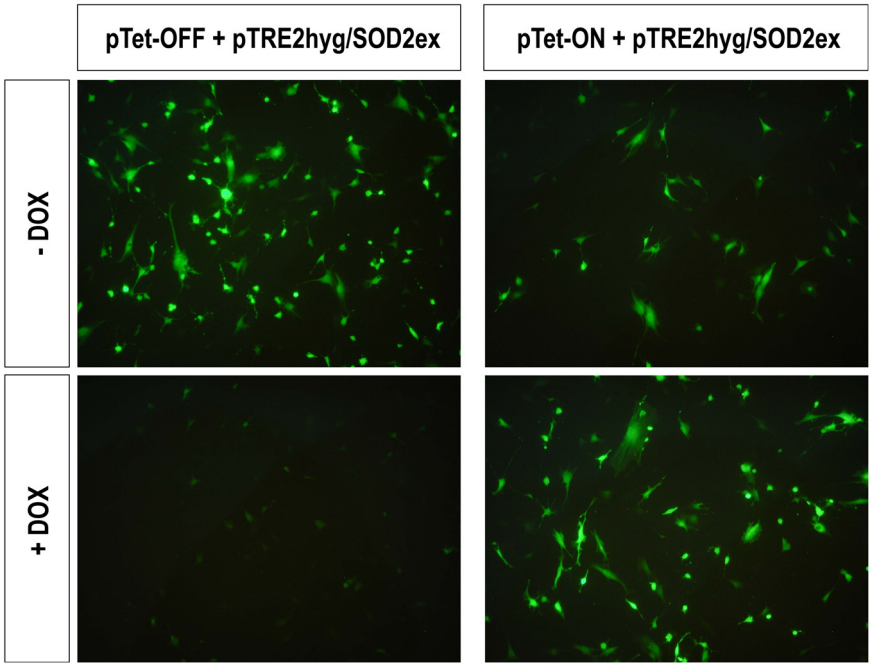

Fig. 3. Transient co-transfections of the pTRE2hyg/SOD2ex expression construct together with the regulatory pTet-On or pTet-Off plasmids. Cells were electroporated and plated at equal densities.

As shown on Fig. 3, pTRE2hyg/SOD2ex construct produced a functional EGFP reporter molecule. Co-transfections of the expression construct together with the pTet-On plasmid made it possible to switch on the expression by administration of doxycycline. However, even in the absence of the antibiotic a significant number of cells produced strong EGFP signals. On the other hand, co-transfections with the pTet-Off regulatory plasmid produced no signal or very weak green fluorescence in the presence of doxycycline, when expression from the pTRE2hyg/SOD2ex construct should be repressed. Cultivation of cells in the absence of

doxycycline allowed the tetracycline receptor (encoded by the pTet-Off) to induce quite strong transcription of the expression construct. Similar results were obtained in four independent experiments as well as in the Phoenix cell line transfected using the calcium phosphate method (data not shown).

3.1.2 The pTRE2hyg/SOD2ex construct produces functional MnSOD

To test whether translation of the expression cassette produces tagged MnSOD protein of the expected size C3H/10T1/2 and Phoenix cells were transiently transfected with the pTRE2hyg/SOD2ex construct and the pTet-Off plasmid. Cells were cultured in the absence of doxycycline to induce MnSOD overexpression. Proteins were isolated from these cells and the presence of recombinant MnSOD molecule was tested with four different methods.

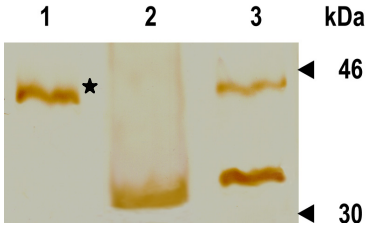

Fig. 4. Western blot of immunoprecipitated protein extracts from transiently transfected C3H/10T1/2 cells. Anti-myc monoclonal 9e10 antibody was used to detect tagged MnSOD protein. 1 – protein extract from non-transfected C3H/10T1/2 cells, immunoprecipitated with 9e10 antibody; 2 – crude protein extract from C3H/10T1/2 cells transiently transfected with the pTRE2hyg/SOD2ex construct and pTet-Off plasmid, not immunoprecipitated; 3 – protein extract as in lane 2 but after immunoprecipitation. An unspecific band is marked with an asterisk. Positions of the protein ladder bands are shown.

Western blotting of immunoprecipitated protein extract revealed a protein of approximately 30 kDa, which most probably corresponds to the recombinant MnSOD monomer of the predicted mass of 34 kDa (24 kDa MnSOD monomer plus 10 kDa myc epitope). Unspecific bands of approximately 46 kDa were visible in all cell extracts which were subjected to immunoprecipitation. Fortunately, they did not interfere with the expected product in transfected cells (Fig. 4).

The unspecific band visualized on Western blot suggested that cross-reaction of the myc antibody with cellular proteins might limit the use of this construct for the *in situ* detection of recombinant MnSOD. To test this, *in situ* stainings with 9e10 antibody were performed.

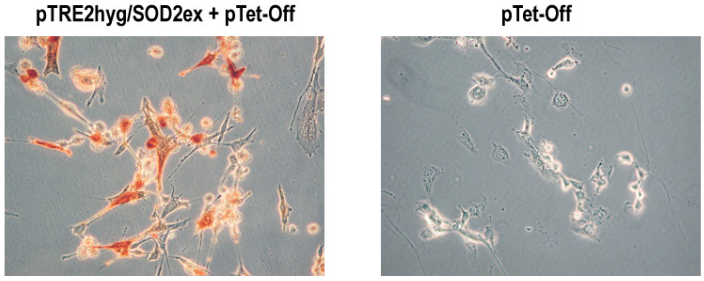

Fig. 5. Expression of recombinant tagged MnSOD in transiently transfected C3H/10T1/2 cells as detected with anti-myc 9e10 antibody. Right panel shows mock transfected cells to prove the specificity of the antibody.

In situ immunostaining for myc epitope shows a strong almost ubiquitous signal in the majority of cells. The lack of signal in some cells is due to transfection efficiency which is below 100%. Cells transfected with pTet-Off plasmid alone served as a control. Results of this staining indicate that 9e10 antibody can be used for *in situ* detection of recombinant MnSOD with no or very low background (Fig. 5).

Since the protein of the expected size is effectively synthesized, determination of its enzymatic activity was the last and most important assay to prove functionality of the expression construct.

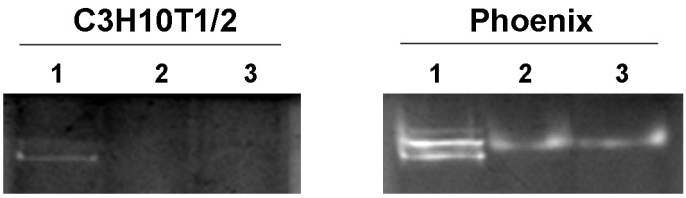

Fig. 6. SOD activity gels showing mitochondrial MnSOD. Protein extracts from transiently transfected cells were loaded at 100 μg per lane. Cytosolic SOD was inhibited with KCN. In native gels proteins migrate not according to their molecular weight. Therefore recombinant MnSOD migrates almost at the same speed as native. For both C3H/10T1/2 and Phoenix cells numbers indicate as follows: 1 – co-transfection of pTRE2hyg/SOD2ex expression construct and pTet-Off regulatory plasmid in 1:1 ratio, 2 – mock transfection (pTet-Off), 3 – non-transfected cells.

The pTRE2hyg/SOD2ex expression construct produced a functional MnSOD protein which was capable of catalyzing the dismutation reaction. Fibroblast cells had a comparatively low MnSOD activity level, hence only transfected cells showed a band corresponding to MnSOD. Phoenix cells had an intrinsically higher MnSOD activity, however, in cells transfected with pTRE2hyg/SOD2ex the band was much stronger. Mock-transfected and non-transfected cells had equal MnSOD activity in both cell lines indicating that the signal in pTRE2hyg/SOD2ex-transfected cells was due to overexpression of active MnSOD from the generated construct (Fig. 6).

	C3H/10T1/2			Phoenix		
	1	2	3	1	2	3
total SOD [U/min/mg protein]	21.51	20.73	22.07	61.67	52.40	44.04
MnSOD [U/min/mg protein]	**6.80**	**5.34**	**4.90**	**26.75**	**15.66**	**13.47**
CuZnSOD [U/min/mg protein]	14.71	15.39	17.17	34.92	36.74	30.57
CAT [μmole/min/mg protein]	14.25	14.37	14.30	7.14	7.06	6.19

Table 2. Activities of mitochondrial (MnSOD) and cytosolic (CuZnSOD) dismutases and catalase in transiently transfected cells. SODs activities were determined by inhibiton of cytochrome c reduction method. Catalase (CAT) was determined by monitoring of H_2O_2 decomposition at 240 nm in the presence of cellular lysates. For both C3H/10T1/2 and Phoenix cells numbers indicate as follows: 1 – co-transfection with pTRE2hyg/SOD2ex expression construct and pTet-Off regulatory plasmid in 1:1 ratio, 2 – mock transfection (pTet-Off), 3 – non-transfected cells.

As mentioned previously, CuZnSOD and MnSOD activities can be precisely determined using the inhibiton of cytochrome c reduction method (Table 2). Transient co-transfections using the pTRE2hyg/SOD2ex expression construct and the pTet-Off plasmid led to a 40% increase in MnSOD activity in C3H/10T1/2 cells and a two-fold increase in Phoenix cells as compared to non-transfected cells. The higher induction in Phoenix cells reflected the efficiency of transfections which were approximately 50% for the latter and 21% for fibroblasts. Interestingly, the overexpression of MnSOD had no significant effect on the activities of other antioxidant enzymes (CuZnSOD and CAT) . A minor upregulation of cytosolic SOD in Phoenix cells was due to transfection method (calcium phosphate). A mock calcium phosphate transfection induced CuZnSOD activity by 20-35% in Phoenix cells and approximately 60% in C3H/10T1/2 cells but had no significant influence on MnSOD and CAT activities (data not shown).

3.2 Regulated MnSOD overexpression in murine fibroblasts

Since transient transfections always generate a mixture of wild type and MnSOD overexpressing cells, which are characterized by a decrease of the strength of the expression over time and since the regulation by doxycycline is often inaccurate, a double-stable cell line based on C3H/10T1/2 murine fibroblasts was established. Double-stable lines were generated by consecutive stable transfections of the regulatory plasmid pTet-Off and of the pZK/SOD expression construct (slightly modified version of the pTRE2hyg/SOD2ex). 30 neomycin and hygromycin resistant clones were obtained. All clones were grown in duplicates: in the presence and absence of doxycycline to check the induction level and the background activity of the expression construct. Based on a rough estimation of EGFP fluorescence under the microscope four clones were selected for a more detailed analysis.

3.2.1 Efficiency of the tetracycline-regulatory system

Four different double-stable clones were cultured for a period of several weeks and EGFP fluorescence was monitored occasionally. Microscopic results are presented in Fig. 7. Quantification of the induction level and background activity of the expression construct are shown in Table 3.

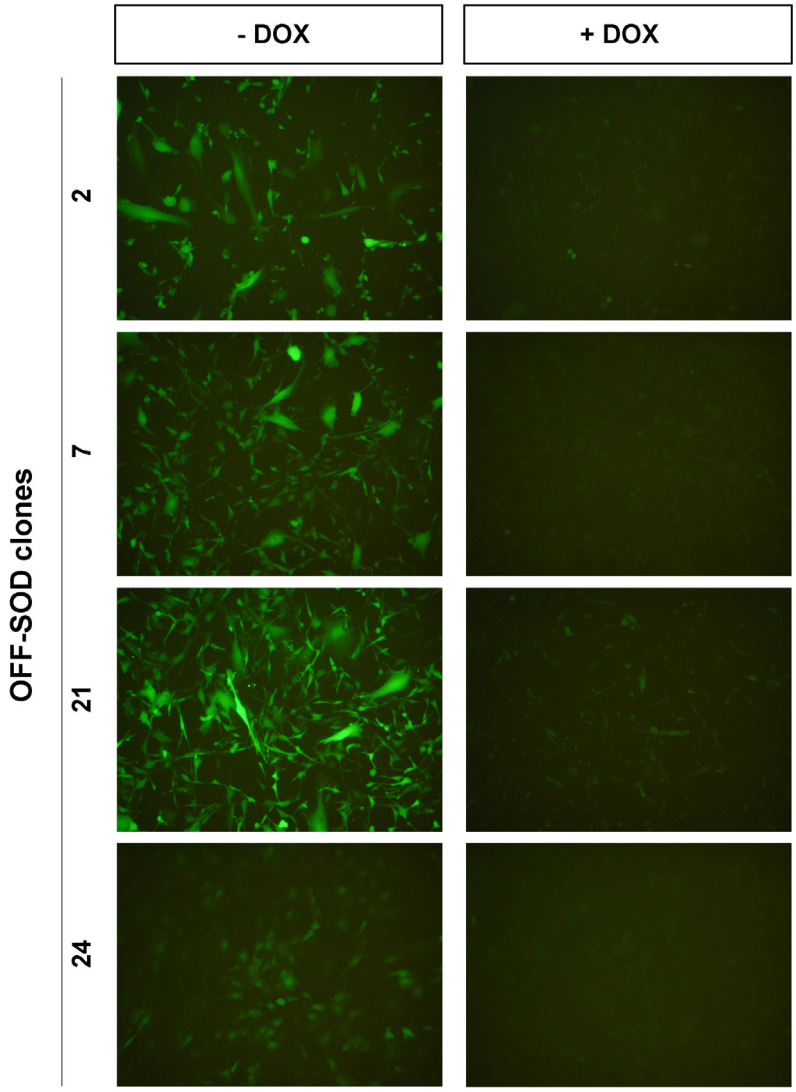

Fig. 7. Four different stable OFF-SOD clones showed diverse EGFP fluorescence level. Photographs do not allow to estimate precisely the background activity level in the switched off state (+ Dox), however induction level in the state on (– Dox) clearly indicates clone 21 as the most tightly regulated clone.

OFF-SOD clone	induction (RFU/mg protein)	background signal (RFU/mg protein)
2	6.5	1.8
7	4.8	2.8
21	6.0	3.0
24	2.4	3.0

Table 3. EGFP fluorescence measured spectrophotometrically in protein extracts from stable OFF-SOD clones. Relative Fluorescence values (RFU) were normalized to the protein content. Induction was calculated as a ratio of EGFP fluorescence in cells in the state "on" to cells in "off" state. Background signal is the ratio of normalized fluorescence values in switched off state to the fluorescence of parental cell line without expression construct. The lower background signal and higher induction the better regulation by Tet-Off system.

Originally, OFF-SOD 2 clone was chosen as the best based on the induction level and background activity. However, longer follow up of the four clones showed substantial decrease in signal intensity of the clone number 2. Finally, clone OFF-SOD 21 showed the most stable and consistent expression of the introduced construct and was used for further studies.

3.2.2 MnSOD overexpression has no effect on activities of main anti-oxidant enzymes

In order to analyze whether MnSOD overexpression induces activity of other antioxidant enzymes OFF-SOD 21 cells were cultured under standard conditions in the presence or absence of doxycycline. C3H/10T1/2 cells served as additional control. Proteins were isolated and activities of antioxidant enzymes were determined in the extracts.

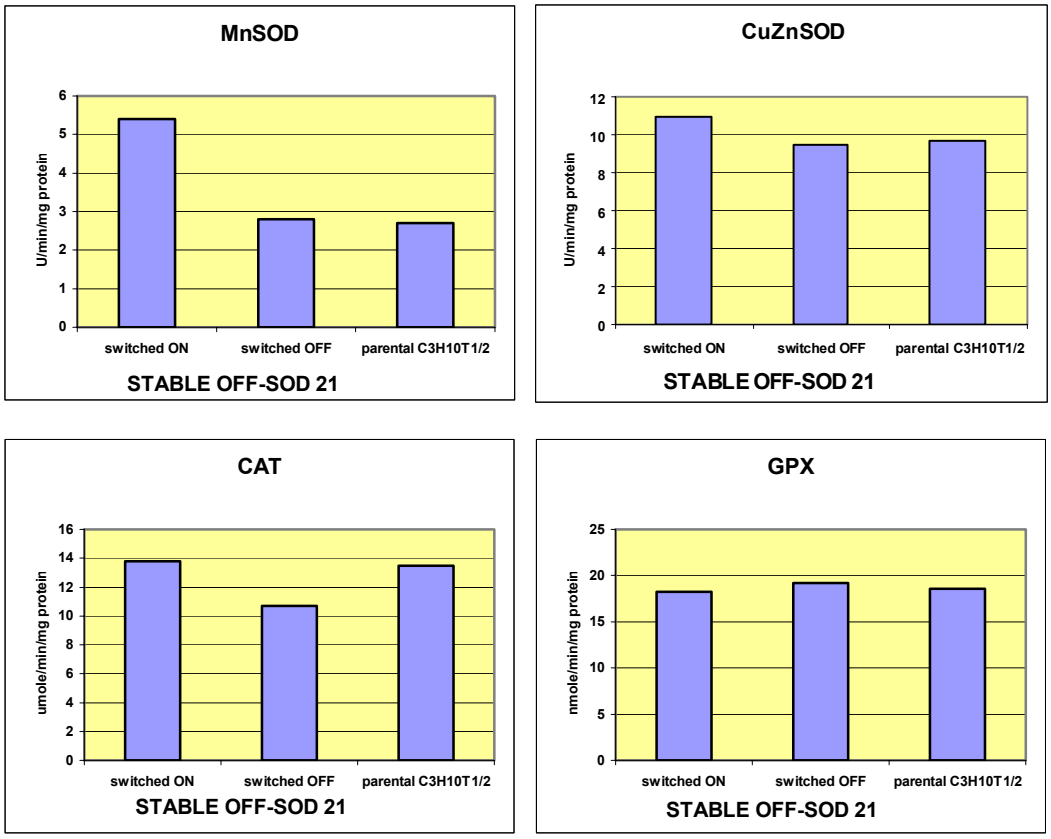

Cell line		Total SOD (U/min/mg protein)	MnSOD (U/min/mg protein)	CuZnSOD (U/min/mg protein)	CAT (μmoles/min /mg protein)	GPX (nmoles/min/ mg protein)
OFF-SOD 21	switched ON	16.4	**5.4**	10.9	13.8	18.2
	switched OFF	12.4	**2.8**	9.5	10.7	19.2
parental C3H/10T1/2		12.4	**2.7**	9.7	13.5	18.6

Fig. 8. Activities of mitochondrial (MnSOD), cytosolic (CuZnSOD) superoxide dismutases, catalase (CAT) and glutathione peroxidase (GPX) in double-stable cell line OFF-SOD 21 cultured in the presence of doxycycline (switched off state) and without (switched on). As a reference parental C3H/10T1/2 cells were used.

Expression of MnSOD was efficiently regulated in the double-stable cell line (OFF-SOD 21) by doxycycline. Administration of the drug suppressed the pTRE2hyg/SOD2ex expression construct in OFF-SOD 21 to MnSOD activity level of the parental C3H/10T1/2 cell line. Cultivation of the stable cell line without doxycycline resulted in a two-fold increase in mitochondrial SOD activity. OFF-SOD 21 cells both in the state “on” and “off” showed no alterations in activities of other enzymes of the antioxidative defense (Fig. 8), which was in agreement with previous observations from transient transfections. The growth rate of this cell line was only slightly slower as compared to the parental cell line.

To confirm that increased MnSOD activity in OFF-SOD 21 cell line was due to expression of the introduced recombinant gene, Western blot hybridization with anti-MnSOD antibody was performed.

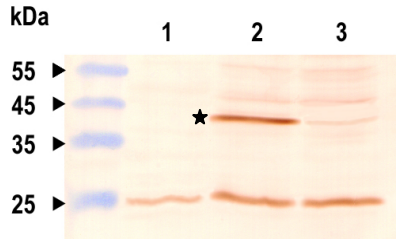

Fig. 9. Western blot hybridization of protein extracts from C3H/10T1/2 – lane 1; OFF-SOD 21 in the state "on" – lane 2; OFF-SOD 21 in the state "off" – lane 3. The asterisk marks recombinant MnSOD protein. 50 μg of protein extract was run in each lane. Anti-MnSOD antibody was used to detect both native and recombinant MnSOD.

Recombinant MnSOD, of molecular mass 34 kDa, was evidently upregulated in OFF-SOD 21 cell line after stimulation (doxycycline withdrawal; Fig. 9, lane 2). Suppression with doxycycline was significant, though not complete (Fig. 9, lane 3). The intensity of native MnSOD (24 kDa) was slightly stronger in both, stimulated and suppressed OFF-SOD 21 cells, as compared to the parental C3H/10T1/2 cell line.

3.2.3 MnSOD overexpression confers resistance to hyperoxia

MnSOD overexpression should support cells to survive oxidative stress. To verify this assumption stable OFF-SOD 21 cells were plated on 4 plates at identical densities. Two of them received doxycycline while the other two were grown without the drug to induce MnSOD overexpression. One plate from each group was placed under hyperoxic conditions (85% oxygen) in a humidified cell culture incubator. The other two plates were grown under standard conditions. After four days of cultivation cells were photographed (Fig. 10).

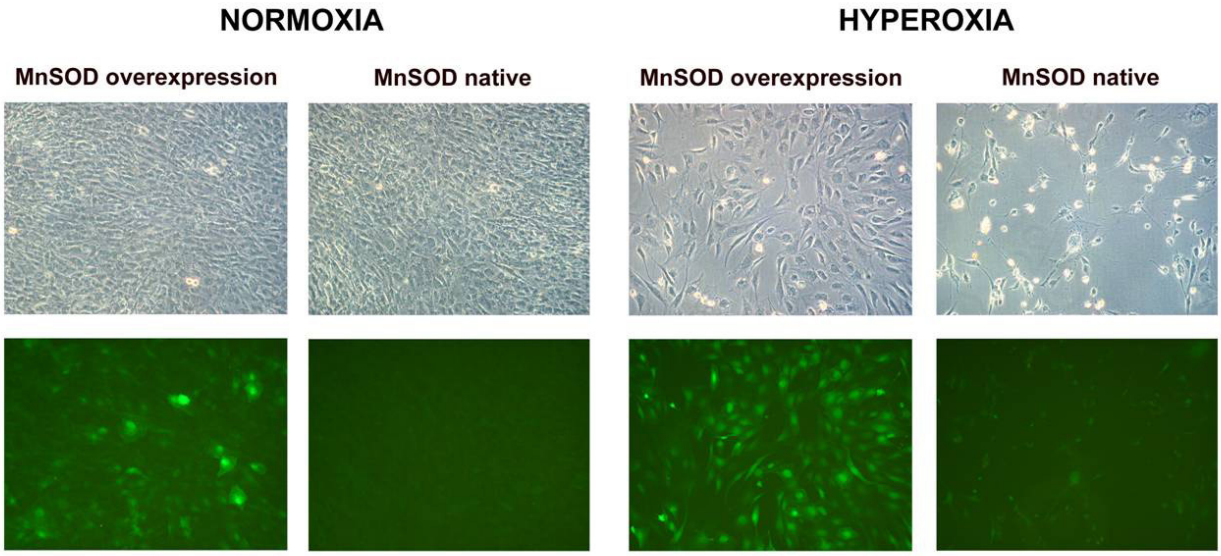

Fig. 10. Resistance of MnSOD overexpressing cells to hyperoxia.

Under hyperoxic conditions only cells with MnSOD overexpression survived. Most cells with native MnSOD level died starting from 3rd day of culture in high oxygen. Growth of cells was slowed as compared to the same cells grown in standard conditions. Cultivation of cells in 85% oxygen for longer periods of time led, eventually, to massive cell death irrespective of their MnSOD level.

3.2.4 Apoptosis resistance of MnSOD overexpressing cells

To test the influence of MnSOD overexpression on apoptosis, OFF-SOD 21 stable cell line was grown under standard conditions in the presence and absence of doxycycline and subjected to 6-hours treatment with 1 mM hydrogen peroxide to induce programmed cell death. Following that, apoptosis-positive cells were visualized with the TUNEL reaction.

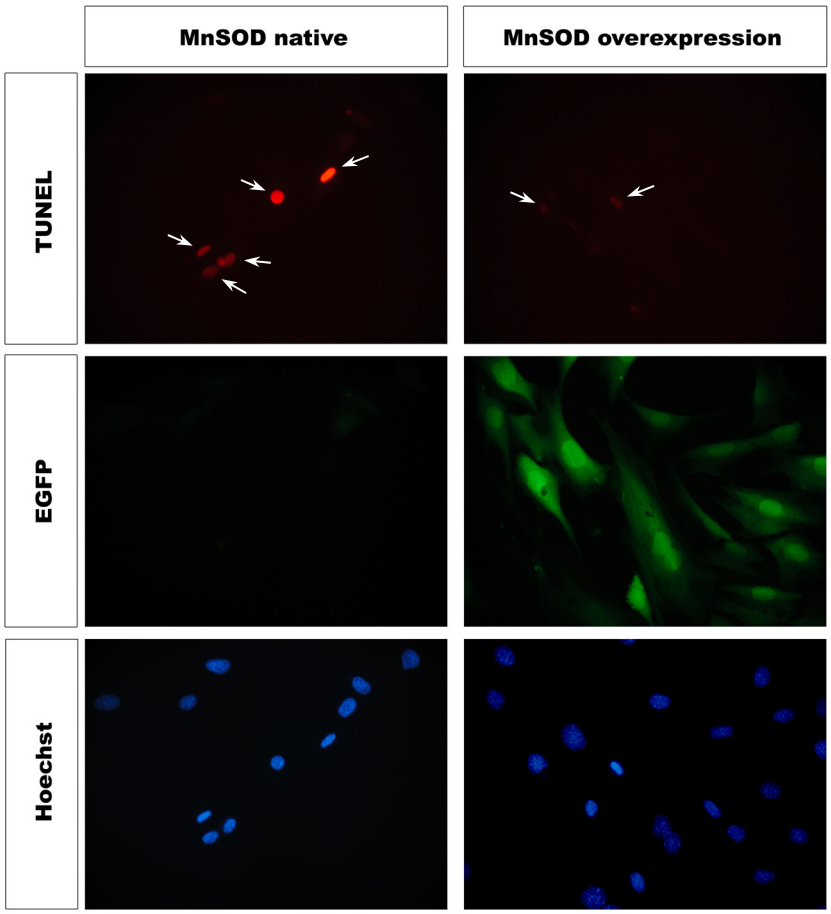

Fig. 11. Apoptosis in H_2O_2 treated OFF-SOD 21 cells. TUNEL-positive cells appear in red, MnSOD overexpressing cells are green. Hoechst stainings of nuclei are shown to visualize EGFP-negative cells. White arrows indicate TUNEL-positive apoptotic cells. Representative images are shown. TUNEL reaction was performed according to manufacturer's protocol (Roche).

The C3H/10T1/2 parental cell line as well as the OFF-SOD 21 double-stable cell line were comparatively resistant to H_2O_2-induced apoptosis. Only 30% of cells with native MnSOD level (OFF-SOD 21 in the presence of Dox) stained positively in the TUNEL reaction. On the other hand, very few MnSOD overexpressing cells (3%) entered apoptotis (Fig. 11).

To test whether MnSOD overexpression protects cells from cytotoxicity induced by doxorubicin, TUNEL assay was performed on OFF-SOD 21 cell line treated with this drug.

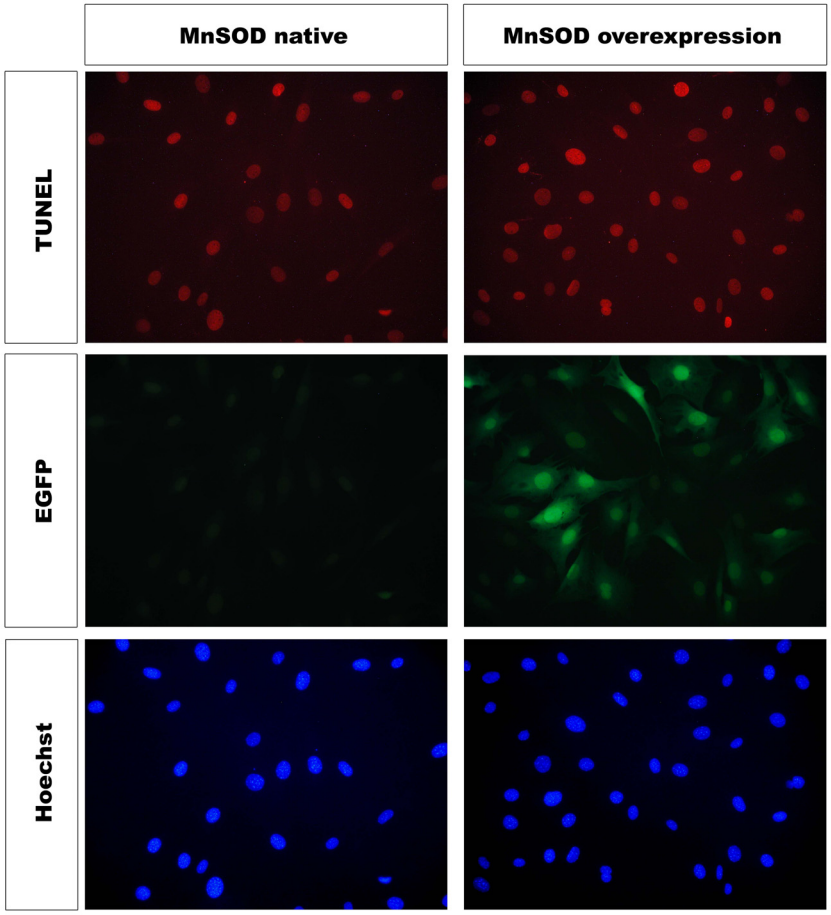

Fig. 12. Apoptosis induced by doxorubicin treatment in OFF-SOD 21 cell line. TUNEL-positive cells appear in red, MnSOD overexpressing cells are green. Hoechst stainings of nuclei are shown to visualize EGFP-negative cells. Representative images are shown. TUNEL reaction was performed according to manufacturer's protocol (Roche).

Contrary to H_2O_2-induced apoptosis, 48 hours incubation in the presence of 400 nM doxorubicin induced cell death in almost all cells. However, slightly stronger TUNEL signal could be observed in fibroblasts overexpressing MnSOD as compared to cells with native level of the enzyme (Fig. 12). No apoptosis was observed in untreated cells.

3.3 Primary mouse embryonic fibroblasts with MnSOD deficiency

To study the effects of MnSOD insufficiency on cellular processes a cell line from $MnSOD^{-/-}$ mice was generated. As SOD/TRE transgenic mice bearing pTG/TRE construct produced no viable homozygotic offspring indicating that the level of MnSOD in homozygotes does not reach the threshold which allows them to carry out key life processes. Three primary fibroblast cell lines were derived from 14 days old embryos: $MnSOD^{-/-}$ from

homozygous SOD/TRE embryos, MnSOD$^{+/-}$ from heterozygous and MnSOD$^{+/+}$ from wild type embryos.

The absence of MnSOD was proven by Western blotting.

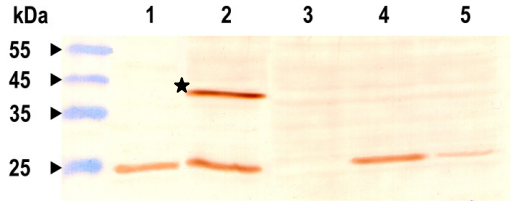

Fig. 13. Western blot hybridization of protein extracts from different cell lines. 1 – C3H/10T1/2; 2 – OFF-SOD 21 in the state 'on'; 3 – MnSOD$^{-/-}$ primary fibroblasts; 4 – MnSOD$^{+/+}$ primary fibroblasts; 5 – MnSOD$^{+/-}$ primary fibroblasts. The asterisk marks recombinant MnSOD which was introduced in the pTRE2hyg/SOD2ex construct to C3H/10T1/2 cells (giving rise to OFF-SOD 21 cell line) and in the pTG/TRE construct for SOD/TRE mice generation. 50 μg of total protein extract was run in each lane. Anti-MnSOD antibody was used to detect both native and recombinant MnSOD.

Though some background expression from the pTG/TRE construct in SOD/TRE mice was expected neither native nor recombinant MnSOD could be detected by Western blotting (Fig. 13, lane 3). This means that at least in fibroblasts from knock-in mice the pTG/TRE construct was silent in the absence of tetracycline receptor. This created an opportunity to study MnSOD deficient cells in an *in vitro* model. MnSOD$^{+/-}$ primary fibroblasts showed strongly reduced levels of MnSOD protein (Fig. 13, lane 5) due to expression from a single allele of the native MnSOD locus.

3.3.1 MnSOD deficient cells produce excessive ROS

To test the influence of oxygen concentration on free radicals' level in the three primary cell lines with different MnSOD level, cells were grown under standard conditions, in hypoxia (3% oxygen) and hyperoxia (85% oxygen). ROS-sensitive dye, carboxy-H_2DCFDA, was used to estimate the production of free radicals in MnSOD$^{-/-}$, MnSOD$^{+/-}$ and MnSOD$^{+/+}$ cells (Fig. 14 and 15).

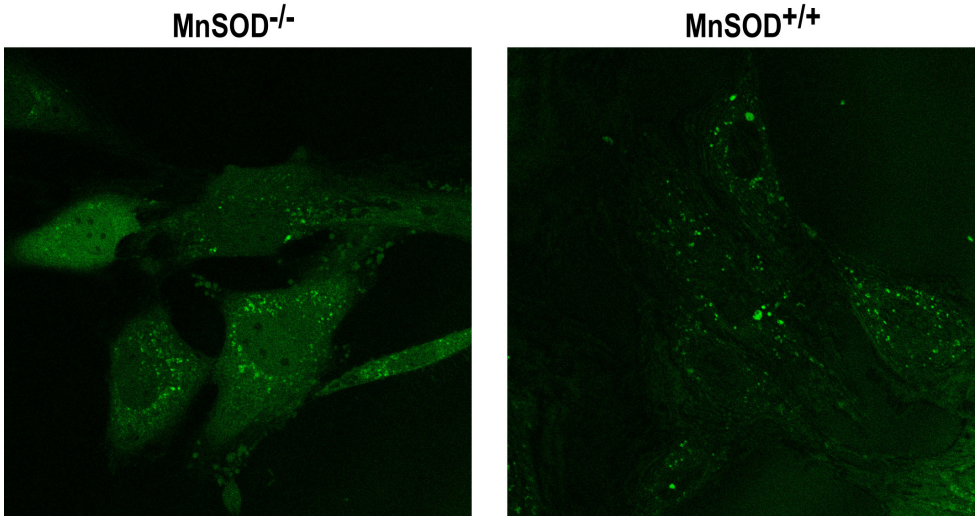

Fig. 14. Carboxy-H_2DCFDA staining of primary fibroblasts cultivated under hyperoxic conditions for 24 hours revealed elevated level of ROS in MnSOD deficient cells. MnSOD deficient ($MnSOD^{-/-}$) and wild type ($MnSOD^{+/+}$) cells were cultivated under hyperoxic conditions for 24 hours. Then the presence of ROS was revealed by staining with 5 μM carboxy-H_2DCFDA in HBS at 37°C for 30 minutes. After three washings with PBS cells were fixed in 5% formalin in PBS for 15 minutes and then observed under a Leica confocal microscope.

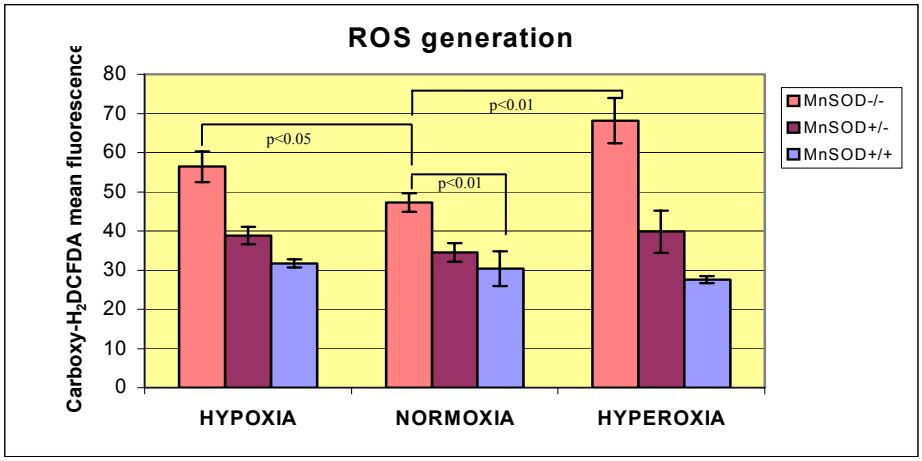

Fig. 15. Reactive oxygen species were produced excessively in MnSOD deficient cells under all conditions. $MnSOD^{+/-}$ cells had slightly elevated ROS level, however, this change did not reach statistical significance. Cells were cultivated in the stated conditions for 24 hours. They were collected in the middle of growth phase and stained with carboxy-H_2DCFDA. Cells were counted by FACS Scan in the continuous presence of carboxy-H_2DCFDA and PI to exclude dead cells. Values represent means, bars indicate SD, n = 3.

Wild type cells showed stable carboxy-H_2DCFDA fluorescence intensity across different cultivation conditions. This fact reflects adaptability of wild type cells to changing environmental conditions through induction of MnSOD. ROS level was increased in MnSOD deficient cells in normoxic conditions (by 50% as compared to wild type cells). Cultivation of cells in elevated oxygen led to a further increase in ROS in $MnSOD^{-/-}$ cells (by 40% as

compared to the same cells in normoxia, by 250% as compared to MnSOD$^{+/+}$ cells also subjected to hyperoxia). The same tendency could also be seen in MnSOD$^{+/-}$ cells, however changes were only minor and not significant. Unexpectedly, ROS level rose in MnSOD$^{-/-}$ cells also in hypoxic conditions. It was 20% higher as compared to the same cells grown under standard conditions and almost 80% when compared to wild type cells grown under hypoxia (Fig. 15).

3.3.2 MnSOD deficiency prevents senescence

Elevated ROS level in MnSOD$^{-/-}$ cells may suggest that these cells undergo accelerated senescence. To test this hypothesis cells after splitting were grown in standard conditions for few days without further passaging. Subsequently cells were subjected to senescence-associated β-galactosidase (SA-β-Gal) staining that identifies senescent cells in culture.

A

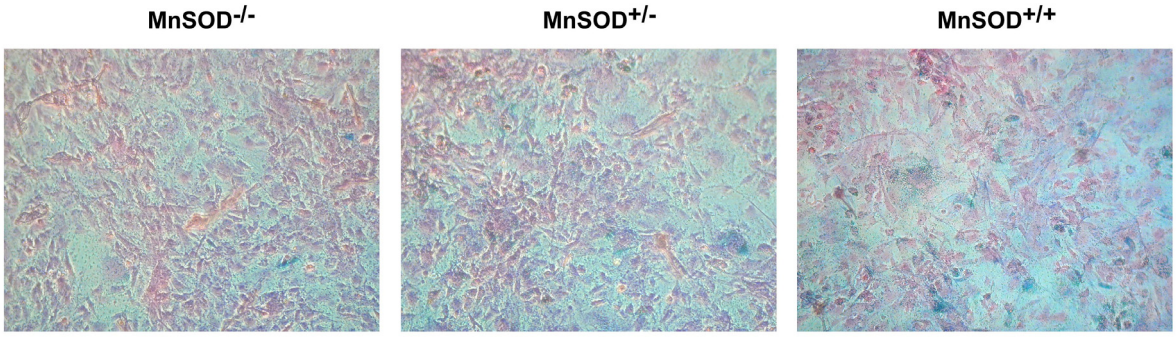

B

	*MnSOD$^{-/-}$	MnSOD$^{+/-}$	MnSOD$^{+/+}$
percent SA-β -Gal positive	**4.7** ±3.12	**23.6** ±7.99	**24.2** ±4.59

Fig. 16. A – Senescence-Associated β-Galactosidase (SA-β-Gal) staining of primary fibroblasts at passage 5. Cells were grown for 8 days without passaging. Then cells were subjected to SA-β-Gal staining. Senescent cells stain blue. Eosin was used for counterstaining. Representative photographs are shown. **B** – Cells were counted under the microscope. 6-7 different fields were selected randomly, 260-390 cells of each type were counted. Values are means ±SD. * – $p<0.01$ vs. MnSOD$^{+/+}$ and MnSOD$^{+/-}$.

MnSOD$^{+/-}$ and MnSOD$^{+/+}$ fibroblasts showed significant number of senescent cells while none or very weak staining was observed in MnSOD$^{-/-}$ cells. The difference was apparent at the first glance. Only a fraction of MnSOD$^{-/-}$ cells showed blue colour (5% of all) whereas

24% of both MnSOD$^{+/-}$ and MnSOD$^{+/+}$ cells were positive (Fig. 16). Similar results were obtained with cells cultured in low oxygen conditions (3%) as well as those treated with doxorubicin to accelerate senescence (data not shown).

3.3.3 Apoptosis is reduced in MnSOD deficient cells

Several studies have indicated that MnSOD overexpression prevents cells from apoptosis induced by variety of stimuli. To check whether MnSOD insufficiency has an effect on apoptosis pathway primary fibroblasts were challenged with hydrogen peroxide to induce apoptosis. Apoptotic cells were visualized with the TUNEL reaction.

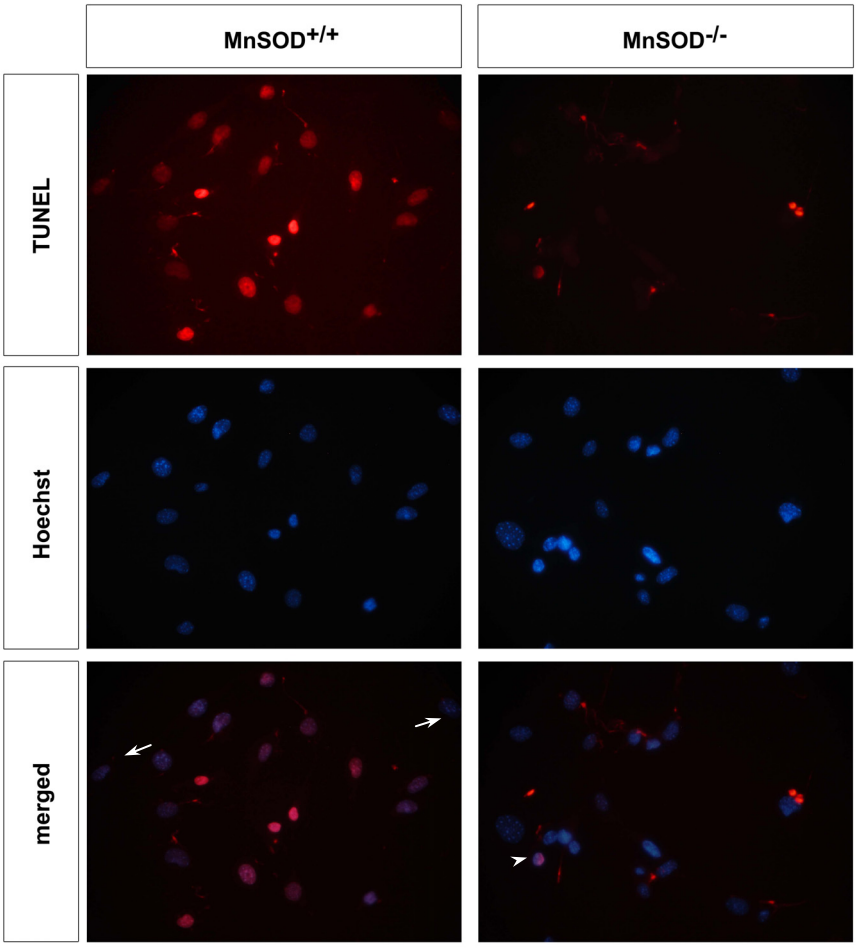

Fig. 17. H_2O_2 induced apoptosis in primary fibroblasts. Apoptotic cells appear red, nuclei in blue. White arrows indicate TUNEL-negative cells. Arrowheads mark singular MnSOD$^{-/-}$ apoptotic cells. Some background staining is visible that does not match stained nuclei. Representative images are shown. TUNEL reaction was performed according to manufacturer's protocol (Roche).

After 4 hours treatment with 1 mM hydrogen peroxide approximately 80% of MnSOD$^{+/+}$ cells underwent apoptosis. Both MnSOD deficient and MnSOD$^{+/-}$ cells appeared resistant to this treatment and showed very few TUNEL-positive cells (1-4%) (Fig. 17, Table 4). To test if p53 activity has an influence on H_2O_2-induced apoptosis, cells were subjected to the same procedure but pifithrin-α (p53 inhibitor) was added at 5 μM concentration to the medium. Interestingly, the inhibition of p53 did not affect the rate of apoptosis in wild type fibroblasts or in MnSOD deficient (data not shown).

The rate of apoptosis was also tested after doxorubicin treatment. This cytotoxic drug was applied to cells for 48 hours which were then assayed by the TUNEL reaction.

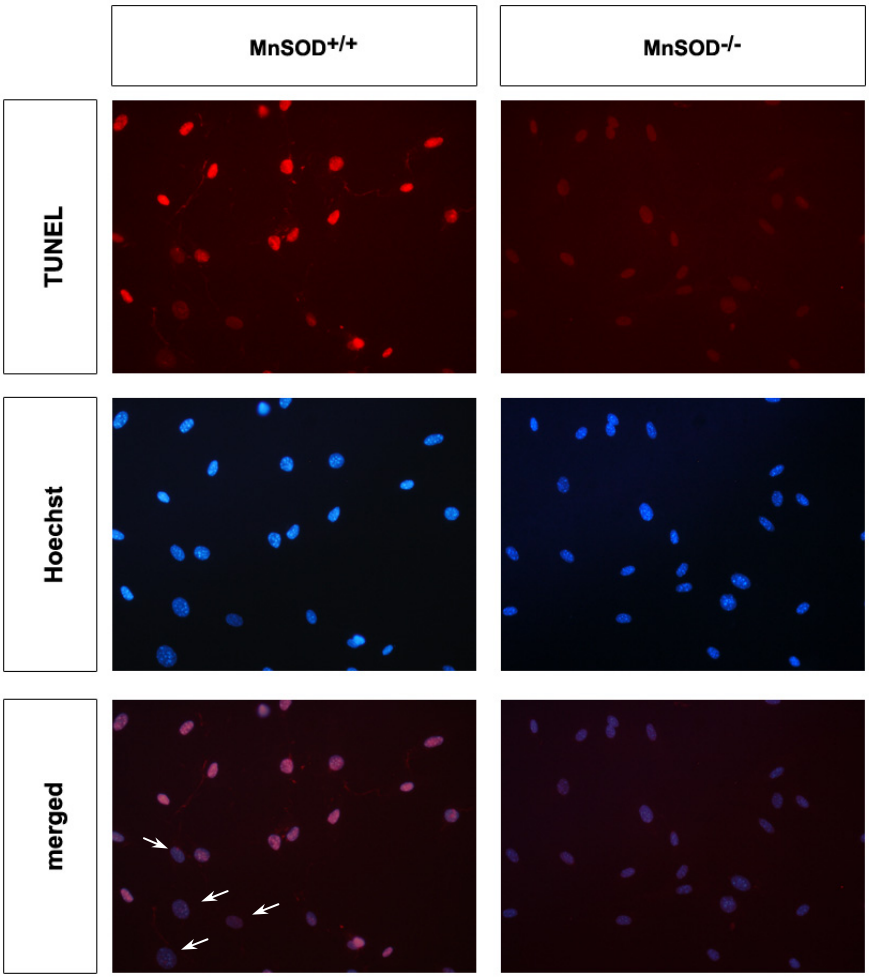

Fig. 18. Apoptosis in primary fibroblasts induced after treatment with doxorubicin. Apoptotic cells appear in red, nuclei in blue. White arrows indicate TUNEL-negative cells. Representative images are shown. TUNEL reaction was performed according to manufacturer's protocol (Roche).

After 48 h treatment with 400 nM doxorubicin almost 60% of MnSOD$^{+/+}$ cells underwent apoptosis while MnSOD$^{-/-}$ cells remained essentially TUNEL-negative with only 3.4% of

cells becoming positive (Fig. 18, Table 4). No significant rate of apoptosis was observed in untreated fibroblasts.

treatment	MnSOD$^{+/+}$	MnSOD$^{+/-}$	MnSOD$^{-/-}$
H_2O_2	***78.9** ±13.6	**1** ±1.92	**3.4** ±4.8
H_2O_2 + PFT-α	**72.5** ±17.9	n.d.	**4.5** ±3.9
Doxorubicin	***59.6** ±28.8	n.d.	**3.4** ±4.8

Table 4. Percentage of TUNEL positive cells following the indicated treatment. Cells were counted under the microscope. 4-11 different fields were selected randomly, 50-240 cells of each type were counted. Values are means ±SD. * – $p<0.01$ vs. MnSOD$^{+/-}$ and MnSOD$^{-/-}$; n.d. – not determined, PFT-α – pifithrin-α.

3.4 Generation of targeting constructs pTG/TRE and pTG/TRE tetR

The generation of transgenic mice required preparation of DNA constructs used to modify the native MnSOD locus in embryonic stem cells by means of homologous recombination.

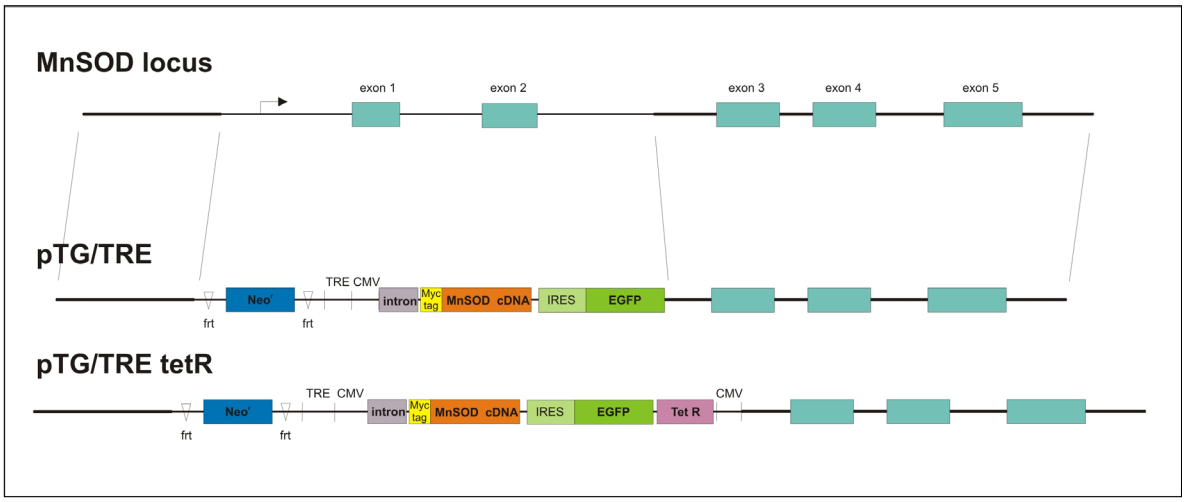

Fig. 19. Schematic representation of targeting constructs used in the generation of transgenic mice. The only difference between the two was that pTG/TRE tetR contained an additional regulatory cassette – tetracycline receptor coding sequence. Abbreviations: CMV – promoter of cytomegalovirus, EGFP – Enhanced Green Fluorescence Protein gene, frt – sequence recognized by Flp recombinase, IRES – Internal Ribosome Entry Site, Neo^r – neomycin resistance gene, Tet R – tetracycline receptor gene, TRE – Tetracycline Responsive Element.

Both constructs had flanking sequences isogenic with sequences of the MnSOD locus. The 3' flanking sequence contained exons 3 to 5 of the original gene in the unchanged genomic configuration. This fragment, genomic BamHI, was 8.75 kb long. The 5' recombination arm comprised the upstream region of the MnSOD gene promoter (lacking essential regulatory sequences), a HindIII fragment, which was 2.5 kb long. All other components were as described in the pTRE2hyg/SOD2ex expression plasmid construction (Fig. 2) except that neomycin resistance gene cassette was added to enable selection of recombinant ES cells. In the pTG/TRE tetR construct, a tetracycline receptor coding sequence was included to obtain regulated expression in mice without the necessity to cross the mice with another strain that contribute the Tet-regulator (Fig. 19).

3.5 MnSOD knock-in mice generation

3.5.1 SOD/TRE mice

The pTG/TRE targeting construct was used to generate SOD/TRE mice. First, the targeting construct was introduced into mouse embryonic stem cells and 25 clones out of 268 analyzed neomycin-resistant ES clones were isolated which carried the correctly integrated pTG/TRE. Recombinant ES cells were used for blastocyst injections to obtain chimeric mice from which, after backcrossing with C57BL/6, the SOD/TRE transgenic strain was established. The desired integration event in ES cells as well as the genotype of the mice were determined by PCR and Southern. Representative genotyping results are shown in Fig. 20.

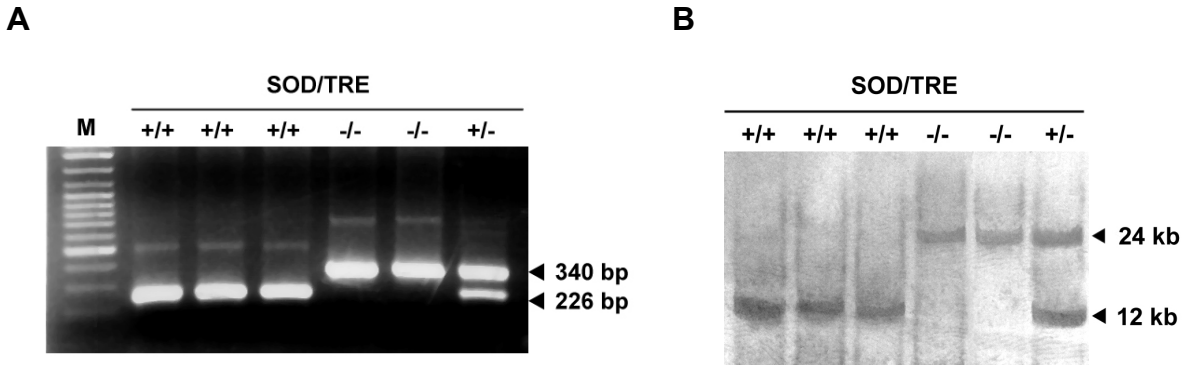

Fig. 20. Genotyping of MnSOD locus in SOD/TRE transgenic mice. **A** – PCR-based with primers designed to anneal to neighbouring exons, products – 340 bp for wild type (-/-), 226 bp for transgenic homozygotes (+/+), two bands for heterozygotes (+/-); M – molecular weight ladder. **B** – Southern blot hybridization with external probe complementary to 3' end of the MnSOD locus; bands – 24 kb for wild type (-/-), 12 kb for transgenic homozygotes (+/+). The same methods were used for embryonic stem cells screening as well as for genotyping of SOD/TRE tetR mice.

Since the pTG/TRE construct did not introduce regulatory tetracycline receptor it was expected that crossing of SOD/TRE heterozygous mice should produce non-viable homozygotes. In agreement with previous reports (Lebovitz et al., 1996; Li et al., 1995) homozygotic animals died a few days after birth and were smaller in size, showed weight reduction of 50% and were not as much active as wild type or heterozygous mice (Fig. 21). Therefore, SOD/TRE homozygous (SOD/TRE$^{+/+}$) and heterozygous mice (SOD/TRE$^{+/-}$) were treated as traditional knock-out (MnSOD$^{-/-}$) and heterozygous animals (MnSOD$^{+/-}$), respectively. This mouse strain was used in further experiments to study effects of MnSOD deficiency. Besides, SOD/TRE mice were used in further crossings to introduce the tetracycline receptor in order to achieve inducible MnSOD expression.

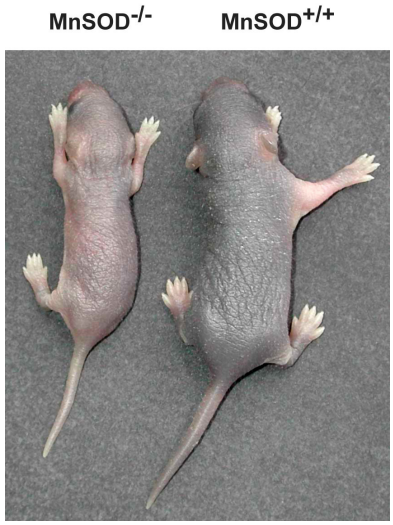

Fig. 21. SOD/TRE homozygous ($MnSOD^{-/-}$) and wild type mice at day P3. The difference in size is readily visible.

3.5.1.1 Increased apoptosis in hearts of MnSOD knock-out mice

Since homozygous SOD/TRE mice do not survive longer than few days after birth, 3 days old pups were sacrificed and their hearts were fixed in PFA and embedded in paraffin. In order to explore the involvement of apoptosis in the previously described heart failure in MnSOD-null mice, paraffin sections were used in TUNEL reaction.

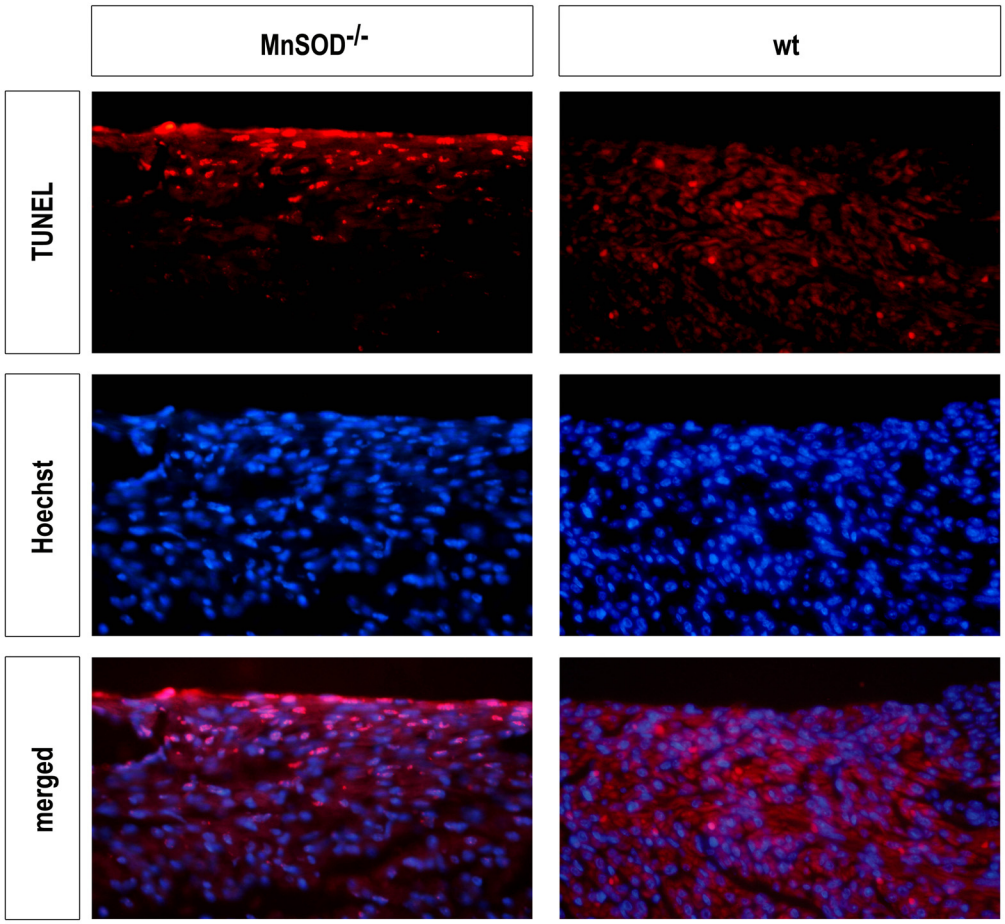

Fig. 22. Apoptosis in the hearts of MnSOD$^{-/-}$ and wt mice as detected by TUNEL reaction. Apoptotic nuclei appear in red. Hoechst staining was performed to visualize all nuclei. Only fragment of the heart is shown. TUNEL reaction was performed according to manufacturer's protocol (Roche).

Accumulation of TUNEL-positive cells was observed only in superficial layers of the heart wall of the left ventricle of MnSOD$^{-/-}$ mice. Staining was not distributed evenly, it was restricted to some areas and was not present in the remaining parts of the heart. In the MnSOD$^{+/+}$ heart false positive signals were produced by erythrocytes since Hoechst staining did not reveal corresponding nuclear signals (Fig. 22). Sections from two distinct individual animals were also analyzed showing the same pattern of staining (data not shown).

3.5.1.2 Increased ANF expression in hearts of MnSOD$^{-/-}$ mice

Expression of atrial natriuretic factor (ANF) is a sensitive marker of cardiac hypertrophy and heart failure. Paraffin sections from the same hearts as the ones used in TUNEL assay were also used for assessment of ANF expression.

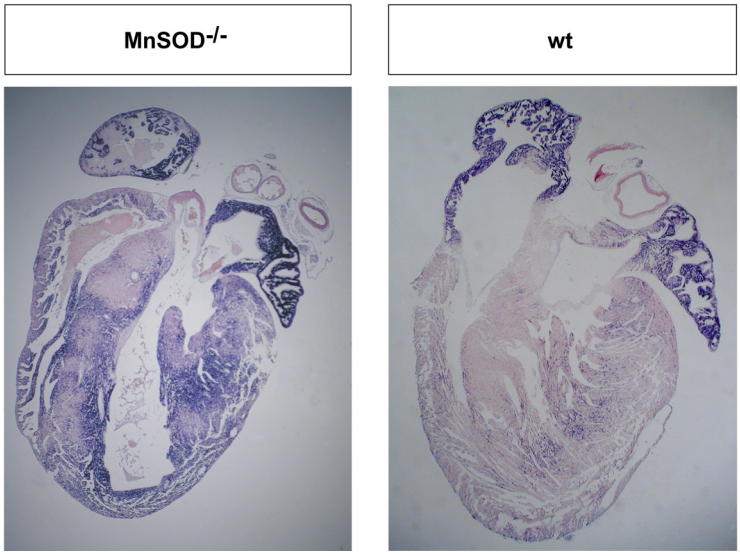

Fig. 23. Expression pattern of atrial natriuretic factor (ANF) in the hearts of wild type and MnSOD deficient mice as detected by *in situ* hybridization. Blue staining detects ANF expression. Sections were slightly counterstained with eosin.

ANF is evenly distributed in the developing heart during embryogenesis. At birth its expression in the ventricles is down-regulated but persists in atria. The results shown on Fig. 23 show significantly enhanced ANF expression in atria and ventricles of the MnSOD deficient mice. In wild type hearts ANF remained exclusively in the atria with faint expression in the left ventricle.

3.5.1.3 AOE's status in MnSOD heterozygous mice

As SOD/TRE mice produced no viable homozygous offspring it was deduced that the activity of the introduced transgene was absent or very low. It has been shown that heterozygous MnSOD mice have 50% reduction in MnSOD activity (Van Remmen et al., 1999). To verify whether the pTG/TRE construct is silent in SOD/TRE mice protein extracts from liver, brain and heart of heterozygous (MnSOD$^{+/-}$) and wild type (wt) mice were

prepared and analyzed for SOD activity. In addition, the influence of a putative MnSOD reduction on catalase (CAT) and glutathione peroxidase (GPX) enzymes was tested.

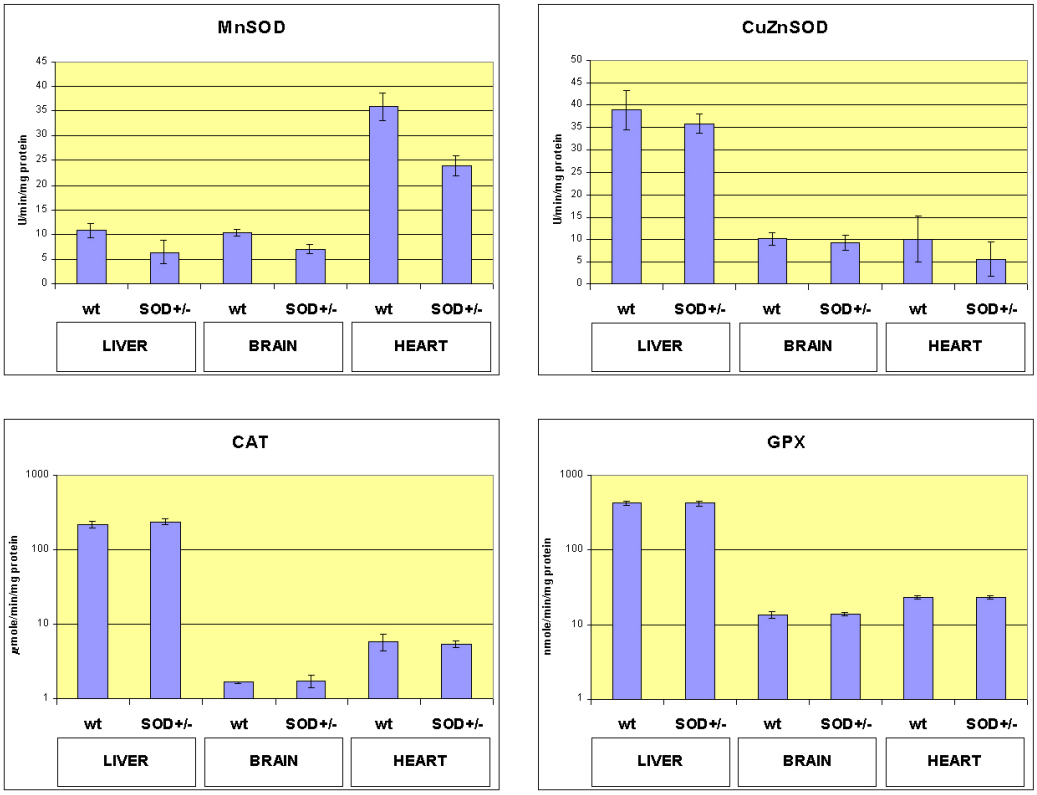

	Total SOD (U/min/mg protein)	MnSOD (U/min/mg protein)	CuZnSOD (U/min/mg protein)	CAT (umoles/min/mg protein)	GPX (nmoles/min/mg protein)
LIVER					
wt	49.73 ± 5.38	10.76 ± 1.39	38.97 ± 4.36	222.22 ± 24.16	426.68 ± 25.49
SOD$^{+/-}$	42.36 ± 2.25	6.42 ± 2.32 *	35.94 ± 2.02	240.12 ± 22.83	420.61 ± 32.46
BRAIN					
wt	20.81 ± 1.64	10.34 ± 0.71	10.18 ± 1.37	1.65 ± 0.16	13.47 ± 1.35
SOD$^{+/-}$	16.23 ± 1.07	7.01 ± 0.80 *	9.22 ± 1.74	1.73 ± 0.33	13.76 ± 0.84
HEART					
wt	45.93 ± 2.21	35.92 ± 2.85	10.01 ± 5.05	5.87 ± 1.44	23.03 ± 1.00
SOD$^{+/-}$	29.29 ± 1.78	24.02 ± 2.07 *	5.54 ± 3.79 * *	5.46 ± 0.61	23.06 ± 1.25

Fig. 24. Activities of antioxidant enzymes in tissue extracts from wild type (wt) and MnSOD heterozygous (SOD+/–) mice. Activities of total SOD and mitochondrial (MnSOD) were determined by the inhibiton of cytochrome c reduction method. Cytosolic dismutase (CuZnSOD) activity was calculated by substracting MnSOD from total SOD. Catalase (CAT) was determined by monitoring of H_2O_2 decomposition at 240 nm in the presence of cellular lysates. Glutathione peroxidase (GPX) activity was measured by following NADPH decomposition at 340 nm. Values are means ±SD, n = 5. * – $p < 0.01$; * * – $p > 0.05$ vs. wild type.

MnSOD activity was reduced in MnSOD$^{+/-}$ mice by 30% in hearts and brains and by 40% in livers. Cytosolic SOD was decreased by 45% exclusively in hearts of MnSOD$^{+/-}$ mice, although this change was statistically not significant. Catalase and glutathione peroxidase showed no alterations (Fig. 24).

The observed reduction of 30% in MnSOD activity might suggest that pTG/TRE construct had some activity independent of the presence of the Tet-regulator or might indicate a compensatory up-regulation of the wild type allele. To answer this question, Western blots with the same protein extracts were made.

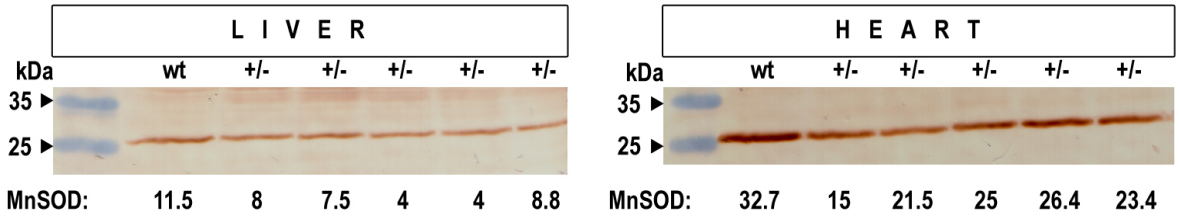

Fig. 25. Western blot hybridization of tissue extracts from 5 distinct heterozygous MnSOD mice (+/–) and one wild type (wt). Only 24 kDa band corresponding to native MnSOD protein is shown. No recombinant MnSOD (34 kDa) could be observed. Below are shown activities of MnSOD as determined by cytochrome c method. Equal amounts of protein were loaded in each lane (25 μg). Anti-MnSOD antibody was used.

No recombinant MnSOD was detected in any of the examined organs. Also larger amounts of protein failed to reveal expression of recombinant MnSOD (data not shown) supporting the idea that up-regulation of the native allele is responsible for MnSOD activity higher than the expected 50% in MnSOD heterozygotes.

Intensities of the bands representing native MnSOD in most cases corresponded to the level of the enzyme activity (Fig. 25).

3.5.1.4 Decreased heart performance in MnSOD heterozygous mice

To test whether decreased MnSOD level has an influence on physiological function of the heart, 9 heterozygous MnSOD mice and 6 wild type were examined by echocardiography.

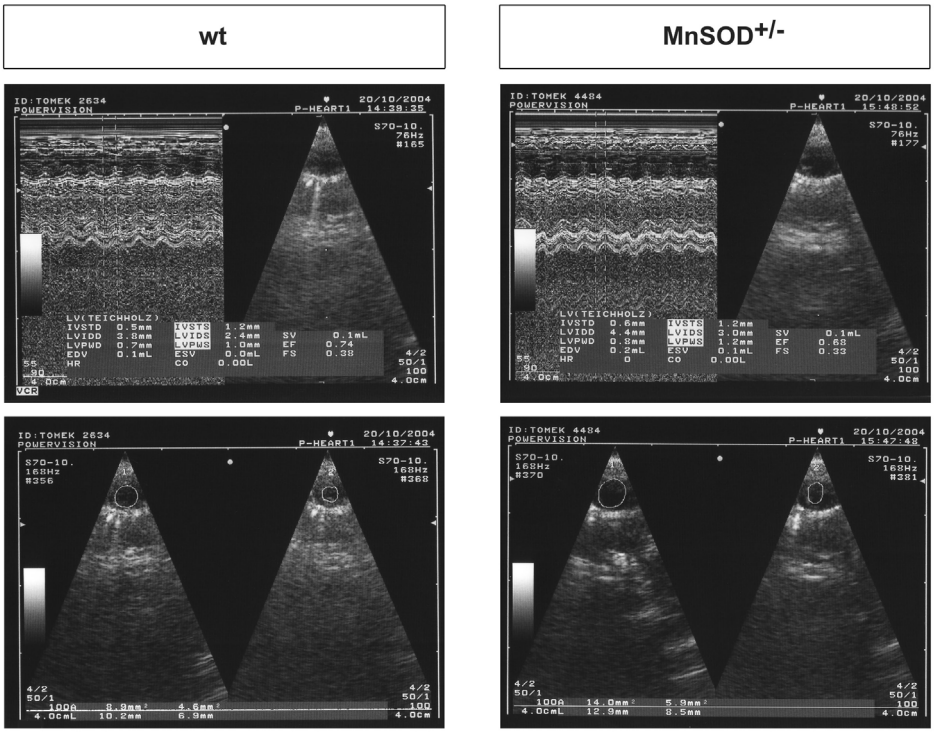

Fig. 26. Representative echocardiographs of wild type and MnSOD$^{+/-}$ mice. In the upper panel left ventricle M-mode recordings are shown. The lower panel shows left ventricle two-dimensional short axis view at papillary muscle level at end diastole and systole. Most important abbreviations: LVIDD – Left Ventricular Internal Diameter in Diastole, LVIDS – Left Ventricular Internal Diameter in Systole, EF – Left Ventricular Ejection Fraction, FS – Fraction Shortening. End-Diastolic Area (EDA) and End-Systolic Area (ESA) are shown at the bottom of the lower panel. Measurements were made on mice anesthetized with isoflurane. Heart rate of mice ranged from 400 to 500 beats per min.

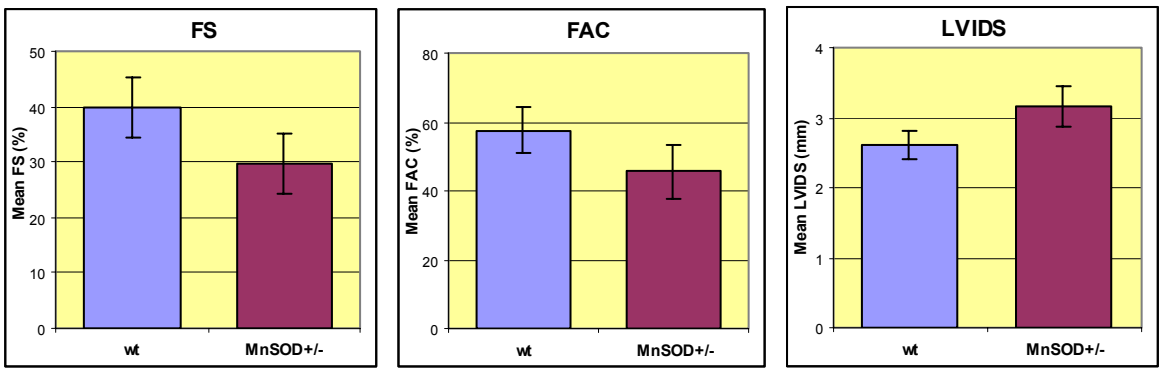

	LVIDD (mm)	LVIDS (mm)	FAC (%)	EF (%)	FS (%)
wt	4.32 ±0.45	2.60 ±0.20	57.62 ±6.83	76 ±5.68	40 ±5.41
MnSOD$^{+/-}$	4.44 ±0.21	3.16 ±0.28*	45.61 ±7.93*	63 ±8.31*	30 ±5.55*

Fig. 27. Left ventricle function assessed by echocardiography. 6 wild type (3 males and 3 females) and 9 MnSOD heterozygous (6 males and 3 females) mice were examined. Animals in both groups were 6 months old. Values are means ±SD. * – $p < 0.01$ vs. wild type mice.

Echocardiographic measurements revealed that left ventricle function was impaired in $MnSOD^{+/-}$ mice. This is indicated by the decrease in fraction shortening (FS) by 26% and fractional area change (FAC) by 21% in $MnSOD^{+/-}$ mice as compared to wild type animals. In addition, the ejection fraction (EF), calculated according to the Teichhozl method, was decreased in the heterozygotes by 18%. All these changes were statistically significant and indicate a decrease in left ventricle systolic function. On the other hand, left ventricle internal diameter in diastole (LVIDD) was similar in both groups. Only left ventricle internal diameter in systole (LVIDS) was significantly increased in the $MnSOD^{+/-}$ animals by 21% (Fig. 26 and 27).

The LVIDS increase, together with the decrease of FAC, FS and EF implicate that MnSOD heterozygous mice suffer from a mild form of dilated cardiomyopathy.

3.5.1.5 Apoptosis in doxorubicin treated MnSOD heterozygous mice

Doxorubicin is a commonly used cytostatic drug. Its known side-effects include dilated cardiomyopathy. Since apoptosis is thought to contribute to this disease by loss of myocyte I decided to check whether hearts of MnSOD deficient mice exposed to doxorubicin are more prone to programmed cell death. For this purpose wild type and MnSOD heterozygous mice were treated with doxorubicin for a period of two weeks. Following that, TUNEL assays were performed on paraffin embedded hearts.

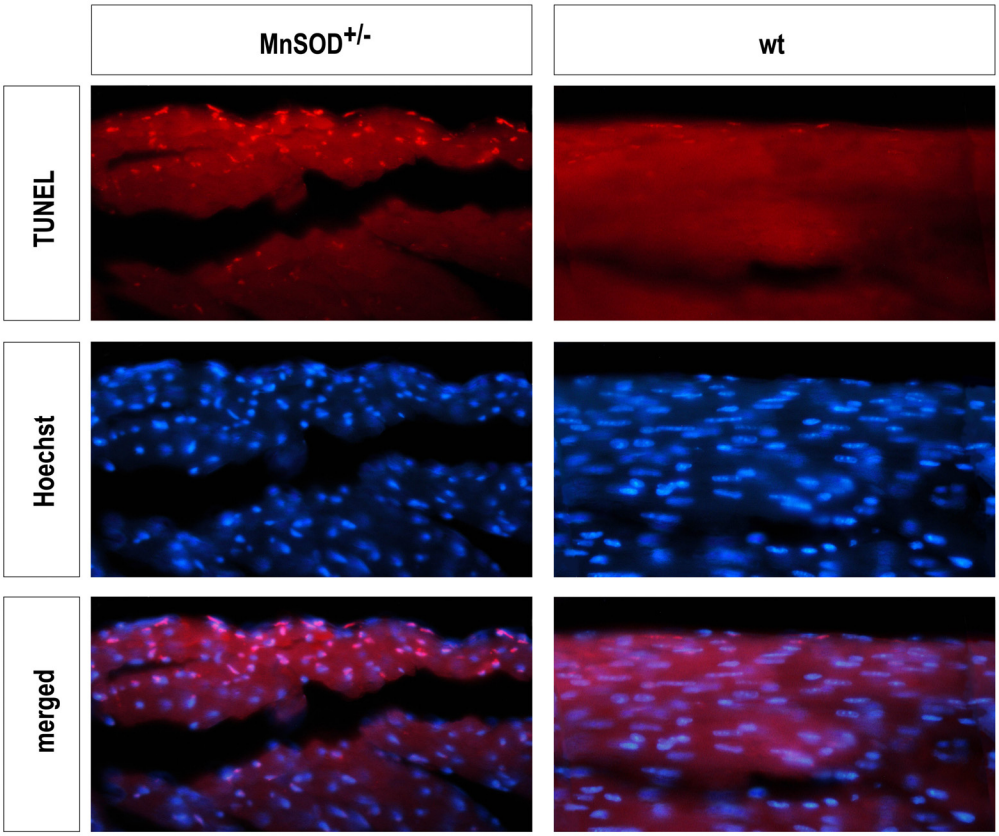

Fig. 28. TUNEL assay detected apoptosis in the hearts of doxorubicin treated mice. Apoptotic nuclei are red. Hoechst staining was performed to visualize all nuclei. Only fragments of the hearts with the strongest signals are shown. Doxorubicin was administered to 4.5 months old mice by means of osmotic pumps (Alzet, model 2002) at a dose of 15 mg/kg body weight. Treatment lasted two weeks. TUNEL reaction was performed according to manufacturer's protocol (Roche).

Hearts of doxorubicin treated MnSOD$^{+/-}$ mice showed significantly more TUNEL-positive cells than wild type animals. TUNEL-positive cells were distributed unevenly and were found in superficial layers of the left ventricle wall (epicardium) forming clusters of apoptotic cells (Fig. 28). However, the majority of the myocard was TUNEL-negative (not shown). No signal was detected in untreated mice (data not shown).

3.5.1.6 ANF up-regulation after doxorubicin treatment of MnSOD$^{+/-}$ mice

The same heart sections were used in *in situ* hybridization experiments to check whether doxorubicin induced expression of atrial natriuretic factor (ANF), a known marker of cardiac pathology. The influence of MnSOD$^{+/-}$ phenotype on heart susceptibility to stress imposed by doxorubicin was examined.

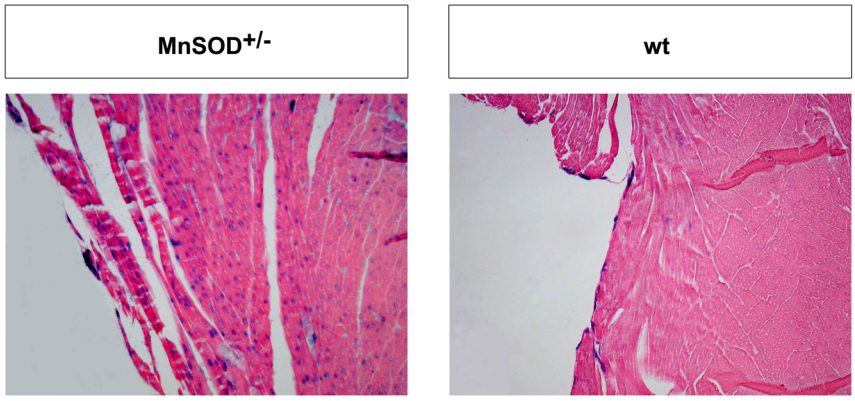

Fig. 29. Expression of ANF in hearts of doxorubicin treated wild type and MnSOD heterozygous mice detected by *in situ* hybridization. ANF expression was visualized by blue staining. Sections were counterstained with eosin. Due to the subtle nature of the signal which is best viewed at higher magnification, only a fragment of septum is shown. Sections were prepared from the same hearts as in 3.5.1.5.

Doxorubicin treatment induced ANF expression in hearts of MnSOD$^{+/-}$ mice but not in wild type mice (Fig. 29). In the latter, in addition to atria – where ANF was readily detected – the signal also appeared as sparse foci on the left ventricular septum surface. The rest of the heart showed no ANF staining.

3.5.1.7 Doxorubicin induced senescence in hearts of MnSOD heterozygous mice

Since doxorubicin generates oxidative stress in cellular environments, hearts of doxorubicin treated mice were assayed for the presence of a senescence marker. For this purpose cryosections of non-fixed hearts were subjected to senescence-associated β-galactosidase staining (SA-β-Gal).

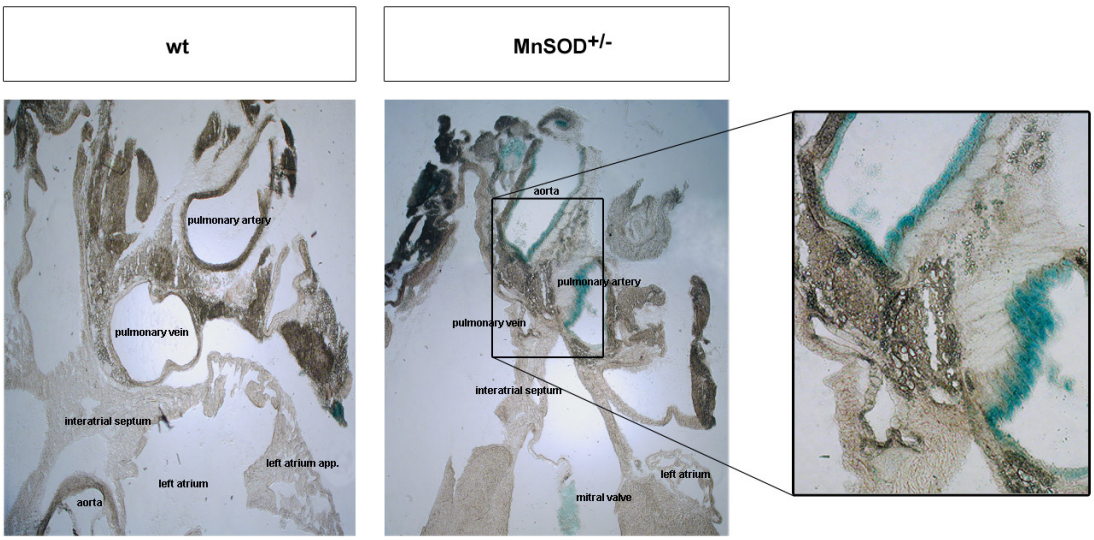

Fig. 30. Senescence-associated β-galactosidase staining in the hearts of wild type and MnSOD$^{+/-}$ mice treated with doxorubicin. The senescence marker stains blue. Non-fixed hearts were embedded in Polyfreeze™ Tissue freezing medium™, then cut with cryotome, briefly fixed in 4% PFA (15 minutes) and stained for SA-β-Gal. Sections were cut at 40µm and were not counterstained to enhance signal.

Blue SA-β-Gal staining was evident in vessels of MnSOD$^{+/-}$ hearts as well as in the mitral valve. The signal was confined to vascular smooth muscle and endothelial cells. In addition, some tissues neighbouring the vessels gave weak signals (Fig. 30). No SA-β-Gal positive cells were observed in other parts of the heart (data not shown). Neither vessels nor mitral valve (not shown) were positive for SA-β-Gal in control wild type mice.

3.5.2 SOD/TRE tetR mice

SOD/TRE tetR mice were generated by introduction of pTG/TRE tetR construct into embryonic stem cells. 29 recombinant ES cell clones were selected out of 196 neomycin-resistant clones. Positive ES clones were used for blastocyst injections from which chimeric mice were obtained. After backcrossing with C57BL/6, SOD/TRE tetR transgenic strain was established. All the screening and genotyping procedures were performed according to the protocol for SOD/TRE mice.

So far 59 animals were born after crossings of heterozygous SOD/TRE tetR mice. Theoretically 15 homozygous pups were expected, however no homozygotes were obtained. The lack of viability of homozygous offspring indicated that the introduced tetracycline receptor-coding cassette was inactive or had a very low expression level. Indeed, expression of tetracycline regulator in heterozygous SOD/TRE tetR mice was not detected by RT-PCR (data not shown). Additionally, EGFP reporter gene expression in these mice appeared at the same level as in animals lacking the tetracycline receptor (SOD/TRE), confirming the assumption that the intended regulation did not work in this mouse strain (Fig. 31). For this reason SOD/TRE tetR strain was not useful for further investigations and was discarded.

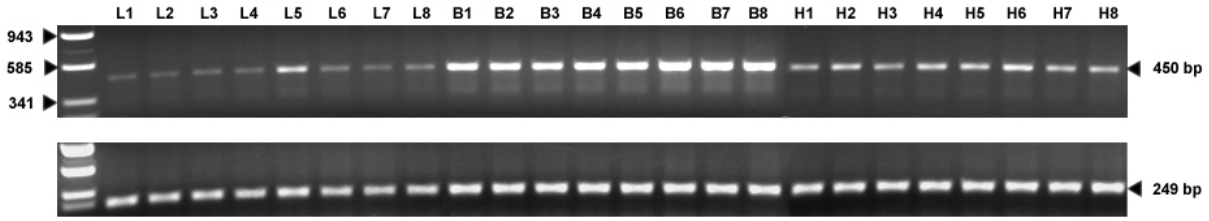

Fig. 31. RT-PCR analysis of EGFP reporter expression in livers (L), brains (B) and hearts (H) of 8 individual mice (upper panel). SOD/TRE tetR heterozygous mice: L1-L3, B1-B3, H1-H3; SOD/TRE heterozygous mice: L4-L8, B4-B8, H4-H8. In the lower panel HPRT expression in the corresponding samples is shown to prove the quality of RNA.

3.5.3 SOD/ROSA mice

The SOD/ROSA strain was generated by crossing SOD/TRE mice with the ROSA t1d strain which was designed to express the rtTA tetracycline receptor ubiquitously from ROSA26 locus. After obtaining heterozygous animals mice were crossed to homozygosity. The occurence of tetracycline receptor in the Tet-On version in ROSA mice means that activation of the targeted MnSOD locus requires administration of doxycycline. Therefore parent animals were treated with this antibiotic in drinking water starting from the first day of crossing until at least three generations of offspring were old enough to be genotyped. This schedule guaranteed that potential homozygous animals would have sufficient doxycycline concentration to drive expression of the targeting construct. Each of the three males were crossed with 2 females until 48 mice were born. However, no homozygotes, either alive or dead, were obtained. Theoretically, 9 homozygous SOD/ROSA mice with rtTA receptor gene were expected. EGFP reporter gene expression analysis in heterozygous animals showed that the regulation of the targeted locus did not work in these animals (Fig. 32). Together with the lack of viable homozygous offspring this indicates that the introduced tetracycline receptor-coding cassette is inactive or has a low expression level. Indeed, expression of tetracycline regulator in heterozygous SOD/ROSA mice was not detected by RT-PCR (data not shown). Therefore further work on this strain was discontinued.

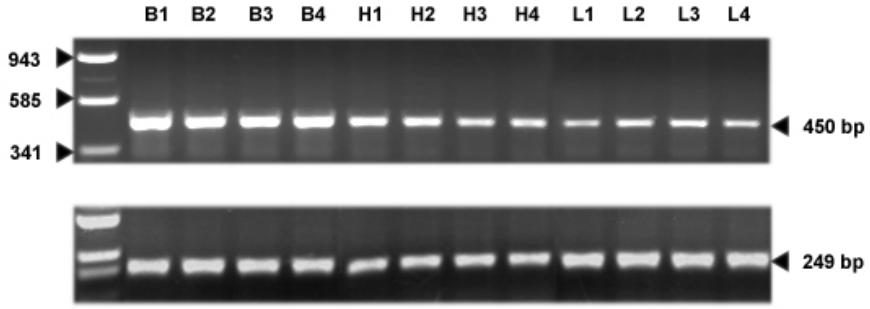

Fig. 32. RT-PCR analysis of EGFP reporter expression in brains (B), hearts (H) and livers (L) of 4 individual mice (upper panel). SOD/ROSA heterozygous mice were divided into two groups: one received doxycycline in drinking water (B1-B2, H1-H2, L1-L2) while the other was kept in standard conditions (B3-B4, H3-H4, L3-L4). In the lower panel HPRT expression in the corresponding samples is shown to prove the quality of RNA.

3.5.4 Transgenic mice with regulated MnSOD expression

SOD/TRE mice were crossed with αMHC-tTA mice which express tetracycline receptor under the control of α-myosin heavy chain promoter. This crossing resulted in generation of a strain (SOD/αMHC tTA) that expressed regulatory tetracycline receptor in Tet-Off configuration exclusively in the heart. Next, double transgenic mice were crossed to homozygosity to obtain fully regulated expression of MnSOD in the heart. However, all homozygotes died within two weeks of life no matter if they inherited αMHC-tTA transgene or not. Therefore activity of the regulated locus was studied in heterozygous animals.

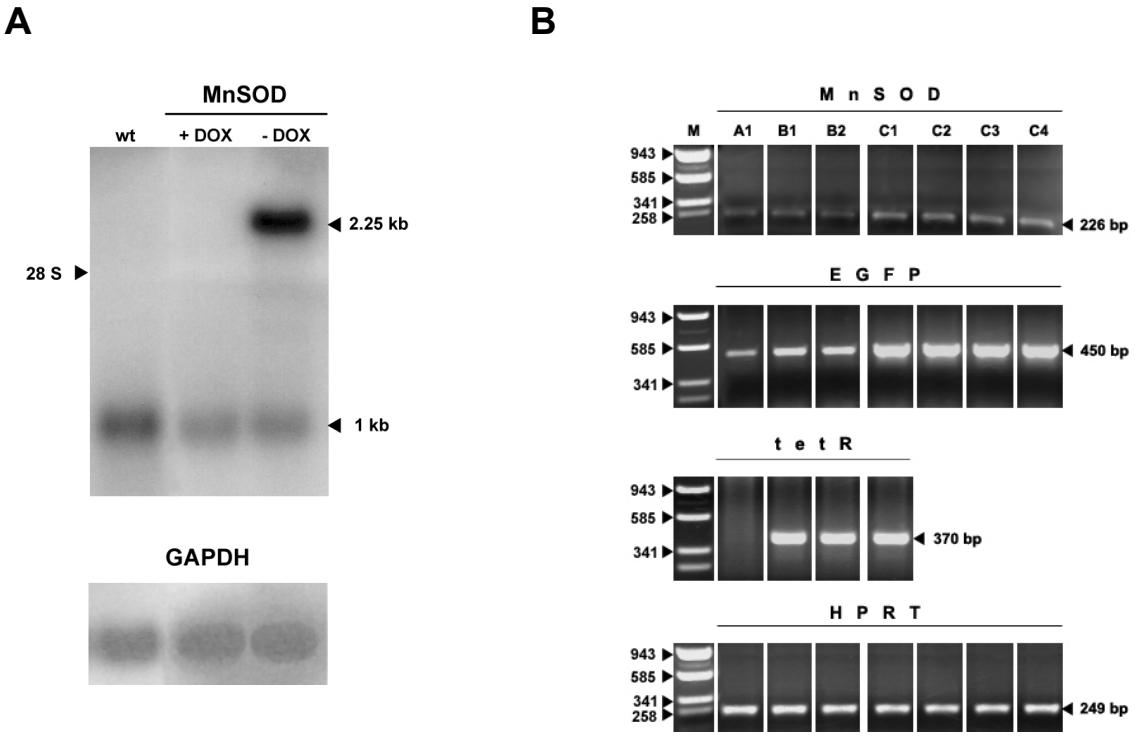

Fig. 33. Regulated expression of the targeted MnSOD locus in hearts of SOD/αMHC tTA heterozygous mice.
A – Northern blot hybridization of total mRNA from hearts of wild type (wt) and two individual SOD/αMHC tTA animals: + DOX – mouse fed with doxycycline in drinking water, – DOX – mouse maintained in standard conditions; whole length MnSOD cDNA was used as a probe; 2.25 kb band represents mRNA expressed from the transgenic locus, 1 kb band – from native locus; position of 28S rRNA is shown; hybridization with GAPDH probe is shown to prove the quality of RNA preparation and equal gel loading.
B – RT-PCR reactions showing expression of MnSOD, EGFP, tetracycline recpetor (tet R) and hypoxanthine phosphoribosyl transferase (HPRT); A1 – SOD/TRE heterozygous mouse, control to show expression in mouse without regulator; B1-B2 – two individual SOD/αMHC tTA heterozygous mice fed with doxycycline in drinking water; C1-C4 – four individual SOD/αMHC tTA heterozygous mice maintained in standard conditions; M – molecular weight marker; calculated lengths of the products are shown.

Both Northern blot hybridization and RT-PCR showed that the targeting construct was fully regulated in animals by means of administration of doxycycline. Standard maintenance of mice activated transcription of the transgene in the heart tissue. This is visualized by the 2.25 kb band in Northern blot hybridization. Native MnSOD mRNA produced 1 kb message while transgene message was longer due to additional sequences (Myc tag, IRES, EGFP). The 2.25 kb band was not detected in animals in which transgene expression was suppressed by doxycycline administration (Fig. 33A). RT-PCR reactions showed higher intensity of the MnSOD and EGFP bands in animals maintained on standard diet (Fig. 33B, lane C1-C4) as compared to those that remained on doxycycline (Fig. 33B, lane B1-B2). An even lower expression was seen in mice that lacked the tetracycline regulatory element (Fig. 33B, lane A1). This level of expression was considered as background expression which was probably due to a leaky CMV_{min} promoter. MnSOD and EGFP were also analyzed in liver and brain of SOD/αMHC tTA mice. As expected, their expression was at the level of background expression (data not shown) also seen in the absence of tetR message in tissues other than heart (data not shown).

To verify that the transgene was effectively translated, Western blot analysis was performed.

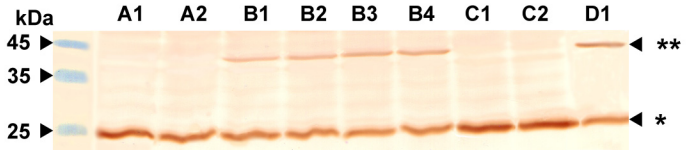

Fig. 34. Western blot analysis of heart extracts. A1-A2 – two individual SOD/αMHC tTA heterozygous mice maintained on doxycycline; B1-B4 – four individual SOD/αMHC tTA heterozygous mice maintained on standard diet; C1-C2 - two individual wild type mice; D1 – positive control - extract from OFF-SOD 21 double stable cell line. Native MnSOD is marked with an asterisk; recombinant MnSOD protein encoded by the pTG/TRE construct is marked with two asterisks. Anti-MnSOD antibody was used. 50 μg of total protein extract was run in each lane.

Regulation of the transgene by administration of doxycycline could also be seen at the protein level. Similarly to Northern blot hybridization, bands representing transgene activity (34 kDa) were visible in animals maintained without doxycycline (Fig. 34, lanes B1-B4, marked with two asterisks), while they were absent in those in which the transgene was suppressed by administration of the antibiotic (Fig. 34, lanes A1-A2). As expected, the intensity of the band corresponding to 24 kDa, native MnSOD protein, (Fig. 34, marked with an asterisk) was lower in all SOD/αMHC tTA heterozygous mice as compared to wild type animals.

4 DISCUSSION

Since conventional MnSOD knock-out mice die early after birth or before delivery, the generation of a mouse strain with spatio-temporally controlled MnSOD expression creates the opportunity to investigate the role of MnSOD during late development and in adult life. Crossing of SOD/TRE conditional transgenic mice with mouse strains capable for an organ specific expression of the regulator (tetracycline receptor) allows to unveil the role of MnSOD in a particular tissue at the desired time. Application of the tetracycline regulatory system makes it possible to switch the MnSOD expression on and off freely.

To obtain such a Tet-operated animal model, a targeting construct for the generation of transgenic mice was developed. This process involved cloning of MnSOD cDNA, addition of reporter gene and elements which facilitate detection of the cloned sequence, supplementation with sequences which provide control over the cDNA expression and finally, functional analysis of the created DNA construct. Test experiments were performed in cell culture system. Both transient and stable transfections were used to assess the efficiency of tetracycline receptor-based regulation, activity of the recombinant protein and *in vitro* effects of MnSOD overexpression. After validation of the applicability of the constructed expression cassette, the DNA construct was used to generate a conditional transgenic mouse strain. The obtained SOD/TRE mouse strain was used to generate a regulated SOD/αMHC tTA strain. SOD/TRE mice were employed to examine effects of complete and partial MnSOD deficiency. Finally, the present work describes the initial characterization of SOD/αMHC tTA conditional transgenic mice and demonstrates effectiveness of tetracycline receptor-based regulation of MnSOD expression.

4.1 Cloning and functional analysis of MnSOD cDNA under control of the Tet-operator

Cloning of MnSOD cDNA into response vector, followed by tagging of MnSOD protein with myc epitope and addition of EGFP reporter molecule resulted in the generation of an expression construct which was functionally analyzed and used in further work. This cell culture construct was meant to be responsive to induction by tetracycline receptor (Fig. 2). Two tetracycline regulatory systems were tested with respect to magnitude of expression induction in the state ‘on’ and effectiveness of suppression in the state ‘off’. Since tetracycline

receptor variants encoded by the pTet-Off plasmid gave lower expression level in the state "off" and higher in "on" as compared to the pTet-On variant (Fig. 3), the former system was used in further work. An additional advantage that argues for the Tet-Off system usage is that MnSOD is essential for cellular physiology and therefore it is less cumbersome to have a regulation where MnSOD expression occurs constantly and only administration of doxycycline suppresses it. This argument is important for the generation of transgenic mice with regulated MnSOD expression. In a Tet-On model animals have to be kept under doxycycline treatment throughout their life while in the Tet-Off model doxycycline needs to be supplied with drinking water only during specified stages of an experiment to suppress MnSOD gene. *In vitro* data showed that regulation mediated by the pTet-Off provides better induction and more effective repression. Concerning the Tet-On system, there is a likelihood that in the animal model this vector could drive MnSOD expression at a level not sufficient for survival or is resistant to a complete shut-down. In addition, much lower concentrations of doxycycline are required to shut off expression in the Tet-Off system as compared to high concentrations required in the Tet-On system to turn the expression on (personal communication from Dr. Bujard group).

Effective regulation of expression cassette by Tet-Off system was shown also in stably transfected C3H/10T1/2 cells (Fig. 7, Table 3). Nevertheless, some cells appeared to lose expression of the transgene during further propagation. Although, a reduction in the activity of transiently transfected plasmids can be explained easily, the observed gradual decrease of expression level observed in some of the generated stable cell lines is harder to understand. One possible explanation is silencing of the locus (by means of DNA methylation, histone deacetylation or other mechanisms) in which the tetracycline receptor coding vector integrated. Other explanation include an instability of the integrated constructs in their integration sites. This might lead to their loss during cell propagation. However this is rather unlikely as cells were constantly propagated in selection medium. Without antibiotic resistance genes these cells do not withstand the selection agents.

Both transient and stable transfections revealed that translation of the expression construct yields enzymatically active MnSOD protein. Also activity gels confirmed the presence of enzymatically active protein of different molecular weight than native MnSOD (Fig. 6). The OFF-SOD 21 stable cell line allowed to achieve reversible two-fold induction in MnSOD activity (Fig. 8).

4.2 Effects of MnSOD overexpression in mouse fibroblasts

The OFF-SOD 21 double-stable cell line with transcription of MnSOD cDNA regulated by tetracycline receptor offered the opportunity to investigate the effects of two-fold higher activity of MnSOD. Many groups have constructed cell lines with MnSOD overexpression having enzyme activity ranging from 1.8-fold to 15-fold above the physiological level of a given cell line (Li et al., 1998; Melendez et al., 1999). MnSOD overexpression was shown to influence activity of CuZnSOD or GPX. In one cell line 3-fold increase in MnSOD caused two-fold decrease in CuZnSOD activity, while in another, 1.8-fold MnSOD overexpression resulted in 1.5-fold up-regulation of GPX (Li et al., 1998). Another group reported either change in CAT activity or no influence on antioxidant enzymes (AOE) (Li et al., 1998). There are also groups which reported absolutely no changes in activities of AOEs (Wenk et al., 1999; Takada et al., 2002).

In my experimental setting a two-fold higher MnSOD activity in OFF-SOD 21 cell line had no influence on other antioxidant enzymes. CAT, GPX and CuZnSOD remained at the physiological level both in transiently and stably transfected cells (Table 2 and Fig. 8). Although it is plausible that activity of one component of the detoxifying pathway might regulate the other, the obtained data suggest that increased MnSOD activity has no direct or indirect regulatory effect on the antioxidant enzymes. Though, it was proposed that SOD overexpression might result in a decrease of hydrogen peroxide levels (Liochev and Fridovich, 1994) most experimental data show an accumulation of H_2O_2 (Li et al., 1998; Rodriguez et al., 2000) which in turn was shown to activate CAT (Shull et al., 1991). Therefore, effects observed in OFF-SOD 21 cell line suggest that the 2-fold higher MnSOD activity fails to produce excessive H_2O_2 and influence other AOEs. Alternatively, alterations of CuZnSOD, CAT and GPX activity reported by some researchers might be explained by vector integration effects or other mechanisms rather than the real adaptation of cells to elevated MnSOD. On the other hand, cells with high MnSOD activity exhibited retarded growth in culture, which was attributed to H_2O_2 over-production. Indeed, OFF-SOD 21 cell line grew more slowly than the parental C3H/10T1/2 fibroblasts, which was evident in the longer population doubling time.

As expected, OFF-SOD 21 cells appeared to be more resistant to hyperoxia than parental cells. Cells with native MnSOD activity (MnSOD overexpression suppressed by doxycycline) started to die on the 3rd day of cultivation in 85% oxygen while MnSOD overexpressing cells

continued to grow (Fig. 10). This observation was in complete agreement with previous reports (Koo et al., 2005; Ilizarov et al., 2001).

MnSOD overexpressing cells were shown to be resistant to apoptosis induced by various stimuli: radiation, TNF-α, IL-3 withdrawal (Epperly et al., 2003), alkaline conditions (Majima et al., 1998), ATP depletion (Cruthirds et al., 2005), taxol, H_2O_2 and okadaic acid (Manna et al., 1998).

In this study, protective effect of two-fold overexpression of MnSOD against H_2O_2-induced apoptosis was tested. Both parental C3H/10T1/2 cell line and OFF-SOD 21 stable line were comparatively resistant to induction of apoptosis by hydrogen peroxide. Therefore 1 mM H_2O_2 solution was used to trigger apoptotic pathway. Under these conditions a two-fold higher MnSOD activity clearly protected cells from apoptosis. Approximately ten times more cells were apoptotic when doxycycline was added to the medium to suppress MnSOD overexpression (Fig. 11). Thus, data obtained in OFF-SOD 21 cells confirmed previous reports on protective effect of MnSOD overexpression on apoptotic cell death induced by H_2O_2.

To test the protective effect of MnSOD overexpression apoptosis was induced by different modes including application of doxorubicin. This drug induces apoptosis through activation of many signalling pathways including generation of ROS and accumulation of ceramide. Almost all cells treated with doxorubicin appeared TUNEL-positive with slightly stronger signal in those overexpressing MnSOD (Fig. 12). The minor augmentation of apoptosis by increased MnSOD in OFF-SOD21 cell line might be explained by induction of the ceramide mediated cell death pathway. Doxorubicin was shown to activate sphingomyelinase, which is responsible for ceramide synthesis. Another anthracycline, daunorubicin, induces ceramide synthesis *de novo*. Ceramide induces dephosphorylation of anti-apoptotic Bcl-2 protein, down-regulates Akt/PKB anti-apoptotic pathway and up-regulates MnSOD (reviewed in Fogli et al., 2004; Pahan et al., 1999). It was shown that ceramide-mediated cell death pathway is regulated by MnSOD. Mitochondrial dismutase appears indispensable for the progression of ceramide-induced apoptosis (Kinscherf et al., 1998) validating the data obtained in MnSOD overexpressing as well as deficient cells (discussed below).

Mechanisms of doxorubicin-induced toxicity include generation of superoxide and nitric oxide (Vasquez-Vivar et al., 1997; Sayed-Ahmed et al., 2001). As peroxynitrite can be formed from $NO^{\bullet}$ in the presence of superoxide, MnSOD activity might control the balance

between NO and $ONOO^-$. Depending on its concentration, $NO^\bullet$ can either induce an apoptotic response or prevent it (Razavi et a., 2005). It was shown that $NO^\bullet$ donors at high concentrations kill MnSOD overexpressing cells preferentially (Melendez et al., 1999). Hence, MnSOD might play significant role in $NO^\bullet$-mediated apoptosis. Moreover, a functional link was proposed for $NO^\bullet$-induced cell death and ceramide synthesis (Fogli et al., 2004), further supporting observations made in MnSOD overexpressing and deficient fibroblasts.

Taken together, the interference of MnSOD with apoptosis depends on the stimuli used in its induction. The effects of MnSOD might range from inhibition, as it is in the case of H_2O_2-induced apoptosis, to augmentation in doxorubicin-induced cell death.

4.3 MnSOD deficiency in primary mouse embryonic fibroblasts

The generation of transgenic mouse strain SOD/TRE created the opportunity to derive primary fibroblast cell lines from homozygous, heterozygous and wild type animals. Hence, cell lines with 3 possible configurations of MnSOD gene were established: absent ($MnSOD^{-/-}$), reduced ($MnSOD^{+/-}$) and native MnSOD level ($MnSOD^{+/+}$) (Fig. 13).
As expected, mouse primary fibroblasts, which were completely or partially deficient in MnSOD, produced greater amounts of ROS than wild type cells ($MnSOD^{+/+}$). After staining with a ROS-sensitive dye, dichlorofluorescein derivative, this was observed using a confocal microscope (Fig. 14) and measured by flow cytometry (Fig. 15). Under standard conditions $MnSOD^{-/-}$ cells clearly produced more ROS than heterozygous and wild type cell lines. Intriguingly, even more ROS was produced in hypoxic conditions whereas, as expected, hyperoxia induced the highest ROS production in $MnSOD^{-/-}$ cells. Interestingly, at least a transient production of ROS was described during hypoxia (Zuo and Clanton, 2005) and $MnSOD^{-/-}$ cells lacking native promoter regulatory elements of the MnSOD gene failed to respond to changing conditions. $MnSOD^{+/+}$ cells, which have native MnSOD locus, adapt to both hypoxia and hyperoxia showing almost stable level of radicals under all circumstances. MnSOD expression is known to respond to a number of stimuli including hypoxia and hyperoxia (Ohman et al., 1999; Clerch, 2000; Visner et al., 1990). $MnSOD^{-/-}$ cell survival in 85% oxygen was clearly reduced compared to $MnSOD^{+/+}$ cell line (data not shown). These data suggests a central role of MnSOD in adaptation of cells to stressful conditions. Additionally, it demonstrates that the construct introduced into the MnSOD locus was transcriptionally isolated and did not respond to native regulatory elements. This observation

might indicate a tight, tetracycline receptor-based, self-contained regulation of MnSOD cDNA expression in transgenic mice.

According to the free radical hypothesis of aging, elevated ROS level in $MnSOD^{-/-}$ cells should lead to accelerated senescence. Unexpectedly, MnSOD deficient cells appeared to senesce more slowly than cells with normal MnSOD level (Fig. 16). This finding was confusing and seemed not fit the role of SODs enzymes for antioxidant defence. However, in the light of the fact that hydrogen peroxide has been shown to induce features of cellular senescence and MnSOD overexpression increases percentage of SA-β-Gal expressing cells (Plymate et al., 2003), the lack of an enzyme that processes oxygen radical to hydrogen peroxide in $MnSOD^{-/-}$ cells might explain the obtained data. The absence of MnSOD might lead to reduced H_2O_2 levels within the cell and therefore to an increased resistance against cellular senescence. This result can also be substantiated by the fact that MnSOD is repressed in many tumors and its overexpression inhibits growth of many tumor cell lines (Li et al., 1998). Probably, acquirement of senescence is a mechanism that counteracts transformation of normal cells while MnSOD deficient cells escape this mechanism and are more susceptible to tumor formation.

As evasion of apoptosis is important in the development of cancer, $MnSOD^{-/-}$ cells were tested for their capacity to execute the cell death program. H_2O_2-induced apoptosis was observed in the vast majority of $MnSOD^{+/+}$ cells, while $MnSOD^{-/-}$ remained largely resistant to this treatment (Fig. 17, Table 4). As MnSOD is able to repress p53 transcription, p53 involvement in this process was tested. Inhibition of p53 activity by pifithrin-α had no influence on apoptosis rate in neither cell line (data not shown) excluding this pathway of cell death induction, which is in line with a previous report showing that inhibition of radiation-induced apoptosis by MnSOD was independent of p53 transactivation function (Drane et al., 2001). Induction of apoptosis by administration of doxorubicin gave similar results (Fig. 18, Table 4). Very few publications deal with apoptosis in $MnSOD^{-/-}$ cells. Van Remmen et al. (2001) showed that cardiomyocytes derived from MnSOD knock-out mice are more susceptible to apoptosis induction than from wild type animals. In another study (Comhair et al., 2005), inhibition of MnSOD by pyrogallol (2-ME) induced cell death in bronchial epithelial cells. While protective effects of MnSOD overexpression on apoptosis are well described (also shown in this work), inhibition of apoptosis in MnSOD deficient cells is a quite unexpected finding. However, low level of MnSOD in many tumors, including hepatomas, pancreas and breast cancer (Galeotti et al., 1989; Ough et al., 2004; Li et al, 1998), indicates that – in some circumstances – MnSOD may be indispensable for the

execution of apoptotic pathways. The postulated role of MnSOD in regulation of ceramide-mediated cell death (discussed above) suggests that, at least in some cell types this mode of dying requires the presence of mitochondrial dismutase.

4.4 Generation of transgenic mice with a conditional MnSOD expression regulated by tetracycline

Two transgenic mice strains were established using embryonic stem cells. The SOD/TRE tetR strain included sequences coding for the tetracycline receptor in the Tet-Off version – to achieve the intended regulation of MnSOD expression without further crossings with established strains expressing the regulator. Though gene targeting succeeded, very low expression level and lack of regulation of the transgene was detected (Fig. 31). Consequently, further breeding of these mice never produced viable homozygotes. This result was anticipated right after identification of successfully targeted ES cells when they were checked for the expression of the EGFP reporter molecule. No fluorescence was detected neither in undifferentiated ES cells nor in cells subjected to differentiation procedure (data not shown). Only a weak regulation was detected by RT-PCR in differentiated ES cells (data not shown). There are at least two explanations for this result. One is the phenomenon known as promoter interference. In this particular case the presence of neomycin cassette with PGK promoter may influence the activity of other promoters in the neighborhood (Dragatsis and Zeitlin, 2001; Zhuang et al., 2001). The other explanation is a low activity of CMV promoter in ES cells. To eliminate the influence of promoter interference SOD/TRE tetR strain was crossed with mouse strain expressing ubiquitously Flp recombinase. As neomycin selection cassette is flanked by Flp recombinase recognition sequences, resulting offspring were free of promoter interference due to the removed cassette. In spite of that, no viable homozygotes were obtained suggesting rather low CMV promoter activity driving the expression of tetracycline receptor. Indeed, no tetR expression was detected by RT-PCR method in extracts from heart, liver or brain in heterozygous SOD/TRE tetR mice (data not shown). For this reason, this strain was regarded as useless and further work was discontinued.

The other starting strain – SOD/TRE – was used in further crossings with the purpose to introduce a regulator. The goal of crossing with ROSA t1d mice was to introduce ubiquitously expressed rtTA tetracycline receptor. Resulting SOD/ROSA strain should express the transgene in all tissues when treated with doxycycline (Tet-On system). However no inducible expression of the EGFP reporter molecule was detected by RT-PCR in hearts,

livers and brains of the heterozygous SOD/ROSA mice. Only a low level basal expression was observed that did not respond to doxycycline administration (Fig. 32). No expression of the rtTA tetracycline receptor was detected in this strain by RT-PCR (data not shown). Consequently these mice also did not produce homozygous offspring and further work was stopped.

Finally, SOD/TRE mice were crossed with αMHC-tTA strain and heart-specific regulation of MnSOD was achieved in SOD/αMHC tTA strain suggesting that the Tet-Off system, at least in my experimental setting was superior and more robust than the Tet-On system (discussed in detail in 4.4.4).

The starting strain SOD/TRE served as a source of heterozygous ($MnSOD^{+/-}$) mice as well as rare homozygotes ($MnSOD^{-/-}$) with early-onset mortality (around day P3). Results obtained in these animals are discussed in the following sections.

4.4.1 Complete MnSOD deficiency causes increased apoptosis in epicardium and strong up-regulation of ANF

Two groups have generated MnSOD knock-out mice on different genetic backgrounds (Li et al., 1995; Lebovitz et al. 1996; Huang et al., 2001). Homozygous mice develop dilated cardiomyopathy on a CD1 and C57BL/6 background and the latter die in uterus or around birth. On mixed genetic background of C57BL/6 and 129/Sv only 10% of animals suffer from this disease and survive up to 18 days. Transgenic mice strains that were generated in this work (both SOD/TRE and SOD/TRE tetR) originated from v6.5 hybrid ES cell line (mixed genetic background of C57BL/6 × 129/Sv mice). The obtained chimeric mice were backcrossed with C57BL/6 for one generation. Resulting offspring was crossed to homozygosity. Then, homozygous and heterozygous litter was used in further research. Hence, genetic background of the analyzed animals was still mixed C57BL/6 and 129/Sv with the prevailing contribution of the former. Homozygotes survived up to 3 days after birth and showed similar phenotypic changes as those described in previous reports (i.e. reduced body weight and size and motor disturbances).

It was expected that apoptosis would contribute to the pathology of the heart leading to death of MnSOD deficient mice. However, TUNEL-positive apoptotic cells were observed only in some areas of hearts of $MnSOD^{-/-}$ mice. These foci of apoptosis were usually found in the left ventricle wall extending from the epicardium to superficial layers of the myocardium (Fig. 22). Hearts of wild type animals of the same age lacked TUNEL-positive cells completely. It

is very unlikely that this low scale of apoptosis in MnSOD$^{-/-}$ mice contributes to the heart failure resulting in death of animals. Therefore, expression of other molecular markers of tissue pathology were tested.

ANF is a well-known marker of heart hypertrophy. However, hearts without ANF elevation as well as ANF elevation without hypertrophy were observed. Normally, its expression is confined to atria while ventricular expression is limited only to cardiac development prior to birth. It is suggested that ANF induction in ventricles is an indicator of cardiac pathogenesis that might result from abnormal tissue architecture, hemodynamic load and other stimuli, including elevated ROS (Vikstrom et al., 1998; Pimentel et al., 2001; Nakagami et al., 2003). In 3 days old MnSOD$^{-/-}$ mice ANF expression was distributed consistently throughout the heart whereas wild type animals showed expression limited largely to atria (Fig. 23). Most probably, this reflects the effect of oxidative stress in MnSOD deficient mice. As hypertrophic response is mediated by $O_2^{\bullet-}$, it can be postulated that MnSOD, through the regulation of redox state, influences cardiac growth. ANF activation, together with somewhat increased rate of apoptosis in the hearts of MnSOD$^{-/-}$ mice, certainly indicates ongoing pathological changes.

4.4.2 Heterozygous SOD/TRE mice have decreased MnSOD activity and impaired heart function

To investigate the effects of MnSOD insufficiency on heart function adult heterozygous mice were used. SOD/TRE mice were utilized since they were based on a DNA construct which, theoretically, should be silent in the absence of regulatory tetracycline receptor. In the beginning, activities of MnSOD and other antioxidant enzymes were determined to better characterize this strain and to test the effect of MnSOD insufficiency on remaining AOEs. Activity of MnSOD was 30-40% lower in SOD/TRE heterozygotes than in wild type mice depending on the tissue examined (Fig. 24). No recombinant MnSOD protein was detected by Western blot analysis in these mice (Fig. 25) arguing for an almost complete inactivity of the introduced targeting construct in the absence of a regulator. This result proves that this mouse model is free from promoter leakage (the effect that might have interfered with expression control) and promises a tight regulation of the transgene after introduction of tetracycline receptor. It was surprising to find a reduction of MnSOD activity of only 30-40% since a 50% reduction was expected in SOD/TRE heterozygotes, as it has already been shown by others (Van Remmen et al., 1999). Assuming accuracy of methods, these findings indicate

that activity of the native MnSOD can be adjusted by the cell as a consequence of oxidative stress. Indeed, it has already been shown that MnSOD heterozygous animals have decreased MnSOD activity in lungs by 40% and that hyperoxia induces MnSOD (Jackson et al., 1999; Allen and Balin, 2003; Freiberger et al., 2004). Additionally, data presented in this work indirectly point to up-regulation of native MnSOD in response to oxidative stress (Fig. 15). Furthermore, oxidative stress induced in C3H/10T1/2 cells by doxorubicin treatment stimulated MnSOD activity (data not shown). In summary, the lower than expected reduction of MnSOD activity in SOD/TRE heterozygous mice might originate from a compensatory up-regulation of the native MnSOD allele rather than from an activity of the transgene. In accordance with previous reports (Van Remmen et al., 1999), no changes in activities of other antioxidant enzymes were observed in these mice.

After determination of the AOEs status in SOD/TRE mice, a functional analysis of hearts was performed to investigate whether MnSOD heterozygosity has an impact on cardiac function. As mentioned above, MnSOD knock-out mice develop dilated cardiomyopathy but so far no studies were performed on MnSOD heterozygous mice to test the influence of MnSOD deficiency on heart performance. Echocardiographic measurements of the left ventricle showed clearly that heart function was impaired in $SOD^{+/-}$ mice. Decreased ejection fraction, fractional area change and fraction shortening together with an increased left ventricle diameter in systole (Fig. 26 and 27) indicate a moderate affection of left ventricular function. However, these changes are minor compared to a ‘true’ dilated cardiomyopathy since the left ventricle diameter in diastole as well as heart wall thickness in SOD/TRE mice did not differ from wild type controls. Nevertheless, a decline in left ventricle systolic function was evident in 6 months old animals and probably will advance with age. Hypothethical reasons for the impaired heart function are presented in the next chapter.

4.4.3 Treatment of heterozygous SOD/TRE mice with doxorubicin leads to elevation of apoptosis, ANF expression and senescence marker (SA-β-Gal)

In order to increase oxidative stress in MnSOD heterozygous mice even further, miniosmotic pumps filled with doxorubicin were implanted subcutaneously for the period of two weeks in 4.5 months old animals. The dose of 15 mg/kg caused an increase in the number of apoptotic cells in hearts of $MnSOD^{+/-}$ mice as compared to wild type. Similarly to hearts of perinatal $MnSOD^{-/-}$ mice, the majority of apoptotic cells accumulated in the epicardium and

were concentrated only in some parts of the left ventricle, while the majority of the heart showed no evidence of cell death (Fig. 28). Doxorubicin induced also a stronger expression of ANF in $MnSOD^{+/-}$ mice as compared to wild type. Although the signal for ANF in doxorubicin treated $MnSOD^{+/-}$ mice was not as strong as in $MnSOD^{-/-}$ mice, it was found in all parts of the heart (Fig. 29). The *in vivo* induction of ANF expression by doxorubicin has recently been shown to correlate with the degree of apoptosis (Bennink et al., 2004). Though, the exact role of ANF in heart pathogenesis is still not understood (induction of apoptosis in cardiomyocytes culture after ANF administration was observed (Wu et al, 1997), its expression in ventricles is a clear sign of cardiac malfunction both in $MnSOD^{-/-}$ and $MnSOD^{+/-}$ mice. However, the lack of massive apoptosis in mice of both genotypes is rather surprising. The TUNEL method detects late stages of programmed cell death, hence a gradual decline in physiological functioning of cells, which is manifested by ANF expression, might finally lead to terminal heart arrest in $MnSOD^{-/-}$ mice and worsening of heart performance in $MnSOD^{+/-}$. The decrease in mitochondrial respiration, increased proton leak, lower aconitase activity and accelerated accumulation of mitochondrial oxidative damage in MnSOD deficient mice do support this assumption (Kokoszka et al., 2001; Melov et al., 1999). In addition, dilated and hypertrophic cardiomyopathies were correlated to respiratory chain dysfunction in humans (Scaglia et al., 2004; Lev et al., 2004).

The presence of sensescence marker in vessels of $MnSOD^{+/-}$ mice most likely reflects their decreased capacity to cope with oxidative stress caused by doxorubicin administration (Fig. 30). Evidence of senescence of endothelial cells in $MnSOD^{+/-}$ mice has been provided recently (Kurz et al., 2004; Minamino et al., 2002) and *in vivo* data point to the importance of this phenomenon in living organisms subjected to oxidative stress. Here, I report that senescence also occurs in smooth muscle cells of vessels. No signs of senescence were observed in vessels of wild type mice indicating that wild type mice are capable to cope with the level of stress imposed by this drug probably by a higher MnSOD activity. In both animals no signs of SA-β-Gal staining were observed in the heart tissue mass except a faint staining in the mitral valve of $MnSOD^{+/-}$ hearts. This might be explained by the fact that heart tissue has limited mitotic capacity and therefore is less prone to senescence. Moreover, the heart is the organ which has a high MnSOD activity and the remaining functional allele might provide substantial protection in heterozygous animals. On the other hand, vascular cells might be more susceptible to induction of senescence. It is conceivable that ROS producing stimuli may in the long term increase the number of senescent endothelial and smooth muscle cells and play an important role in the pathophysiology of vascular disorders.

4.4.4 Successful generation of a mouse strain with a conditional heart-specific expression of MnSOD under control of the tetracycline system

Based on the SOD/TRE mouse strain, a SOD/αMHC tTA compound strain was established that employed the regulatory tetracycline receptor under the transcriptional control of the α–myosin heavy chain promoter. The α–MHC promoter drives heart–specific expression of the tetracycline receptor in the Tet-Off version solely in cardiac tissue. Therefore, it was anticipated that homozygous animals show the MnSOD knock-out phenotype with the exception of heart in which mitochondrial dismutase expression, in the absence of doxycycline, might approach normal levels. Unfortunately, no homozygous mice were generated so far and for this reason heterozygous animals were used to test the effectiveness of tetracycline system. Both, Northern blot hybridization and RT-PCR showed that the transgene was strongly expressed in the absence of doxycycline in SOD/αMHC tTA mice. Administration of doxycycline vitually completely suppressed the expression of MnSOD so that no MnSOD was detectable by Northern blotting. Only a faint signal which was hardly above background (i.e. SOD/TRE strain), was found by the RT-PCR (Fig. 33). At the protein level, regulation of the transgene was demonstrated by the appearance of a band of higher molecular weight (Fig. 34). Most probably, this corresponds to the active MnSOD protein, as it already did at cellular level in OFF-SOD21 cell line. Expression of the transgene in tissues other than heart were at the background level and unresponsive to doxycycline (data not shown) further corroborating the effectiveness of the system.

Homozygous SOD/αMHC tTA mice lived maximally 14 days. The expression of the αMHC tTA transgene did not influence their survival. Phenotypically, they showed the same abnormalities (reduced body size and weight, motor disturbances) as traditional knock-outs. The extension of the lifespan in SOD/TRE strain, stems probably from the introduction of a different genetic background after crossing SOD/TRE with αMHC tTA mice (the influence of the genetic background on longevity was discussed in 4.4.1). The activity of MnSOD in hearts of SOD/αMHC tTA homozygous mice remains to be determined, however, it is highly likely that MnSOD activity will be close to the level of heterozygous wild type animals. Based on the obtained data, it can be hypothesized that the lethality of MnSOD deficient mice stems from degenerative lesions in the central nervous system rather than heart failure. Motor disturbances and injuries to central nervous system were reported in MnSOD knock-out mice that survived up to two weeks (Lebovitz et al., 1996). Interestingly, attempts to rescue animals

from cardiomyopathy by means of administration of MnSOD mimetics (which do not cross blood-brain barrier) does not protect them from severe neurological pathologies (Melov et al., 1998), while administration of antioxidants that cross blood-brain barrier extends $MnSOD^{-/-}$ mice lifespan and protects them from spongiform encephalopathy. Nevertheless, these animals die of unidentified neurological disorder (Melov et al., 2001). Cultivation of $MnSOD^{-/-}$ neuronal cells *in vitro* shows that they are more susceptible to ambient oxygen than corresponding cardiomyocytes (Patel, 2003; Van Remmen et al., 2001). Another factor which might contribute to the premature death of MnSOD deficient mice was the accumulation of lipids in liver and metabolic acidosis (Li et al., 1995). However liver-specific conditional knock-out mice did not confirm previous observations and implied brain or heart failure as primary cause of mortality (Ikegami et al., 2002). SOD/αMHC tTA homozygous mice were weaker and had serious problems with walking and maintaining balance. Most probably, the level of MnSOD activity in the heart was high enough to protect them from cardiac failure but failed to prevent neurological malfunctions.

Further efforts that will take advantage of the established SOD/αMHC tTA strain will contribute to a better understanding of effects of MnSOD on brain and heart development and function. Additional crossings with mice strains carrying tissue-specifically and ubiquitously expressed tetracycline receptor in the Tet-Off version will provide models that might be useful in many areas of research.

5 CONCLUSIONS

MnSOD gain and loss of function experiments in cell culture as well as in transgenic mice led me to the following conclusions:

- Neither overexpression of MnSOD in murine fibroblasts nor its deficiency in mice led to changes in activities of the main antioxidant enzymes i.e. CuZnSOD, CAT and GPX.
- Mitochondrial dismutase is indispensable for the progression of apoptosis under certain circumstances. Lack of MnSOD in primary mouse fibroblasts inhibited hydrogen peroxide and doxorubicin induced apoptosis.
- MnSOD probably regulates programmed cell death through interference with ceramide-mediated apoptosis pathway. This was supported by two observations on doxorubicin-induced apoptosis: 1) inhibition in MnSOD null fibroblasts and 2) mild increase in MnSOD overexpressing cells.
- MnSOD, through its $O_2^{\bullet -}$ scavenging activity, may be involved in the regulation of balance between nitric oxide and peroxynitrite, hence controlling apoptosis. Experiments with doxorubicin-treated murine fibroblasts support this assumption.
- Reduction of senescence in MnSOD deficient cells implicates an important role of MnSOD in the progression of cellular aging.
- Strong up-regulation of ANF expression in hearts of homozygous SOD/TRE mice indicates that complete MnSOD deficiency leads to cardiac disorder, while the lack of massive cell death suggests that a gradual decline of cellular physiology contributes to this pathology.
- Life-long reduction in MnSOD activity in heterozygous SOD/TRE mice leads to an impairment of heart performance.
- Heterozygous SOD/TRE mice are more susceptible to oxidative stress imposed by doxorubicin. This was manifested by induction of ANF expression in the heart and senescence of endothelial and smooth muscle cells in vessels proximal to the heart.
- The conditional SOD/αMHC tTA mouse strain allows conditional heart-specific expression of MnSOD, which can be controlled by administration of doxycycline. Other organs are devoid of the transgenic MnSOD expression.

- Lethality of homozygous SOD/αMHC tTA mice and their apparent neurological problems may suggest that heart dysfunction is not the primary cause of deaths of animals lacking MnSOD.
- SOD/TRE and SOD/αMHC tTA animal models provide convenient research tools suitable for spatio-temporal studies of MnSOD deficiency.

The proposed involvement of MnSOD in the regulation of apoptosis by means of regulation of nitric oxide and peroxynitrite balance is presented on Fig. 35.

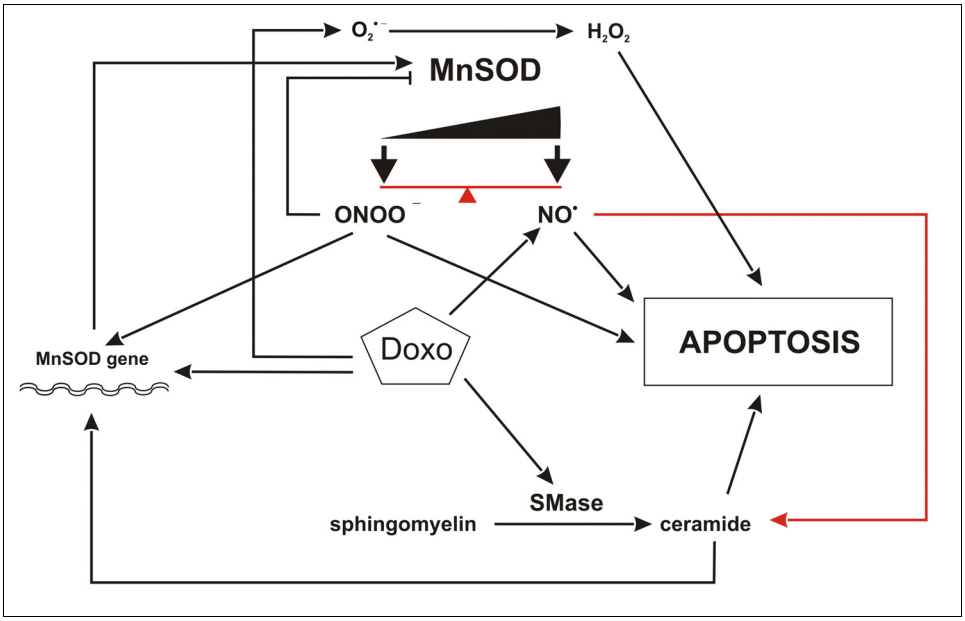

Fig. 35. Proposed involvement of MnSOD in nitric oxide and ceramide-mediated apoptosis. Black arrows depict interactions described in the literature. Elements in red show suggested mechanisms of apoptosis induction that partially emerge from the obtained data, however, stimulation of ceramide synthesis by $NO^\bullet$ has been described in the literature. Depending on concentration, $NO^\bullet$ can activate proliferation or cell death. It seems that through the stimulation of ceramide, $NO^\bullet$ at certain concentration, is able to induce apoptosis more efficiently than peroxynitrite. Further studies are necessary to prove this possibility. Abbreviations: Doxo – doxorubicin; SMase – sphingomyelinase.

Acknowledgements

I am greatly indebted to many people for collaboration and support. Katja Kölditz from the Max Planck Institute for Heart and Lung Research, Bad Nauheim, taught me to handle cell culture and the mouse colony. Henning Ebelt from the Institute of Physiological Chemistry, the University of Halle-Wittenberg, introduced me to FACS analysis and performed all echocardiography measurements. Jacek Kaczor and Wiesław Ziółkowski from the J. Śniadecki University School of Physical Education and Sport, Gdańsk, Poland, taught me determination of antioxidant enzymes' activities and helped a lot to complete this aspect of the work. Izabela Piotrowska and Michał Mielcarek from the Max Planck Institute for Heart and Lung Research, Bad Nauheim, performed *in situ* hybridization experiment and helped in many other ways. Sawa Kostin from the Max Planck Institute, Bad Nauheim, interpreted the morphology of hearts stained for senescence. I want to thank Thilo Borchardt from the Max Planck Institute for Heart and Lung Research, Bad Nauheim, for helpful advice on tetracycline expression system and handling of transgenic mouse colony. I am grateful to Gabriele Hoang for her secretarial work and helping hand in many situations.

Sincere thanks are given to all people at the Institute of Physiological Chemistry, the University of Halle-Wittenberg, for their willingness to help in various situations and for introducing me to techniques and equipment.

Finally, I would like to specially thank Dr. Eva Bober from the Institute of Physiological Chemistry, the University of Halle-Wittenberg, for giving me the opportunity to pursue the doctoral thesis in her research group. Her trust, encouragement and enthusiasm were very helpful in my work.

I would especially like to thank Prof. Thomas Braun, currently at the Max Planck Institute for Heart and Lung Research, Bad Nauheim, for helpful discussions and providing the organisational framework. His continuous availability and expertise were invaluable for successful work.

6 REFERENCES

Ausubel, F. M., Brent, R., Kingston, R. E., Moore, D. D., Seidman, J. G., Smith, J. A., Struhl, K. (1992) Current Protocols in Molecular Biology. John Wiley & Sons

Akashi, M., Hachiya, M., Paquette, R. L., Osawa, Y., Shimizu, S., Suzuki, G. (1995) Irradiation increases manganese superoxide dismutase mRNA levels in human fibroblasts. Possible mechanisms for its accumulation. *J Biol Chem* **270**: 15864-9

Allen, R. G. and Balin, A. K. (2003) Effects of oxygen on the antioxidant responses of normal and transformed cells. *Exp Cell Res* **289**: 307-16

Ambrosone, C. B., Freudenheim, J. L., Thompson, P. A., Bowman, E., Vena, J. E., Marshall, J. R., Graham, S., Laughlin, R., Nemoto, T., Shields, P. G. (1999) Manganese superoxide dismutase (MnSOD) genetic polymorphisms, dietary antioxidants, and risk of breast cancer. *Cancer Res* **59**: 602-6

Amstad, P. A., Liu, H., Ichimiya, M., Berezesky, I. K., Trump, B. F. (1997) Manganese superoxide dismutase expression inhibits soft agar growth in JB6 clone41 mouse epidermal cells. *Carcinogenesis* **18**: 479-84

Arnold, W. P., Mittal, C. K., Katsuki, S., Murad, F. (1977) Nitric oxide activates guanylate cyclase and increases guanosine 3':5'-cyclic monophosphate levels in various tissue preparations. *Proc Natl Acad Sci U S A* **74**: 3203-7

Atmaca, G. (2004) Antioxidant effects of sulfur-containing amino acids. *Yonsei Med J* **45**: 776-88

Aust, S. D., Roerig, D. L., Pederson, T. C. (1972) Evidence for superoxide generation by NADPH-cytochrome c reductase of rat liver microsomes. *Biochem Biophys Res Commun* **47**: 1133-7

Avissar, N., Ornt, D. B., Yagil, Y., Horowitz, S., Watkins, R. H., Kerl, E. A., Takahashi, K., Palmer, I. S., Cohen, H. J. (1994) Human kidney proximal tubules are the main source of plasma glutathione peroxidase. *Am J Physiol* **266**: C367-75

Baker, A. M., Oberley, L. W., Cohen, M. B. (1997) Expression of antioxidant enzymes in human prostatic adenocarcinoma. *Prostate* **32**: 229-33

Beauchamp, C. and Fridovich, I. (1971) Superoxide dismutase: improved assays and an assay applicable to acrylamide gels. *Anal Biochem* **44**: 276-87.

Becker, B. F. (1993) Towards the physiological function of uric acid. *Free Radic Biol Med* **14**: 615-31

Bergman, M., Ahnstrom, M., Palmeback, Wegman, P., Wingren, S. (2005) Polymorphism in the manganese superoxide dismutase (MnSOD) gene and risk of breast cancer in young women. *J Cancer Res Clin Oncol* **131**: 439-44

Borgstahl, G. E., Parge, H. E., Hickey, M. J., Beyer, W. F. Jr., Hallewell, R. A., Tainer, J. A. (1992) The structure of human mitochondrial manganese superoxide dismutase reveals a novel tetrameric interface of two 4-helix bundles. *Cell* **71**: 107-18

Bourdon, E., Loreau, N., Lagrost, L., Blache, D. (2005) Differential effects of cysteine and methionine residues in the antioxidant activity of human serum albumin. *Free Radic Res* **39**: 15-20

Boveris, A. and Chance, B. (1973) The mitochondrial generation of hydrogen peroxide. General properties and effect of hyperbaric oxygen. *Biochem J* **134**: 707-16

Brookes, P. S., Levonen, A. L., Shiva, S., Sarti, P., Darley-Usmar, V. M. (2002) Mitochondria: regulators of signal transduction by reactive oxygen and nitrogen species. *Free Radic Biol Med* **33**: 755-64

Butterfield, L. H., Merino, A., Golub, S. H., Shau, H. (1999) From cytoprotection to tumor suppression: the multifactorial role of peroxiredoxins. *Antioxid Redox Signal* **1**: 385-402

Cai, Q., Shu, X. O., Wen, W., Cheng, J. R., Dai, Q., Gao, Y. T., Zheng, W. (2004) Genetic polymorphism in the manganese superoxide dismutase gene, antioxidant intake, and breast cancer risk: results from the Shanghai Breast Cancer Study. *Breast Cancer Res* **6**: R647-55

Carlsson, L. M., Jonsson, J., Edlund, T., Marklund, S. L. (1995) Mice lacking extracellular superoxide dismutase are more sensitive to hyperoxia. *Proc Natl Acad Sci U S A* **92**: 6264-6268

Chang, L. Y., Slot, J. W., Geuze, H. J., Crapo, J. D. (1988) Molecular immunocytochemistry of the CuZn superoxide dismutase in rat hepatocytes. *J Cell Biol* **107**: 2169-79

Chen, Z., Oberley, T. D., Ho, Y., Chua, C. C., Siu, B., Hamdy, R. C., Epstein, C. J., Chua, B. H. (2000) Overexpression of CuZnSOD in coronary vascular cells attenuates myocardial ischemia/reperfusion injury. *Free Radic Biol Med* **29**: 589-96

Chen, Z., Siu, B., Ho, Y. S., Vincent, R., Chua, C. C., Hamdy, R. C., Chua, B. H. (1998) Overexpression of MnSOD protects against myocardial ischemia/reperfusion injury in transgenic mice. *J Mol Cell Cardiol* **30**: 2281-9

Chu, F. F., Doroshow, J. H., Esworthy, R. S. (1993) Expression, characterization, and tissue distribution of a new cellular selenium-dependent glutathione peroxidase, GSHPx-GI. *J Biol Chem* **268**: 2571-6

Church, S. L., Grant, J. W., Ridnour, L. A., Oberley, L. W., Swanson, P. E., Meltzer, P. S., Trent, J. M. (1993) Increased manganese superoxide dismutase expression suppresses the malignant phenotype of human melanoma cells. *Proc Natl Acad Sci U S A* **90**: 3113-7

Clerch, L. B. (2000) Post-transcriptional regulation of lung antioxidant enzyme gene expression. *Ann N Y Acad Sci* **899**: 103-11

Cobbs, C. S., Levi, D. S., Aldape, K., Israel, M. A. (1996) Manganese superoxide dismutase expression in human central nervous system tumors. *Cancer Res* **56**: 3192-5

Comhair, S. A., Xu, W., Ghosh, S., Thunnissen, F. B., Almasan, A., Calhoun, W. J., Janocha, A. J., Zheng, L., Hazen, S. L., Erzurum, S. C. (2005) Superoxide dismutase inactivation in pathophysiology of asthmatic airway remodeling and reactivity. *Am J Patho*. **166**: 663-74

Copin, J. C., Gasche, Y., Chan, P. H. (2000) Overexpression of copper/zinc superoxide dismutase does not prevent neonatal lethality in mutant mice that lack manganese superoxide dismutase. *Free Radic Biol Med* **28**: 1571-6

Crack, P. J., Taylor, J. M., Flentjar, N. J., de Haan, J., Hertzog, P., Iannello, R. C., Kola, I. (2001) Increased infarct size and exacerbated apoptosis in the glutathione peroxidase-1 (Gpx-1) knockout mouse brain in response to ischemia/reperfusion injury. *J Neurochem* **78**: 1389-99

Cruthirds, D. L., Saba, H., Macmillan-Crow, L. A. (2005) Overexpression of manganese superoxide dismutase protects against ATP depletion-mediated cell death of proximal tubule cells. *Arch Biochem Biophys* **437**: 96-105

Cullen, J. J., Weydert, C., Hinkhouse, M. M., Ritchie, J., Domann, F. E., Spitz, D., Oberley, L. W. (2003) The role of manganese superoxide dismutase in the growth of pancreatic adenocarcinoma. *Cancer Res* **63**: 1297-303

Darby Weydert, C. J., Smith, B. B., Xu, L., Kregel, K. C., Ritchie, J. M., Davis, C. S., Oberley, L. W. (2003) Inhibition of oral cancer cell growth by adenovirusMnSOD plus BCNU treatment. *Free Radic Biol Med* **34**: 316-29

Davies, M. J. (2005) The oxidative environment and protein damage. *Biochim Biophys Acta* **1703**: 93-109

de Haan, J. B., Cristiano, F., Iannello, R., Bladier, C., Kelner, M. J., Kola, I. (1996) Elevation in the ratio of Cu/Zn-superoxide dismutase to glutathione peroxidase activity induces features of cellular senescence and this effect is mediated by hydrogen peroxide. *Hum Mol Genet* **5**: 283-92

Dimri, G. P., Lee, X., Basile, G., Acosta, M., Scott, G., Roskelley, C., Medrano, E. E., Linskens, M., Rubelj, I., Pereira-Smith, O., Peacocke, M., Campisi, J. (1995) A biomarker that identifies senescent human cells in culture and in aging skin *in vivo*. *Proc Natl Acad Sci U S A* **92**: 9363-9367.

Dougall, W. C. and Nick, H. S. (1991) Manganese superoxide dismutase: a hepatic acute phase protein regulated by interleukin-6 and glucocorticoids. *Endocrinology* **129**: 2376-84

Dragatsis, I., Zeitlin, S. (2001) A method for the generation of conditional gene repair mutations in mice. *Nucleic Acids Res* **29**: E10

Drane, P., Bravard, A., Bouvard, V., May E. (2001) Reciprocal down-regulation of p53 and SOD2 gene expression-implication in p53 mediated apoptosis. *Oncogene* **20**: 430-9

Dringen, R., Pawlowski, P. G., Hirrlinger, J. (2005) Peroxide detoxification by brain cells. *J Neurosci Res* **79**: 157-65

Dröge, W. (2002) Free radicals in the physiological control of cell function. *Physiol Rev* **82**: 47-95

Duan, H., Zhang, H. J., Yang, J. Q., Oberley, L. W., Futscher, B. W., Domann, F. E. (2003) MnSOD up-regulates maspin tumor suppressor gene expression in human breast and prostate cancer cells. *Antioxid Redox Signal* **5**: 677-88

Elchuri, S., Oberley, T. D., Qi, W., Eisenstein, R. S., Jackson Roberts, L., Van Remmen, H., Epstein, C. J., Huang, T. T. (2005) CuZnSOD deficiency leads to persistent and widespread oxidative damage and hepatocarcinogenesis later in life. *Oncogene* **24**: 367-80

Epperly, M. W., Bernarding, M., Gretton, J., Jefferson, M., Nie, S., Greenberger, J. S. (2003) Overexpression of the transgene for manganese superoxide dismutase (MnSOD) in 32D cl 3 cells prevents apoptosis induction by TNF-alpha, IL-3 withdrawal, and ionizing radiation. *Exp Hematol* **31**: 465-74

Esworthy, R. S., Ho, Y. S., Chu, F. F. (1997) The Gpx1 gene encodes mitochondrial glutathione peroxidase in the mouse liver. *Arch Biochem Biophys* **340**: 59-63

Evans, M. D. and Cooke, M. S. (2004) Factors contributing to the outcome of oxidative damage to nucleic acids. *Bioessays* **26**: 533-42

Finkel, T. and Holbrook, N. J. (2000) Oxidants, oxidative stress and the biology of ageing. *Nature* **408**: 239-247

Fogli, S., Nieri, P., Breschi, M. C. (2004) The role of nitric oxide in anthracycline toxicity and prospects for pharmacologic prevention of cardiac damage. *FASEB J* **18**: 664-75

Folz, R. J., Abushamaa, A. M., Bland, R. D. (1999) Extracellular superoxide dismutase in the airways of transgenic mice reduces inflammation and attenuates lung toxicity following hyperoxia. *J Clin Invest* **103**: 1055-1066

Folz, R. J. and Crapo, J. D. (1994) Extracellular superoxide dismutase (SOD3): tissue-specific expression, genomic characterization, and computer assisted sequence analysis of the human EC-SOD gene. *Genomics* **22**: 162-171

Folz, R. J., Guan, J., Seldin, M. F., Oury, T. D., Enghild, J. J., Crapo, J. D. (1997) Mouse extracellular superoxide dismutase: primary structure, tissue-specific gene expression, chromosomal localization, and lung in situ hybridization. *Am J Respir Cell Mol Biol* **17**: 393-403

Foresti, R., Green, C. J., Motterlini, R. (2004) Generation of bile pigments by haem oxygenase: a refined cellular strategy in response to stressful insults. *Biochem Soc Symp* **71**: 177-92

Forsberg, L., de Faire, U., Morgenstern, R. (2001) Oxidative stress, human genetic variation, and disease. *Arch Biochem Biophys* **389**: 84-93

Freiberger, J., Coulombe, K., Suliman, H., Carraway, M., Piantadosi, C. (2004) Superoxide dismutase responds to hyperoxia in rat hippocampus. *Undersea Hyperb Med* **31**: 227-32

Fridovich, I. (1975) Superoxide dismutases. *Annu Rev Biochem* **44**: 147-59

Fridovich, I. (2004) Mitochondria: are they the seat of senescence? *Aging Cell* **3**: 13-6

Fridovich, I. and Freeman, B. (1986) Antioxidant defenses in the lung. *Annu Rev Physiol* **48**: 693-702

Fujimura, M., Morita-Fujimura, Y., Kawase, M., Copin, J. C., Calagui, B., Epstein, C. J., Chan, P. H. (1999) Manganese superoxide dismutase mediates the early release of mitochondrial cytochrome C and subsequent DNA fragmentation after permanent focal cerebral ischemia in mice. *J Neurosci* **19**: 3414-22

Galeotti, T., Wohlrab, H., Borrello, S., De Leo, M. E. (1989) Messenger RNA for manganese and copper-zinc superoxide dismutases in hepatomas: correlation with degree of differentiation. *Biochem Biophys Res Commun* **165**: 581-9

Geller, B. L. and Winge, D. R. (1982) Rat liver Cu,Zn-superoxide dismutase. Subcellular location in lysosomes. *J Biol Chem* **257**: 8945-52

Giordano, F. J. (2005) Oxygen, oxidative stress, hypoxia, and heart failure. *J Clin Invest* **115**: 500-8

Guo, Z., Van Remmen, H., Yang, H., Chen, X., Mele, J., Vijg, J., Epstein, C. J., Ho, Y. S., Richardson, A. (2001) Changes in expression of antioxidant enzymes affect cell-mediated LDL oxidation and oxidized LDL-induced apoptosis in mouse aortic cells. *Arterioscler Thromb Vasc Biol* **21**: 1131-8

Hamilton, M. L., Van Remmen, H., Drake, J. A., Yang, H., Guo, Z. M., Kewitt, K., Walter, C. A., Richardson, A. (2001) Does oxidative damage to DNA increase with age? *Proc Natl Acad Sci U S A* **98**: 10469-74

Harris, N., Costa, V., MacLean, M., Mollapour, M., Moradas-Ferreira, P., Piper, P. W. (2003) Mnsod overexpression extends the yeast chronological (G(0)) life span but acts independently of Sir2p histone deacetylase to shorten the replicative life span of dividing cells. *Free Radic Biol Med* **34**: 1599-606

Hendrickson, D. J., Fisher, J. H., Jones, C., Ho, Y.-S. (1990) Regional localization of human extracellular superoxide dismutase gene to 4pter-q21. *Genomics* **8**: 736-738

Hjalmarsson, K., Marklund, S. L., Engstrom, A., Edlund, T. (1987) Isolation and sequence of complementary DNA encoding human extracellular superoxide dismutase. *Proc Natl Acad Sci U S A* **84**: 6340-6344

Ho, Y. S. (2002) Transgenic and knockout models for studying the role of lung antioxidant enzymes in defense against hyperoxia. *Am J Respir Crit Care Med* **166**: S51-6

Ho, Y. S., Dey, M. S., Crapo, J. D. (1996) Antioxidant enzyme expression in rat lungs during hyperoxia. *Am J Physiol* **270**: L810-8

Ho, Y. S., Magnenat, J. L., Gargano, M., Cao, J. (1998) The nature of antioxidant defense mechanisms: a lesson from transgenic studies. *Environ Health Perspect* **5**: 1219-28

Ho, Y. S., Xiong, Y., Ma, W., Spector, A., Ho, D. S. (2004) Mice lacking catalase develop normally but show differential sensitivity to oxidant tissue injury. *J Biol Chem* **279**: 32804-12

Honda, K., Smith, M. A., Zhu, X., Baus, D., Merrick, W. C., Tartakoff, A. M., Hattier, T., Harris, P. L., Siedlak, S. L., Fujioka, H., Liu, Q., Moreira, P. I., Miller, F. P., Nunomura, A., Shimohama, S., Perry, G. (2005) Ribosomal RNA in Alzheimer disease is oxidized by bound redox-active iron. *J Biol Chem* **280**: 20978-86

Huang, T. T., Carlson, E. J., Gillespie, A. M., Shi, Y., Epstein, C. J. (2000) Ubiquitous overexpression of CuZn superoxide dismutase does not extend life span in mice. *J Gerontol A Biol Sci Med Sci* **55**: B5-9

Huang, T. T., Carlson, E. J., Kozy, H. M., Mantha, S., Goodman, S. I., Ursell, P. C., Epstein, C. J. (2001) Genetic modification of prenatal lethality and dilated cardiomyopathy in Mn superoxide dismutase mutant mice. *Free Radic Biol Med* **31**: 1101-10

Hudson, E. K., Hogue, B. A., Souza-Pinto, N. C., Croteau, D. L., Anson, R. M., Bohr, V. A., Hansford, R. G. (1998) Age-associated change in mitochondrial DNA damage. *Free Radic Res* **29**: 573-9

Huret, J. L., Delabar, J. M., Marlhens, F., Aurias, A., Nicole, A., Berthier, M., Tanzer, J., Sinet, P. M. (1987) Down syndrome with duplication of a region of chromosome 21 containing the CuZn superoxide dismutase gene without detectable karyotypic abnormality. *Hum Genet* **75**: 251-7

Hussain, S. P., Amstad, P., He, P., Robles, A., Lupold, S., Kaneko, I., Ichimiya, M., Sengupta, S., Mechanic, L., Okamura, S., Hofseth, L. J., Moake, M., Nagashima, M., Forrester, K. S., Harris, C. C. (2004) p53-induced up-regulation of MnSOD and GPx but not catalase increases oxidative stress and apoptosis. *Cancer Res* **64**: 2350-6

Ikegami, T., Suzuki, Y., Shimizu, T., Isono, K., Koseki, H., Shirasawa, T. (2002) Model mice for tissue-specific deletion of the manganese superoxide dismutase (MnSOD) gene. *Biochem Biophys Res Commun* **296**: 729-36

Ilizarov, A. M., Koo, H. C., Kazzaz, J. A., Mantell, L. L., Li, Y., Bhapat, R., Pollack, S., Horowitz, S., Davis, J. M. (2001) Overexpression of manganese superoxide dismutase protects lung epithelial cells against oxidant injury. *Am J Respir Cell Mol Biol* **24**: 436-41

Jackson, S. H., Devadas, S., Kwon, J., Pinto, L. A., Williams, M. S. (2004) T cells express a phagocyte-type NADPH oxidase that is activated after T cell receptor stimulation. *Nat Immunol* **5**: 818-27

Jackson, R. M., Helton, E. S., Viera, L., Ohman, T. (1999) Survival, lung injury, and lung protein nitration in heterozygous MnSOD knockout mice in hyperoxia. *Exp Lung Res* **25**: 631-46

Jackson, R. M., Parish, G., Helton, E. S. (1998) Peroxynitrite modulates MnSOD gene expression in lung epithelial cells. *Free Radic Biol Med* **25**: 463-72

Janssen, A. M., Bosman, C. B., Kruidenier, L., Griffioen, G., Lamers, C. B., van Krieken, J. H., van de Velde, C. J., Verspaget, H. W. (1999) Superoxide dismutases in the human colorectal cancer sequence. *J Cancer Res Clin Oncol* **125**: 327-35

Janssen, A. M., Bosman, C. B., Sier, C. F., Griffioen, G., Kubben, F. J., Lamers, C. B., van Krieken, J. H., van de Velde, C. J., Verspaget, H. W. (1998) Superoxide dismutases in relation to the overall survival of colorectal cancer patients. *Br J Cancer* **78**: 1051-7

Janssen, A. M., Bosman, C. B., van Duijn, W., Oostendorp-van de Ruit, M. M., Kubben, F. J., Griffioen, G., Lamers, C. B., van Krieken, J. H., van de Velde, C. J., Verspaget, H. W. (2000) Superoxide dismutases in gastric and esophageal cancer and the prognostic impact in gastric cancer. *Clin Cancer Res* **6**: 3183-92

Jones, S. P., Hoffmeyer, M. R., Sharp, B. R., Ho, Y. S., Lefer, D. J. (2003) Role of intracellular antioxidant enzymes after in vivo myocardial ischemia and reperfusion. *Am J Physiol Heart Circ Physiol* **284**: H277-82

Jones, P. L., Kucera, G., Gordon, H., Boss, J. M. (1995) Cloning and characterization of the murine manganous superoxide dismutase-encoding gene. *Gene* **153**: 155-61

Jones, P. L., Ping, D., Boss, J. M. (1997) Tumor necrosis factor alpha and interleukin-1beta regulate the murine manganese superoxide dismutase gene through a complex intronic enhancer involving C/EBP-beta and NF-kappaB. *Mol Cell Biol* **17**: 6970-81

Jornot, L. and Junod, A. F. (1995) Differential regulation of glutathione peroxidase by selenomethionine and hyperoxia in endothelial cells. *Biochem J* **306**: 581-7

Kahl, R., Kampkötter, A., Wätjen, W., Chovolou, Y. (2004) Antioxidant enzymes and apoptosis. *Drug Metab Rev* **36**: 747-62

Kang, Y. J., Chen, Y., Epstein, P. N. (1996) Suppression of doxorubicin cardiotoxicity by overexpression of catalase in the heart of transgenic mice. *J Biol Chem* **271**: 12610-6

Keele, B. B. Jr., McCord, J. M., Fridovich, I. (1971) Further characterization of bovine superoxide dismutase and its isolation from bovine heart. *J Biol Chem* **246**: 2875-80

Keller, G. A., Warner, T. G., Steimer, K. S., Hallewell, R. A. (1991) Cu,Zn superoxide dismutase is a peroxisomal enzyme in human fibroblasts and hepatoma cells. *Proc Natl Acad Sci U S A* **88**: 7381-5

Kinnula, V. L., Crapo, J. D., Raivio, K. O. (1995) Generation and disposal of reactive oxygen metabolites in the lung. *Lab Invest* **73**: 3-19

Kinouchi, H., Epstein, C. J., Mizui, T., Carlson, E., Chen, S. F., Chan, P. K. (1991) Attenuation of focal cerebral ischemic injury in transgenic mice overexpressing CuZn superoxide dismutase. *Proc Natl Acad Sci U S A* **88**: 11158-11162

Kinscherf, R., Claus, R., Wagner, M., Gehrke, C., Kamencic, H., Hou, D., Nauen, O., Schmiedt, W., Kovacs, G., Pill, J., Metz, J., Deigner, H.P. (1998) Apoptosis caused by oxidized LDL is manganese superoxide dismutase and p53 dependent. *FASEB J* **12**: 461-7

Kinscherf, R., Deigner, H. P., Usinger, C., Pill, J., Wagner, M., Kamencic, H., Hou, D., Chen, M., Schmiedt, W., Schrader, M., Kovacs, G., Kato, K., Metz, J. (1997) Induction of mitochondrial manganese superoxide dismutase in macrophages by oxidized LDL: its relevance in atherosclerosis of humans and heritable hyperlipidemic rabbits. *FASEB J* **11**: 1317-28

Knirsch, L. and Clerch, L. B. (2001) Tyrosine phosphorylation regulates manganese superoxide dismutase (MnSOD) RNA-binding protein activity and MnSOD protein expression. *Biochemistry* **40**: 7890-5

Kocabas, N. A., Sardas, S., Cholerton, S., Daly, A. K., Elhan, A. H., Karakaya, A. E. (2005) Genetic polymorphism of manganese superoxide dismutase (MnSOD) and breast cancer susceptibility. *Cell Biochem Funct* **23**: 73-6

Kokoszka, J. E., Coskun, P., Esposito, L. A., Wallace, D. C. (2001) Increased mitochondrial oxidative stress in the Sod2 (+/-) mouse results in the age-related decline of mitochondrial function culminating in increased apoptosis. *Proc Natl Acad Sci U S A* **98**: 2278-83

Koo, H. C., Davis, J. M., Li, Y., Hatzis, D., Opsimos, H., Pollack, S., Strayer, M. S., Ballard, P. L., Kazzaz, J. A. (2005) Effects of transgene expression of superoxide dismutase and glutathione peroxidase on pulmonary epithelial cell growth in hyperoxia. *Am J Physiol Lung Cell Mol Physiol* **288**: L718-26

Kurz, D. J., Decary, S., Hong, Y., Trivier, E., Akhmedov, A., Erusalimsky, J. D. (2004) Chronic oxidative stress compromises telomere integrity and accelerates the onset of senescence in human endothelial cells. *J Cell Sci* **117**: 2417-26

Lebovitz, R. M., Zhang, H., Vogel, H., Cartwright, J. Jr., Dionne, L., Lu, N., Huang, S., Matzuk, M. M. (1996) Neurodegeneration, myocardial injury, and perinatal death in mitochondrial superoxide dismutase-deficient mice. *Proc Natl Acad Sci U S A* **93**: 9782-7

Lee, J. M. and Johnson, J. A. (2004) An important role of Nrf2-ARE pathway in the cellular defense mechanism. *J Biochem Mol Biol* **37**: 139-43

Lev, D., Nissenkorn, A., Leshinsky-Silver, E., Sadeh, M., Zeharia, A., Garty, B. Z., Blieden, L., Barash, V., Lerman-Sagie, T. (2004) Clinical presentations of mitochondrial cardiomyopathies. *Pediatr Cardiol* **25**: 443-50

Li, H., Kantoff, P. W., Giovannucci, E., Leitzmann, M. F., Gaziano, J. M., Stampfer, M. J., Ma, J. (2005) Manganese superoxide dismutase polymorphism, prediagnostic antioxidant status, and risk of clinical significant prostate cancer. *Cancer Res* **65**: 2498-504

Li, J. J., Oberley L. W., Fan M., Colburn N. H. (1998) Inhibition of AP-1 and NF-kappaB by manganese-containing superoxide dismutase in human breast cancer cells. *FASEB J* **12**: 1713-23

Li, J. J., Oberley, L. W., St Clair, D. K., Ridnour, L. A., Oberley, T. D. (1995) Phenotypic changes induced in human breast cancer cells by overexpression of manganese-containing superoxide dismutase. *Oncogene* **10**: 1989-2000

Li, N., Oberley, T. D., Oberley, L. W., Zhong, W. (1998) Inhibition of cell growth in NIH/3T3 fibroblasts by overexpression of manganese superoxide dismutase: mechanistic studies. *J Cell Physiol* **175**: 359-69

Li, N., Oberley, T. D., Oberley, L. W., Zhong, W. (1998) Overexpression of manganese superoxide dismutase in DU145 human prostate carcinoma cells has multiple effects on cell phenotype. *Prostate* **35**: 221-33

Li, Y., Huang, T. T., Carlson, E. J., Melov, S., Ursell, P. C., Olson, J. L., Noble, L. J., Yoshimura, M. P., Berger, C., Chan, P. H., Wallace, D. C., Epstein, C. J. (1995) Dilated cardiomyopathy and neonatal lethality in mutant mice lacking manganese superoxide dismutase. *Nat Genet* **11**: 376-81

Lim, S., Groneberg, D., Fischer, A., Oates, T., Caramori, G., Mattos, W., Adcock, I., Barnes, P. J., Chung, K. F. (2000) Expression of heme oxygenase isoenzymes 1 and 2 in normal and asthmatic airways: effect of inhaled corticosteroids. *Am J Respir Crit Care Med* **162**: 1912-8

Liochev, S. I. and Fridovich, I. (1994) The role of $O2^{\bullet-}$ in the production of $HO^{\bullet}$: in vitro and in vivo. *Free Radic Biol Med* **16**: 29-33

Liu, R., Oberley, T. D., Oberley, L. W. (1997) Transfection and expression of MnSOD cDNA decreases tumor malignancy of human oral squamous carcinoma SCC-25 cells. *Hum Gene Ther* **8**: 585-95

Loenders, B., van Mechelen, E., Nicolai, S., Buyssens, N., van Osselaer, N., Jorens, P. G., Willems, J., Herman, A. G., Slegers, H. (1998) Localization of extracellular superoxide dismutase in rat lung: neutrophils and macrophages as carriers of the enzyme. *Free Rad Biol Med* **24**: 1097-1106

Majima, H. J., Oberley, T. D., Furukawa, K., Mattson, M. P., Yen, H. C., Szweda, L. I., St Clair, D. K. (1998) Prevention of mitochondrial injury by manganese superoxide dismutase reveals a primary mechanism for alkaline-induced cell death. *J Biol Chem* **273**: 8217-24

Manna, S. K., Zhang, H. J., Yan, T., Oberley, L. W., Aggarwal, B. B. (1998) Overexpression of manganese superoxide dismutase suppresses tumor necrosis factor-induced apoptosis and activation of nuclear transcription factor-κB and activated protein-1. *J Biol Chem* **273**: 13245-13254

Marklund S. L. (1984) Extracellular superoxide dismutase in human tissues and human cell lines. *J Clin Invest* **74**: 1398-1403

Marklund, S. L. (1992) Regulation of cytokines of extracellular superoxide dismutase and other superoxide dismutase isoenzymes in fibroblasts. *J Biol Chem* **267**: 6696-6701

Marklund, S. L., Holme, E., Hellner, L. (1982) Superoxide dismutase in extracellular fluids. *Clin Chim Acta* **126**: 41-51

Matsuda, Y., Higashiyama, S., Kijima, Y., Suzuki, K., Kawano, K., Akiyama, M., Kawata, S., Tarui, S., Deutsch, H. F., Taniguchi, N. (1990) Human liver manganese superoxide dismutase. Purification and crystallization, subunit association and sulfhydryl reactivity. *Eur J Biochem* **194**: 713-20

McCord, J. M., Fridovich, I. (1969) Superoxide dismutase: an enzymic function for erythrocuprein (hemocuprein). *J Biol Chem* **244**: 6049-6055

Meagher, E. A. and FitzGerald, G. A. (2000) Indices of lipid peroxidation in vivo: strengths and limitations. *Free Radic Biol Med* **28**: 1745-50

Melendez, J. A., Melathe, R. P., Rodriguez, A. M., Mazurkiewicz, J. E., Davies, K. J. (1999) Nitric oxide enhances the manganese superoxide dismutase-dependent suppression of proliferation in HT-1080 fibrosarcoma cells. *Cell Growth Differ* **10**: 655-64

Melov, S., Coskun, P., Patel, M., Tuinstra, R., Cottrell, B., Jun, A. S., Zastawny, T. H., Dizdaroglu, M., Goodman, S. I., Huang, T. T., Miziorko, H., Epstein, C. J., Wallace, D. C. (1999) Mitochondrial disease in superoxide dismutase 2 mutant mice. *Proc Natl Acad Sci U S A* **96**: 846-51

Melov, S., Doctrow, S. R., Schneider, J. A., Haberson, J., Patel, M., Coskun, P. E., Huffman, K., Wallace, D. C., Malfroy, B. (2001) Lifespan extension and rescue of spongiform encephalopathy in superoxide dismutase 2 nullizygous mice treated with superoxide dismutase-catalase mimetics. *J Neurosci* **21**: 8348-53

Melov, S., Schneider, J. A., Day, B. J., Hinerfeld, D., Coskun, P., Mirra, S. S., Crapo, J. D., Wallace, D. C. (1998) A novel neurological phenotype in mice lacking mitochondrial manganese superoxide dismutase. *Nat Genet* **18**: 159-63

Meyers, E. N., Lewandoski, M., Martin G. R. (1998) An Fgf8 mutant allelic series generated by Cre- and Flp-mediated recombination. *Nat Genet* **18**: 136-41.

Meyrick, B. and Magnuson, M. A. (1994) Identification and functional characterization of the bovine manganous superoxide dismutase promoter. *Am J Respir Cell Mol Biol* **10**: 113-21

Miles, A. T., Hawksworth, G. M., Beattie, J. H., Rodilla, V. (2000) Induction, regulation, degradation, and biological significance of mammalian metallothioneins. *Crit Rev Biochem Mol Biol* **35**: 35-70

Millikan, R. C., Player, J., de Cotret, A. R., Moorman, P., Pittman, G., Vannappagari, V., Tse, C. K., Keku, T. (2004) Manganese superoxide dismutase Ala-9Val polymorphism and risk of breast cancer in a population-based case-control study of African Americans and whites. *Breast Cancer Res* **6**: R264-74

Minamino, T., Miyauchi, H., Yoshida, T., Ishida, Y., Yoshida, H., Komuro, I. (2002) Endothelial cell senescence in human atherosclerosis: role of telomere in endothelial dysfunction. *Circulation* **105**: 1541-4

Misra, H. P. and Fridovich, I. (1972) The generation of superoxide radical during the autoxidation of hemoglobin. *J Biol Chem* **247**: 6960-2

Mitrunen, K., Sillanpaa, P., Kataja, V., Eskelinen, M., Kosma, V. M., Benhamou, S., Uusitupa, M., Hirvonen, A. (2001) Association between manganese superoxide dismutase (MnSOD) gene polymorphism and breast cancer risk. *Carcinogenesis* **22**: 827-9

Mittal, C. K. and Murad, F. (1977) Activation of guanylate cyclase by superoxide dismutase and hydroxyl radical: a physiological regulator of guanosine 3',5'-monophosphate formation. *Proc Natl Acad Sci U S A* **74**: 4360-4

Mylonas, C. and Kouretas, D. (1999) Lipid peroxidation and tissue damage. *In Vivo* **13**: 295-309

Nakagami, H., Takemoto, M., Liao, J. K. (2003) NADPH oxidase-derived superoxide anion mediates angiotensin II-induced cardiac hypertrophy. *J Mol Cell Cardiol* **35**: 851-9

Nakagawa, Y. (2004) Role of mitochondrial phospholipid hydroperoxide glutathione peroxidase (PHGPx) as an antiapoptotic factor. *Biol Pharm Bull* **27**: 956-60

Nakano, T., Oka, K., Taniguchi, N. (1996) Manganese superoxide dismutase expression correlates with p53 status and local recurrence of cervical carcinoma treated with radiation therapy. *Cancer Res* **56**: 2771-5

Nelson, K. K., Ranganathan, A. C., Mansouri, J., Rodriguez, A. M., Providence, K. M., Rutter, J. L., Pumiglia, K., Bennett, J. A., Melendez, J. A. (2003) Elevated sod2 activity augments matrix metalloproteinase expression: evidence for the involvement of endogenous hydrogen peroxide in regulating metastasis. *Clin Cancer Res* **9**: 424-32

Nilakantan, V., Zhou, X., Hilton, G., Roza, A. M., Adams, M. B., Johnson, C. P., Pieper, G. M. (2005) Hierarchical change in antioxidant enzyme gene expression and activity in acute cardiac rejection: role of inducible nitric oxide synthase. *Mol Cell Biochem* **270**: 39-47

Nishida, S., Akai, F., Iwasaki, H., Hosokawa, K., Kusunoki, T., Suzuki, K., Taniguchi, N., Hashimoto, S., Tamura, T. T. (1993) Manganese superoxide dismutase content and localization in human thyroid tumours. *J Pathol* **169**: 341-5

Nunomura, A., Chiba S., Lippa, C. F., Cras, P., Kalaria, R. N., Takeda, A., Honda, K., Smith, M. A., Perry, G. (2004) Neuronal RNA oxidation is a prominent feature of familial Alzheimer's disease. *Neurobiol Dis* **17**: 108-13

Ohman, T., Parish, G., Jackson, R. M. (1999) Hypoxic modulation of manganese superoxide dismutase promoter activity and gene expression in lung epithelial cells. *Am J Respir Cell Mol Biol* **21**: 119-27

Okado-Matsumoto, A. and Fridovich, I. (2001) Subcellular distribution of superoxide dismutases (SOD) in rat liver: Cu,Zn-SOD in mitochondria. *J Biol Chem* **276**: 38388-93

Orrell, R. W., Habgood, J. J., Gardiner, I., King, A. W., Bowe, F. A., Hallewell, R. A., Marklund, S. L., Greenwood, J., Lane, R. J., deBelleroche, J. (1997) Clinical and functional investigation of 10 missense mutations and a novel frameshift insertion mutation of the gene for copper-zinc superoxide dismutase in UK families with amyotrophic lateral sclerosis. *Neurology* **48**: 746-51

Ough, M., Lewis, A., Zhang, Y., Hinkhouse, M. M., Ritchie, J. M., Oberley, L. W., Cullen, J. J. (2004) Inhibition of cell growth by overexpression of manganese superoxide dismutase (MnSOD) in human pancreatic carcinoma. *Free Radic Res* **38**: 1223-33

Oury, T. D., Day, B. J., Crapo, J. D. (1996) Extracellular superoxide dismutase in vessels and airways of humans and baboons. *Free Radic Biol Med* **20**: 957-965

Oury, T. D., Day, B. J., Crapo, J. D. (1996) Extracellular superoxide dismutase: a regulator of nitric oxide bioavailability. *Lab Invest* **75**: 617-636

Pahan, K., Dobashi, K., Ghosh, B., Singh, I. (1999) Induction of the manganese superoxide dismutase gene by sphingomyelinase and ceramide. *J Neurochem* **73**: 513-20

Pani, G., Bedogni, B., Anzevino, R., Colavitti, R., Palazzotti, B., Borrello, S., Galeotti, T. (2000) Deregulated manganese superoxide dismutase expression and resistance to oxidative injury in p53-deficient cells. *Cancer Res* **60**: 4654-60

Parkes, T. L., Elia, A. J., Dickinson, D., Hilliker, A. J., Phillips, J. P., Boulianne, G. L. (1998) Extension of Drosophila lifespan by overexpression of human SOD1 in motorneurons. *Nat Genet* **19**: 171-4

Patel, M. N. (2003) Metalloporphyrins improve the survival of Sod2-deficient neurons. *Aging Cell* **2**: 219-22

Patton, S. E., Rosen, G. M., Rauckman, E. J. (1980) Superoxide production by purified hamster hepatic nuclei. *Mol Pharmacol* **18**: 588-93

Pimentel, D. R., Amin, J. K., Xiao, L., Miller, T., Viereck, J., Oliver-Krasinski, J., Baliga, R., Wang, J., Siwik, D. A., Singh, K., Pagano, P., Colucci, W. S., Sawyer, D. B. (2001) Reactive oxygen species mediate amplitude-dependent hypertrophic and apoptotic responses to mechanical stretch in cardiac myocytes. *Circ Res* **89**: 453-60

Plymate, S. R., Haugk, K. H., Sprenger, C. C., Nelson, P. S., Tennant, M. K., Zhang, Y., Oberley, L. W., Zhong, W., Drivdahl, R., Oberley, T. D. (2003) Increased manganese superoxide dismutase (SOD-2) is part of the mechanism for prostate tumor suppression by Mac25/insulin-like growth factor binding-protein-related protein-1. *Oncogene* **22**: 1024-34

Powers, S. K., Criswell, D., Lawler, J., Ji, L. L., Martin, D., Herb, R. A., Dudley, G. (1994) Influence of exercise and fiber type on antioxidant enzyme activity in rat skeletal muscle. *Am J Physiol* **266**(2 Pt 2): R375-80

Powers, S. K., Ji, L. L., Leeuwenburgh, C. (1999) Exercise training-induced alterations in skeletal muscle antioxidant capacity: a brief review. *Med Sci Sports Exerc* **31**: 987-97

Powis, G. and Montfort, W. R. (2001) Properties and biological activities of thioredoxins. *Annu Rev Biophys Biomol Struct* **30**: 421-55

Pryor, W. A. (1986) Oxy-radicals and related species: their formation, lifetimes, and reactions. *Annu Rev Physiol* **48**: 657-67

Quan, F., Korneluk, R. G., Tropak, M. B., Gravel, R. A. (1986) Isolation and characterization of the human catalase gene. *Nucleic Acids Res* **14**: 5321-35

Radi, R., Turrens, J. F., Chang, L. Y., Bush, K. M., Crapo, J. D., Freeman, B. A. (1991) Detection of catalase in rat heart mitochondria. *J Biol Chem* **266**: 22028-34

Radomski, M. W., Palmer, R. M., Moncada, S. (1987) The anti-aggregating properties of vascular endothelium: interactions between prostacyclin and nitric oxide. *Br J Pharmacol* **92**: 639-46

Raineri, I., Carlson, E. J., Gacayan, R., Carra, S., Oberley, T. D., Huang, T. T., Epstein, C. J. (2001) Strain-dependent high-level expression of a transgene for manganese superoxide dismutase is associated with growth retardation and decreased fertility. *Free Radic Biol Med* **31**: 1018-30

Raineri, I., Huang, T. T., Epstein, C. J., Epstein, L. B. (1996) Antisense manganese superoxide dismutase mRNA inhibits the antiviral action of interferon-gamma and interferon-alpha. *J Interferon Cytokine Res* **16**: 61-8

Razavi, H. M., Hamilton, J. A., Feng, Q. (2005) Modulation of apoptosis by nitric oxide: implications in myocardial ischemia and heart failure. *Pharmacol Ther* **106**: 147-162

Reiter, R. J. (1995) Oxidative processes and antioxidative defense mechanisms in the aging brain. *FASEB J* **9**: 526-33

Reiter, R. J., Tan, D. X., Cabrera, J., D'Arpa, D. (1999) Melatonin and tryptophan derivatives as free radical scavengers and antioxidants. *Adv Exp Med Biol* **467**: 379-87

Rice-Evans, C. (2001) Flavonoid antioxidants. *Curr Med Chem* **8**: 797-807

Rodriguez, A. M., Carrico, P. M., Mazurkiewicz, J. E., Melendez, J. A. (2000) Mitochondrial or cytosolic catalase reverses the MnSOD-dependent inhibition of proliferation by enhancing respiratory chain activity, net ATP production, and decreasing the steady state levels of H_2O_2. *Free Radic Biol Med* **29**: 801-13

Sambrook, J., Fritsch, E. F., and Maniatis, T. (1989) Molecular Cloning: A LaboartoryManual. CSHL, Cold Spring Harbor

Sandstrom, J., Carlsson, L., Marklund, S. L., Edlund, T. (1992) The heparin-binding domain of extracellular superoxide dismutase C and formation of variants with reduced heparin affinity. *J Biol Chem* **267**: 18205-18209

Sayed-Ahmed, M. M., Khattab, M. M., Gad, M. Z., Osman, A. M. (2001) Increased plasma endothelin-1 and cardiac nitric oxide during doxorubicin-induced cardiomyopathy. *Pharmacol Toxicol* **89**: 140-4

Scaglia, F., Towbin, J. A., Craigen, W. J., Belmont, J. W., Smith, E. O., Neish, S. R., Ware, S. M., Hunter, J. V., Fernbach, S. D., Vladutiu, G. D., Wong, L. J., Vogel, H. (2004) Clinical spectrum, morbidity, and mortality in 113 pediatric patients with mitochondrial disease. *Pediatrics* **114**: 925-31

Shackelford, R. E., Kaufmann, W. K., Paules, R. S. (2000) Oxidative stress and cell cycle checkpoint function. *Free Radic Biol Med* **28**: 1387-404

Shull, S., Heintz, N. H., Periasamy, M., Manohar, M., Janssen, Y. M., Marsh, J. P., Mossman, B. T. (1991) Differential regulation of antioxidant enzymes in response to oxidants. *J Biol Chem* **266**: 24398-403

Skulachev, V. P. (1997) Aging is a specific biological function rather than the result of a disorder in complex living systems: biochemical evidence in support of Weismann's hypothesis. *Biochemistry (Mosc)* **62**: 1191-5

Stamler, J. S., Singel, D. J., Loscalzo, J. (1992) Biochemistry of nitric oxide and its redox-activated forms. *Science* **258**: 1898-902

Sturtz, L. A., Diekert, K., Jensen, L. T., Lill, R., Culotta, V. C. (2001) A fraction of yeast Cu,Zn-superoxide dismutase and its metallochaperone, CCS, localize to the intermembrane space of mitochondria. A physiological role for SOD1 in guarding against mitochondrial oxidative damage. *J Biol Chem* **276**: 38084-9

Sun, Y., Colburn, N. H., Oberley, L. W. (1993) Decreased expression of manganese superoxide dismutase mRNA and protein after immortalization and transformation of mouse liver cells. *Oncol Res* **5**: 127-32

Sutton, A., Imbert, A., Igoudjil, A., Descatoire, V., Cazanave, S., Pessayre, D., Degoul, F. (2005) The manganese superoxide dismutase Ala16Val dimorphism modulates both mitochondrial import and mRNA stability. *Pharmacogenet Genomics* **15**: 311-9

Takada, Y., Hachiya, M., Park, S.H., Osawa, Y., Ozawa, T., Akashi, M. (2002) Role of reactive oxygen species in cells overexpressing manganese superoxide dismutase: mechanism for induction of radioresistance. *Mol Cancer Res* **1**: 137-46

Tamimi, R. M., Hankinson, S. E., Spiegelman, D., Colditz, G. A., Hunter, D. J. (2004) Manganese superoxide dismutase polymorphism, plasma antioxidants, cigarette smoking, and risk of breast cancer. *Cancer Epidemiol Biomarkers Prev* **13**: 989-96

Tan, Y. H., Tischfield, J., Ruddle, F. H. (1973) The linkage of genes for the human interferon-induced antiviral protein and indophenol oxidase-B traits to chromosome G-21. *J Exp Med* **137**: 317-330

Thannickal, V. J. and Fanburg, B. L. (2000) Reactive oxygen species in cell signaling. *Am J Physiol Lung Cell Mol Physiol* **279**: L1005-28

Thomas, D. D., Liu, X., Kantrow, S. P., Lancaster, J. R. Jr. (2001) The biological lifetime of nitric oxide: implications for the perivascular dynamics of NO and O2. *Proc Natl Acad Sci U S A* **98**: 355-60

Tsan, M. F. (2001) Superoxide dismutase and pulmonary oxygen toxicity: lessons from transgenic and knockout mice (Review). *Int J Mol Med* **7**: 13-9

Tsan, M. F., White, J. E., Caska, B., Epstein, C. J., Lee, C. Y. (1998) Susceptibility of heterozygous MnSOD gene-knockout mice to oxygen toxicity. *Am J Respir Cell Mol Biol* **19**: 114-20

Tsan, M. F., White, J. E., Santana, T. A., Lee, C. Y. (1990) Tracheal insufflation of tumor necrosis factor protects rats against oxygen toxicity. *J Appl Physiol* **68**: 1211-1219

Tsuda, T., Kato, Y., Osawa, T. (2000) Mechanism for the peroxynitrite scavenging activity by anthocyanins. *FEBS Lett* **484**: 207-10

Turrens, J. F. (1997) Superoxide production by the mitochondrial respiratory chain. *Biosci Rep* **17**: 3-8

Van Remmen, H., Ikeno, Y., Hamilton, M., Pahlavani, M., Wolf, N., Thorpe, S. R., Alderson, N. L., Baynes, J. W., Epstein, C. J., Huang, T. T., Nelson, J., Strong, R., Richardson, A. (2003) Life-long reduction in MnSOD activity results in increased DNA damage and higher incidence of cancer but does not accelerate aging. *Physiol Genomics* **16**: 29-37

Van Remmen, H., Salvador, C., Yang, H., Huang, T. T., Epstein, C. J., Richardson, A. (1999) Characterization of the antioxidant status of the heterozygous manganese superoxide dismutase knockout mouse. *Arch Biochem Biophys* **363**: 91-7

Van Remmen, H., Williams, M. D., Guo, Z., Estlack, L., Yang, H., Carlson, E. J., Epstein, C. J., Huang, T. T., Richardson, A. (2001) Knockout mice heterozygous for Sod2 show alterations in cardiac mitochondrial function and apoptosis. *Am J Physiol Heart Circ Physiol* **281**: H1422-32

Vasquez-Vivar, J., Martasek, P., Hogg, N., Masters, B. S., Pritchard, K. A. Jr., Kalyanaraman, B. (1997) Endothelial nitric oxide synthase-dependent superoxide generation from adriamycin. *Biochemistry* **36**: 11293-7

Vikstrom, K. L., Bohlmeyer, T., Factor, S. M., Leinwand, L. A. (1998) Hypertrophy, pathology, and molecular markers of cardiac pathogenesis. *Circ Res* **82**: 773-8

Vile, G. F., Basu-Modak, S., Waltner, C., Tyrrell, R. M. (1994) Heme oxygenase 1 mediates an adaptive response to oxidative stress in human skin fibroblasts. *Proc Natl Acad Sci U S A* **91**: 2607-10

Visner, G. A., Block, E. R., Burr, I. M., Nick, H. S. (1991) Regulation of manganese superoxide dismutase in porcine pulmonary artery endothelial cells. *Am J Physiol* **260**: L444-9

Visner, G. A., Dougall, W. C., Wilson, J. M., Burr, I. A., Nick, H. S. (1990) Regulation of manganese superoxide dismutase by lipopolysaccharide, interleukin-1, and tumor necrosis factor. Role in the acute inflammatory response. *J Biol Chem* **265**: 2856-64

Wan, X. S., Devalaraja, M. N., St Clair, D. K. (1994) Molecular structure and organization of the human manganese superoxide dismutase gene. *DNA Cell Biol* **13**: 1127-36

Weisiger, R. A. and Fridovich, I. (1973) Mitochondrial superoxide simutase. Site of synthesis and intramitochondrial localization. *J Biol Chem* **248**: 4793-6

Wenk, J., Brenneisen, P., Wlaschek, M., Poswig, A., Briviba, K., Oberley, T.D., Scharffetter-Kochanek, K. (1999) Stable overexpression of manganese superoxide dismutase in mitochondria identifies hydrogen peroxide as a major oxidant in the AP-1-mediated induction of matrix-degrading metalloprotease-1. *J Biol Chem* **274**: 25869-76

White, A. A., Crawford, K. M., Patt, C. S., Lad, P. J. (1976) Activation of soluble guanylate cyclase from rat lung by incubation or by hydrogen peroxide. *J Biol Chem* **251**: 7304-12

White, C. W., Ghezzi, P., McMahon, S., Dinarello, C. A., Repine, J. E. (1989) Cytokines increase rat lung antioxidant enzymes during exposure to hyperoxia. *J Appl Physiol* **66**: 1003-1007

Whitin, J. C., Bhamre, S., Tham, D. M., Cohen, H. J. (2002) Extracellular glutathione peroxidase is secreted basolaterally by human renal proximal tubule cells. *Am J Physiol Renal Physiol* **283**: F20-8

Wispe, J. R., Clark, J. C., Burhans, M. S., Kropp, K. E., Korfhagen, T. R., Whitsett, J. A. (1989) Synthesis and processing of the precursor for human mangano-superoxide dismutase. *Biochim Biophys Acta* **994**: 30-6

Wispe, J. R., Warner, B. B., Clark, J. C., Dey, C. R., Neuman, J., Glasser, S. W., Crapo, J. D., Chang, L. Y., Whitsett, J. A. (1992) Human Mn-superoxide dismutase in pulmonary epithelial cells of transgenic mice confers protection from oxygen injury. *J Biol Chem* **267**: 23937-41

Woodson, K., Tangrea, J. A., Lehman, T. A., Modali, R., Taylor, K. M., Snyder, K., Taylor, P. R., Virtamo, J., Albanes, D. (2003) Manganese superoxide dismutase (MnSOD) polymorphism, alpha-tocopherol supplementation and prostate cancer risk in the alpha-tocopherol, beta-carotene cancer prevention study (Finland). *Cancer Causes Control* **14**: 513-8

Wu, C. F., Bishopric, N. H., Pratt, R. E. (1997) Atrial natriuretic peptide induces apoptosis in neonatal rat cardiac myocytes. *J Biol Chem* **272**: 14860-6

Xu, Y., Porntadavity, S., St Clair, D. K. (2004) Transcriptional regulation of the human manganese superoxide dismutase gene: the role of specificity protein 1 (Sp1) and activating protein-2 (AP-2). *Biochem J* **362**: 401-12

Yen, H. C., Oberley, T. D., Vichitbandha, S., Ho, Y. S., St Clair, D. K. (1996) The protective role of manganese superoxide dismutase against adriamycin-induced acute cardiac toxicity in transgenic mice. *J Clin Invest* **98**: 1253-60

Yoon, S. O., Yun C. H., Chung, A. S. (2002) Dose effect of oxidative stress on signal transduction in aging. *Mech Ageing Dev* **123**: 1597-604

Zhao, Y., Kiningham, K. K., Lin, S. M., St Clair, D. K. (2001) Overexpression of MnSOD Protects Murine Fibrosarcoma Cells (FSa-II) from Apoptosis and Promotes a Differentiation Program upon Treatment with 5-Azacytidine: Involvement of MAPK and NFκB Pathways. *Antioxid Redox Signal* **3**: 375-86

Zhao, Y., Oberley, T. D., Chaiswing, L., Lin, S. M., Epstein, C. J., Huang, T. T., St Clair, D. (2002) Manganese superoxide dismutase deficiency enhances cell turnover via tumor promoter-induced alterations in AP-1 and p53-mediated pathways in a skin cancer model. *Oncogene* **21**: 3836-46

Zhao, Y., Xue, Y., Oberley, T. D., Kiningham, K. K., Lin, S. M., Yen, H. C., Majima, H., Hines, J., St Clair, D. (2001) Overexpression of manganese superoxide dismutase suppresses tumor formation by modulation of activator protein-1 signaling in a multistage skin carcinogenesis model. *Cancer Res* **61**: 6082-8

Zhong, W. and Oberley, T. D. (2001) Redox-mediated effects of selenium on apoptosis and cell cycle in the LNCaP human prostate cancer cell line. *Cancer Res* **61**: 7071-8

Zhong, W., Oberley, L. W., Oberley, T. D., St Clair, D. K. (1997) Suppression of the malignant phenotype of human glioma cells by overexpression of manganese superoxide dismutase. *Oncogene* **14**: 481-90

Zhuang, X., Oosting, R. S., Jones, S. R., Gainetdinov, R. R., Miller, G. W., Caron, M. G., Hen, R. (2001) Hyperactivity and impaired response habituation in hyperdopaminergic mice. *Proc Natl Acad Sci U S A* **98**: 1982-7

Zuo, L. and Clanton, T. L. (2005) Reactive oxygen formation in the transition to hypoxia in skeletal muscle. *Am J Physiol Cell Physiol* **289**: C207-16

7 APPENDIX

7.1 Abbreviations

A	Adenine
BCNU	1,3-bis(2-chloroethyl)-1-nitrosourea
bp	base pair
BSA	Bovine Serum Albumine
C	Cytosine
CAT	Catalase
cDNA	DNA complementary to RNA
DMBA	7,12-dimethylbenz(α)anthracene
Dox	Doxycycline
DTT	Dithiothreitol
EGFP	Enhanced Green Fluorescent Protein
EtOH	Ethanol
FBS	Fetal Bovine Serum
FCS	Fetal Calf Serum
G	Guanine
GPx	Glutathione Peroxidase
GSH	reduced glutathione
GSSG	oxidized glutathione
h	hour
kb	kilo base pair
kDa	kilo Dalton
KO	Knock Out
LDL	Low-Density Lipoprotein
MeOH	Methanol
min.	minute
mRNA	messenger RNA
PBS	Phosphate Buffered Saline
PCR	Polymerase Chain Reaction
PFA	Paraformaldehyde
ROS	Reactive Oxygen Species
RT-PCR	Reverse Transcriptase Polymerase Chain Reaction
SD	Standard Deviation
T	Thymine
TPA	12-O-tetradecanoylphorbol-13-acetate
TUNEL	Terminal deoxynucleotidyl transferase mediated UTP Nick End Labeling
U	Uracil
wt	wild type

7.2 Solutions and media

BPTE	Piperazine-N,N'-bis(ethanesulfonic acid) – 10 mM; Bis-Tris – 30 mM; EDTA – 1 mM
cell homogenization buffer	potassium phosphate buffer pH 7.2 – 50 mM; EDTA – 1 mM; Triton X-100 – 0.01% (v/v)
electroblotting buffer	methanol – 20% ; Tris – 20 mM; glycine – 150 mM
ES lysis buffer	Tris·HCl pH 8.5 – 100 mM; EDTA – 5 mM; SDS – 0.2%; NaCl – 200 mM; proteinase K – 40 μg/ml
ES medium	FCS – 15%; MEM Non-Essential Amino Acids Solution – 1×; Penicillin-Streptamycin-Glutamine – 1×; β-mercaptoethanol – 0.7% (v/v/); Leukaemia Inhibitory Factor – 1000 U/ml; all components in Dulbecco's Modified Eagle Medium (D-MEM) 4,500 mg/L D-glucose, 25 mM HEPES without sodium pyruvate; filter sterilized
glyoxal mixture	DMSO – 60% (v/v); BPTE – 0.12×; deionized glyoxal – 8%; glycerol – 4.8%; ethidium bromide – 0.2 mg/ml
HBS	glucose – 5 mM; NaCl – 140 mM; KCl – 5 mM; EDTA – 0.2 mM; $CaCl_2$ – 1 mM; $MgCl_2$ – 1 mM; HEPES – 5 mM; filter sterilized
HEPES buffer	NaCl – 120 mM; KCl – 5 mM; KH_2PO_4 – 440 μM; $Na_2HPO_4 \cdot 7H_2O$ – 300 μM; glucose – 5.5 mM; Phenol Red – 0.01% (w/v); HEPES – 20 mM; autoclaved
HEPES/EDTA buffer	HEPES buffer with 120 mM EDTA; autoclaved
hybrydization buffer	formamide – 50% in 5× SSC pH 4.5 (citric acid to adjust pH), tRNA – 50 μg/ml, SDS – 1%, heparin – 50 μg/ml
NTMT	NaCl – 100 mM, TrisHCl pH 9.5 – 100 mM, $MgCl_2$ – 50 mM, Tween-20 – 0.1%
PFA	PFA – 40g in 1litre of 1× PBS, pH 7.0; heated to 60º C, 2 M NaOH added to solubilize PFA; filter sterilized
RNA loading buffer	deionized formamide – 90% (v/v); Bromophenol Blue – 0.025% (w/v); Xylene Cyanol FF – 0.025% (w/v); EDTA – 5 mM; SDS – 0.025% (w/v)
solution I	formamide – 50%, SDS – 1% in 5× SSC pH 4.5
solution III	formamide – 50% in 2× SSC pH 4.5
tail lysis buffer	Tris·HCl pH 8.5 – 100 mM; EDTA – 5 mM; SDS – 0.2%; NaCl – 200 mM; proteinase K – 500 μg/ml
TBS	Tris·HCl pH 7.4 – 50 mM; NaCl - 150 mM
TBST	TBS with 0.1% (v/v) Tween-20
tissue homogenization buffer	potassium phosphate buffer pH 7.2 – 50 mM; EDTA – 1 mM; DTT – 1 mM; KCl – 1.15% (w/v); Triton X-100 – 0.01% (v/v)

7.3 Erklärung

Hiermit erkläre ich, daß ich mich mit der vorliegenden wissenschaftlichen Arbeit erstmals um die Erlangung des Doktorgrades bewerbe, die Arbeit selbständig und nur unter Verwendung der angegebenen Quellen und Hilfsmittel angefertigt und die den benutzen Werken wörtlich oder inhaltlich entnommenen Stellen als solche kenntlich gemacht habe.

Halle/Saale, January 2006 Tomasz Loch

7.4 Curriculum vitae

Personal data

Name	Tomasz Loch
Born	22.11.1971 in Siemianowice Śląskie, Poland
Citizenship	Polish
Marital status	Married

Education

1978 – 1986	Primary School No. 59, Katowice, Poland
1986 – 1990	Jan Kawalec IX Grammar School, Katowice, Poland

Master degree studies

1990 – 1996	University of Silesia, Faculty of Biology and Environmental Protection, Katowice, Poland
1993 – 1994	University of Greenwich, Tempus Exchange
17.05.1996	Master of Sciences Degree Scientific supervisor: Prof. Zdzisław Krawczyk Research subject: Microsatellite sequences

Ph.D. studies

2001 – 2004	Martin-Luther-University, Institute of Physiological Chemistry, Halle, Germany Scientific supervisor: Prof. Thomas Braun Research subject: Manganese Superoxide Dismutase

Employment

1997 – 2001	Medical University of Silesia, Department of Molecular Biology and Medical Genetics, Katowice, Poland Scientific supervisor: Prof. Tadeusz Wilczok Research subject: Human Papillomavirus, angiogenesis
2001 – 2004	Martin-Luther-University, Institute of Physiological Chemistry, Halle, Germany
2005 – present	Medical University of Silesia, Department of Molecular Biology and Medical Genetics, Katowice, Poland Scientific supervisor: Dr. Urszula Mazurek Research subject: Manganese Superoxide Dismutase

7.5 Publications and Presentations

Published

Neuhaus, P., Oustanina, S., Loch, T., Kruger, M., Bober, E., Dono, R., Zeller, R., Braun, T. (2003) Reduced mobility of fibroblast growth factor (FGF)-deficient myoblasts might contribute to dystrophic changes in the musculature of FGF2/FGF6/mdx triple-mutant mice. Mol. Cell. Biol. 23(17): 6037-48

Loch, T., Bober, E., Braun, T. (2003) Regulated overexpression of mitochondrial superoxide dismutase in 10T1/2 cell line. Acta Biochim. Pol., Supplement 2003: 49

Michalski, B., Mazurek, U., Olejek, A., Loch, T., Graniczka, M., Poręba, R., Wilczok, T. (2003) Expression patterns in isoforms of vascular endothelial growth-factors in tissue samples of vulval cancer T1 N2M0 stage. Ginekol. Pol. 74(1): 40-7

Michalski, B., Mazurek, U., Graniczka, M., Loch, T., Poręba, R., Wilczok, T. (2001) Significance of human papillomavirus testing and colposcopy for diagnostic of minor-grade cytological abnormalities. Ginekologia Praktyczna 54, 11-13

Michalski, B., Mazurek, U. Olejek, A., Graniczka, M., Loch, T., Poręba, R., Wilczok, T. (2001) Quantitative RT-PCR assay for mRNA of VEGF and histone H4 in the determination of proliferative and angiogenic activity in vulvar pathology. Folia Histochem. Cytobiol. 2001;39 Suppl 2:108-9.

Michalski, B., Mazurek, U., Graniczka, M., Loch, T., Poręba, R., Wilczok, T., Ćwiklicki, J. (2001) Human papillomavirus testing significance for cervical cancer screening based on the Bethesda System. Ginekologia Praktyczna 54, 8-10

Loch, T., Michalski, B., Mazurek, U., Graniczka, M. (2001) Vascular endothelial growth factor (VEGF) and its contribution to carcinogenesis. Postepy Hig. Med. Dosw. 55, 257-274

Lisowska, K., Loch, T., Fiszer-Kierzkowska, A., Ścieglińska, D., Krawczyk, Z. (1997) Identification of a microsatellite region composed of a long homopurine-homopyrimidine

tract surrounded by AT-rich sequences upstream of the rat stress inducible hsp70.1 gene. Acta Biochim. Pol. 44, 147-152

Posters

Loch, T., Bober, E., Braun, T. Regulated overexpression of mitochondrial superoxide dismutase in 10T1/2 cell line. 39th Congress of the Polish Biochemical Society, Gdańsk, Poland, September 16-20, 2003

Michalski, B., Mazurek, U., Olejek, A., Loch, T., Graniczka, M., Poręba, R., Wilczok, T. Quantitative analysis of mRNA level of selected angiogenesis genes in ovarian cancer by QRT-PCR technique using ABI PRISM™ 770 (TaqMan). 8th Scientific Workshop of the Polish Society of Oncological Gynaecology, Kraków - Przegorzały, Poland, June 22-24, 2000

Michalski, B., Mazurek, U., Olejek, A., Loch, T., Graniczka, M., Poręba, R., Wilczok, T. mRNA expression profile of vascular endothelial growth factor isoforms in determination of pathology gradation of vulval cancer T1 N2M0 stage. 28th Congress of the Polish Gynaecological Society, Szczecin, Poland, September 13-16, 2000

Graniczka, M., Loch, T., Mazurek, U., Wilczok, T., Michalski, B., Poręba, R. Expression of E6 and E7 HPV genes in the oncogenesis of the cervix. 2nd Congress of the Polish Society of Human Genetics, Poznań, Poland, May 24-26, 1999

32nd Congress of the Polish Biochemical Society, Cracow, September 17-20, 1996

31st Congress of the Polish Biochemical Society, Warsaw, September 6-8, 1995

14th International Workshop on the Cell Nucleus: Spa, Belgium, May 27-31, 1995

8 SUMMARY

Manganese superoxide dismutase (MnSOD) is the only antioxidant enzyme which is indispensable for the existence of higher eukaryotes. To gain better insight into the essential role of MnSOD, I developed a conditional transgenic mouse strain in which MnSOD expression was put under the control of the tetracycline regulatory system.

The present work describes the generation of the transgenic mouse strain and characterizes consequences of MnSOD suppression for the physiology of the genetically altered animals. Furthermore, I describe the effects of MnSOD overexpression and deficiency in different cell culture systems.

My results demonstrate that a two-fold higher activity of MnSOD had no influence on activities of other antioxidant enzymes, namely CuZnSOD, CAT and GPX. As expected, the increased level of MnSOD expression protected cells from death under hyperoxic conditions. It also prevented apoptosis induced by hydrogen peroxide administration. Unexpectedly, however, overexpression of MnSOD did slightly enhance doxorubicin-induced programmed cell death although I observed an almost complete inhibition of apoptosis induced by doxorubicin or hydrogen peroxide in primary fibroblasts isolated from $MnSOD^{-/-}$ mice. These results suggest an involvement of MnSOD in ceramide mediated apoptosis and in the regulation of the balance between nitric oxide and peroxynitrite. These findings represent a new aspect of the regulation of programmed cell death.

I also detected that MnSOD deficient cells contained higher level of free radicals and were more susceptible to hyperoxia. Surprisingly, but in accordance with the proposed role of hydrogen peroxide in senescence, $MnSOD^{-/-}$ fibroblasts appeared to senesce slower than corresponding wild type cells. Taken together, the results of *in vitro* studies demonstrated a central role of MnSOD in the regulation of cellular oxidative stress and revealed that MnSOD is indispensable for the progression of apoptosis and senescence.

In order to generate an animal model for the regulated expression of MnSOD four strains of transgenic mice were produced. Two of them showed a comparatively low expression of SOD and an ineffective regulation of SOD transcription. One of the remaining strains was used to study the effects of a partial and complete MnSOD deficiency *in vivo* (SOD/TRE) while the last strain allowed a regulated MnSOD expression in the heart (SOD/αMHC tTA).

In the absence of an additional allele, which carries the tetracycline receptor to achieve tissue specific or ubiquitous expression of MnSOD, the SOD/TRE strain might be used as

a constitutive knock-out model for SOD. In the presence of the tetracycline receptor, however, the expression of MnSOD can be reversibly switched on and off by administration of doxycycline in drinking water.

Complete MnSOD deficiency in homozygous SOD/TRE mice led to early-onset lethality and to massive phenotypical changes as indicated by a reduced body size and weight together with neurological abnormalities. Strong up-regulation of ANF expression in hearts of 3 days old animals was observed. The same hearts showed a slightly increased rate of apoptosis, although TUNEL-positive cells were rare and accumulated only in the epicardium. Despite earlier description of phenotypical changes, my immunohistochemical stainings suggest that apoptosis in the hearts of $MnSOD^{-/-}$ mice is not the primary cause of cardiac failure.

Heterozygous SOD/TRE mice showed a 30-40% reduced MnSOD activity in the heart, brain and liver. This attenuation of mitochondrial dismutase did not affect the activity of CuZnSOD, CAT or GPX. Interestingly, the 30% reduction of MnSOD activity in the hearts of 6 months old mice clearly reduced the cardiac performance of heterozygous mutant SOD mice. Left ventricle fraction shortening and fractional area change were decreased in these animals by 26% and 21%, respectively.

Furthermore, treatment with doxorubicin, a cytotoxic drug which causes heart dilation, induced apoptosis in the hearts of SOD/TRE heterozygotes and stimulated expression of ANF. The first effect was confined to restricted areas of epicardium, the latter was detectable throughout the heart. Senescence-associated β-galactosidase staining revealed that endothelial and smooth muscle cells in vessels proximal to the heart were less resistant to the stress induced by doxorubicin and displayed a senescent phenotype. In contrast, the heart tissue itself showed no signs of senescence in heterozygous SOD/TRE or in wild type mice.

Taken together, my results demonstrate for the first time that even a partial reduction of MnSOD activity might impair heart function and might contribute to vascular pathogenesis.

SOD/αMHC tTA homozygous mice survived up to 14 days and showed the same phenotypical changes as homozygous SOD/TRE and knock-out mice, which have been constructed previously. I found that the transcription of the engineered SOD allele was readily regulated *in vivo* by administration of doxycycline in drinking water and gave rise to a transcript of the predicted size, which generated a protein of the expected molecular weight. Regulation was shown to be effective also at the protein level. Since transcription of the tetracycline receptor was driven by α-myosin heavy chain promoter, expression of the transgene was achieved exclusively in the heart thereby successfully establishing a mouse model with heart-specific regulated expression of MnSOD.

8 Summary

In the presented work I described experiments performed *in vivo* and *in vitro,* which contribute to the understanding of the function of MnSOD in cellular and physiological processes. The SOD/TRE and SOD/αMHC tTA animal models generated in the course of this work will provide convenient research tools which might help to elucidate the role of MnSOD in many pathological processes in various tissues at different time points.

9 ZUSAMMENFASSUNG

Die vorliegende Arbeit leistet einen Beitrag zum besseren Verständnis der physiologischen Rolle des mitochondrialen Enzyms Mangan Superoxid Dismutase (MnSOD/SOD2). MnSOD ist das erste Enzym in der Kette der mitochondrialen anti-oxidativen Abwehr und die Ausschaltung des MnSOD Gens in Mäusen führt zur frühen perinatalen Letalität. Das Ziel dieser Arbeit war in vitro und in vivo Systeme zur regulierten MnSOD Expression zu etablieren.

Im Zellkulturmodel zur MnSOD Überexpression wurde eine zweifache Erhöhung des MnSOD Expressionslevels beobachtet. Die Expression anderer Enzyme der anti-oxidativen Abwehr (CuZnSOD, CAT, GPX) blieb unverändert. Die erhöhte MnSOD Aktivität führte zu einer verminderten Apoptoserate nach Induktion mit H_2O_2 oder durch Hyperoxie. Dagegen war die Doxorubicin-induzierte Apoptose unter MnSOD Überexpression leicht erhöht.
Ein unerwarteter Effekt wurde in primären MnSOD defizienten ($MnSOD^{-/-}$) Mausfibroblasten beobachtet. Zunächst konnte gezeigt werden, dass $MnSOD^{-/-}$ Zellen tatsächlich höhere Mengen an freien Radikalen produzierten und empfindlicher als die Wildtyp Zellen auf Hyperoxie reagierten. Die $MnSOD^{-/-}$ Fibroblasten waren jedoch resistent gegenüber H_2O_2 -oder Doxorubicin-induzierten Apoptose. Diese Ergebnisse deuten auf eine mögliche Involvierung der MnSOD in die Ceramid-gesteuerte Apoptose und in die Aufrechterhaltung der Balance zwischen Nitritoxid und Peroxydnitrit Levels hin. Weiterhin zeigten MnSOD defiziente Zellen eine verlangsamte Seneszenz. Zusammenfassend lässt sich feststellen, dass die Ergebnisse der in vitro Untersuchungen eine zentrale Rolle der MnSOD in der Regulierung des zellulären oxidativen Stresses sowie der Apoptose- und Seneszenz-Vorgängen unterstützen.

Als erster Schritt zur Etablierung eines adäquaten Tiermodells zur regulierten MnSOD Expression wurde ein transgener „Ausgangsmausstamm“ SOD/TRE generiert. Mittels homologer Rekombination wurde der endogene Genlocus durch eine Expressionskassette ersetzt. Diese Kassette beinhaltet die MnSOD cDNA, der ein basaler Genpromotor inklusive eines Tetracyclin-responsiven-Elements (TRE) vorgesetzt wurde. Eine regulierte MnSOD Expression kann in den transgenen Tieren nur in Anwesenheit eines Tetracyclin-Regulators (TetR) stattfinden. Ohne weitere Verkreuzung wurde der hier generierte SOD/TRE Mausstamm als ein konventioneller Knockout Stamm verwendet. Wie erwartet hat die vollständige MnSOD Defizienz in den SOD/TRE Homozygoten zur frühen Mortalität und

phenotypischen Veränderungen wie reduzierte Körpergröße und Gewicht, sowie motorische Störungen geführt. Des Weiteren wurde eine starke Erhöhung der ANF-Expression in den Herzen der 3 Tage alten Tiere beobachtet. Im Epicardium der analysierten Herzen wurden auch verstreute TUNEL-positive apoptotische Zellen beobachtet. Entgegen den phenotypischen Herzveränderungen, die zuvor bei anderen MnSOD Mutanten beschrieben worden sind, weisen die hier präsentierten immunhistochemischen Analysen nicht auf einen ursächlichen Zusammenhang zwischen der Apoptose in Herzen und dem Ausfall der Herzfunktion und Tod der homozygoten $MnSOD^{-/-}$ Tiere hin.

Um den Einfluss einer verminderten MnSOD Aktivität auf die Herzfunktion zu studieren, wurden anschließend heterozygote SOD/TRE Tiere analysiert. Es zeigte sich, dass die MnSOD Enzymaktivität um 30 bis 40% reduziert war. Diese verminderte Aktivität der mitochondrialen Dismutase hatte keine Aktivitätsveränderungen der CuZnSOD, CAT oder GPX zu Folge. Diese relativ milde 30% Reduktion der MnSOD Aktivität führte jedoch zu einer ca. 20% Einschränkung der linksventrikulären Herzfunktion, wie an Herzen von 6 Monate alten Tieren mittels Echokardiographie demonstriert werden konnte. Nach Behandlung der heterozygoten SOD/TRE Mutanten mit einem cytotoxischen Medikament, dem Doxorubicin, konnten in den Herzen der behandelten Tiere Apoptoseinduktion und ektopische ANF Expression beobachtet werden. Dabei waren die apoptotischen Zellen auf einige Bereiche des Epicardiums begrenzt, die ANF Expression dagegen wurde im gesamten Herzen detektiert. Darüber hinaus wurden seneszente endotheliale und glatte Muskelzellen mittels einer Seneszenz-spezifischen ß-Gal-Anfärbung in den proximalen Herzgefäßen sichtbar gemacht. Die verminderte Resistenz gegenüber Doxorubicin-induziertem oxidativem Stress und das Auftauchen seneszenter Zellen traten nur in Gefäßen der heterozygoten Tiere auf. Das Herzgewebe selbst wies keine seneszenten Zellen auf. Insgesamt dokumentieren die an den heterozygoten MnSOD Mutanten gewonnenen Daten zum ersten Mal, dass eine partielle MnSOD Defizienz bereits die Herzfunktion beeinträchtigt und der oxidative Stress zur vaskulären Pathogenese beitragen kann.

Der SOD/TRE Mausstamm wurde weiterhin zur Generierung eines Tierstamms, SOD/αMHC tTA, verwendet, in dem die MnSOD Expression nur im Myocardium stattfindet; die übrigen Gewebe bleiben MnSOD defizient. Die herzspezifische MnSOD Expression sollte reversibel und zum beliebigen Zeitpunkt durch Tetracyclingabe im Trinkwasser abgeschaltet werden können. Die Analyse der aus Herzgewebe der transgenen Tiere isolierten mRNA zeigte, dass von dem inserierten Konstrukt ein mRNA-Transkript von korrekter Größe produziert wird. Die Transkription konnte durch Tetracyclingabe im Trinkwasser vollständig

unterdrückt werden. Diese regulierte MnSOD Expression konnte ebenso auf Proteinebene dokumentiert werden. Die hier generierten SOD/αMHC tTA homozygoten Tiere zeigten jedoch eine Überlebensdauer von ca. 14 Tagen nach der Geburt und wiesen vergleichbare phenotypische Veränderungen, wie die SOD/TRE homozygoten Knockout Mäuse auf.

Zusammenfassend wurden in dieser Arbeit in vivo und vitro Experimente durchgeführt, die zum Verständnis der MnSOD Funktion in zellulären und physiologischen Prozessen beitragen. Die hier etablierten Tiermodelle, SOD/TRE und SOD/αMHC tTA stellen ausgezeichnete Werkzeuge, die die Erforschung der Rolle der MnSOD in vielen pathologischen Prozessen, gewebsspezifisch und zu definierten Zeitpunkten möglich machen.